USGS
science for a changing world

RESISTIVITY STRUCTURE ACROSS THE HUMBOLDT RIVER BASIN, NORTH-CENTRAL NEVADA

by

Brian D. Rodriguez
and
Jackie M. Williams [1]

Open-File Report 02-39
paper edition

2002

U.S. DEPARTMENT OF THE INTERIOR
U.S. GEOLOGICAL SURVEY

---

[1] Denver, Colorado

TABLE OF CONTENTS

ILLUSTRATIONS

ABSTRACT

Magnetotelluric data collected along five profiles show deep resistivity structures beneath the Battle Mountain-Eureka and Carlin gold trends in north-central Nevada, which appear consistent with tectonic breaks in the crust that possibly served as channels for hydrothermal fluids. It seems likely that gold deposits along these linear trends were, therefore, controlled by deep regional crustal fault systems.

Two-dimensional resistivity modeling of the magnetotelluric data generally show resistive (30 to 1,000 ohm-m) crustal blocks broken by sub-vertical, two-dimensional, conductive (1 to 10 ohm-m) zones that are indicative of large-scale crustal fault zones. These inferred fault zones are regional in scale, trend northeast-southwest, north-south, and northwest-southeast, and extend to mid-crustal (20 km) depths. The conductors are about 2- to 15-km wide, extend from about 1 to 4 km below the surface to about 20 km depth, and show two-dimensional electrical structure. By connecting the locations of similar trending conductors together, individual regional crustal fault zones within the upper crust can be inferred that range from about 4- to 10-km wide and about 30- to 150-km long. One of these crustal fault zones coincides with the Battle Mountain-Eureka mineral trend. The interpreted electrical property sections also show regional changes in the resistive crust from south to north. Most of the subsurface in the upper 20 km beneath Reese River Valley and southern Boulder Valley are underlain by rock that is generally more conductive than the subsurface beneath Kelly Creek Basin and northern Boulder Valley. This suggests that either elevated-temperature or high-salinity fluids, alteration, or carbonaceous rocks are more pervasive in the more conductive area (Battle Mountain Heat-Flow High), which implies that the crust beneath these valleys is either more fractured or has more carbonaceous rocks than in the area surveyed along the 41st parallel.

INTRODUCTION

Many sediment-hosted gold deposits occur along linear trends in northern Nevada (Struhsacker and others, 1996). The distribution and genesis of these deposits along the Battle Mountain-Eureka (BME) and Carlin gold trends is not fully understood. In general, most geologic models suggest that regional structures played an important role in the spatial distribution of these deposits (e.g. Arehart and others, 1993; Ilchik and Barton, 1997; Radtke, 1985; Shawe, 1991; Sillitoe and Bonham, 1990; Tosdal, 1998). To investigate crustal structures that may be related to the genesis of gold deposits along these trends, five profiles of magnetotelluric (MT) soundings were acquired in 1998, 1999, and 2000 (lines MT5 to MT9, Figure 1). Modeling of the MT data can be used to infer the deep resistivity structure of the crust. Such structures may reflect possible

tectonic controls on the emplacement of mineral deposits along these linear trends, and so may be used to help improve critical gold endowment estimates in the Humboldt River Basin.

MAGNETOTELLURIC METHOD

The magnetotelluric (MT) method is a passive surface geophysical technique, which uses the earth's natural electromagnetic fields to investigate the electrical resistivity structure of the subsurface. The resistivity of geologic units is largely dependent upon their fluid content, porosity, degree of fracturing, temperature, and conductive mineral content (Keller, 1989). Saline fluids within the pore spaces and fracture openings can reduce resistivities in a resistive rock matrix. Also, resistivity can be lowered by the presence of conductive clay minerals, carbon, and metallic mineralization. It is common for altered volcanic rocks to contain authigenic minerals that have resistivities ten times lower than those of the surrounding rocks (Nelson and Anderson, 1992). Increased temperatures cause higher ionic mobility and mineral activation energy, reducing rock resistivities significantly. Unaltered, unfractured igneous rocks are normally very resistive (typically 1,000 ohm-m or greater), whereas fault zones will show low resistivity (less than 100 ohm-m) when they are comprised of rocks fractured enough to have hosted fluid transport and consequent mineralogical alteration (Eberhart-Phillips and others, 1995). Carbonate rocks are moderately to highly resistive (hundreds to thousands of ohm-m) depending upon their fluid content, porosity, fracturing, and impurities. Marine shales, mudstones, and clay-rich alluvium are normally very conductive (a few ohm-m to tens of ohm-m). Unaltered, metamorphic rocks (non-graphitic) are moderately to highly resistive (hundreds to thousands of ohm-m). Tables of electrical resistivity for a variety of rocks, minerals and geological environments may be found in Keller (1987) and Palacky (1987).

The MT method can be used to probe the crust from depths of tens of meters to depths of tens of kilometers (Vozoff, 1991). Natural variations of the Earth's magnetic and electric field are measured and recorded at each MT station. The primary frequency bands used by the MT method are 10,000 Hz to 1 Hz from worldwide lightning activity and 1 Hz to 0.0001 Hz from geomagnetic micro-pulsations. The natural electric and magnetic fields propagate vertically in the earth because the very large resistivity contrast between the air and the earth causes a vertical refraction of both fields transmitted into the earth (Vozoff, 1972).

The natural electric and magnetic fields are recorded in two orthogonal, horizontal directions. The vertical magnetic field ("tipper") is also recorded. The resulting time-series signals are used to derive the tensor apparent resistivities and phases. First, the signals are converted to complex cross-spectra using

FFT (fast-Fourier-transform) techniques. Then, least-squares, cross-spectral analysis (Bendat and Piersol, 1971) is used to solve for a transfer function that relates the observed electric fields to the magnetic fields under the assumption that the Earth consists of a two-input, two-output, linear system with the magnetic fields as input and the electric fields as output (Rodriguez and others, 1996b). Prior to conversion to apparent resistivity and phase, the electromagnetic tensor is normally rotated into principal directions that correspond to the direction of maximum and minimum apparent resistivity. For a two-dimensional (2-D) Earth, the MT fields can be de-coupled into transverse electric (TE) and transverse magnetic (TM) modes; 2-D modeling is generally done to fit both modes. When the geology satisfies the 2-D assumption, the MT data for the TE mode is for the electric field parallel to geologic strike, and the data for the TM mode is for the electric field across strike. The MT method is well suited for studying complicated geological environments because the electric and magnetic relations are sensitive to vertical and horizontal variations in resistivity. The method is capable of establishing whether the electromagnetic fields result from subsurface terranes of effectively 1-, 2-, or 3-dimensions. An introduction to the MT method and references for a more advanced understanding are contained in Dobrin and Savit (1988) and Vozoff (1991).

MAGNETOTELLURIC SURVEYS

Thirty-eight MT soundings were located along five profiles (MT5 to MT9, Figure 1) of lengths varying from 20 to 110 km and spacing that varied from 1.5 to 13.5 km. The MT soundings reported here span from 117.48972 degrees west and 41.14575 degrees north to 116.22838 degrees west and 40.58591 degrees north. Results of sixty-nine other MT soundings located along four profiles (MT1 to MT4, Figure 1) of lengths varying from 40 to 110 km and spacing that varied from 1.3 to 19.5 km are described in Rodriguez and Williams (2001).

The following table lists the MT station locations of the five profiles (MT5 to MT9). These locations were found using either on-site GPS measurements or digitized from 100,000 scale field maps (Williams and Rodriguez, 2001b; 2001c; 2001d). Coordinates are referenced to the 1866 Clarke spheroid and North American 1927 Western United States datum. Longitude and latitude format below is decimal degrees. Elevation (derived from 100,000 scale field maps) is in meters.

Station	Longitude	Latitude	Elev(m)
	MT5		
53	-117.46039	41.03561	1450
61	-117.37602	41.05213	1430
48	-117.23083	41.04530	1340
62	-117.12730	41.03736	1350

45	-116.99049	40.99599	1420
60	-116.95005	41.01850	1460
43	-116.88703	41.00584	1650
42	-116.80737	41.00304	1600
59	-116.64933	40.98375	1530
58	-116.54706	40.98970	1650
57	-116.45419	41.00731	1700
34	-116.41038	40.98637	1600
37	-116.39134	40.98808	1650
33	-116.36519	40.98794	1700
32	-116.33897	40.99409	1800
35	-116.26639	40.99996	1800
56	-116.22838	40.99611	1740
	MT6		
72	-116.65770	40.76352	1400
67	-116.59319	40.76856	1400
65	-116.52693	40.76426	1410
64	-116.49056	40.75211	1420
	MT7		
63	-116.46887	40.69744	1450
66	-116.49212	40.79785	1415
68	-116.50533	40.84150	1430
69	-116.49231	40.89135	1470
70	-116.47627	40.94122	1530
	MT8		
76	-116.98241	40.58591	1400
75	-116.96516	40.60841	1400
74	-116.90120	40.66956	1374
73	-116.86531	40.70358	1463
	MT9		
90	-117.48972	40.74573	1440
91	-117.41152	40.78297	1390
92	-117.38475	40.83747	1390
93	-117.31868	40.87867	1370
94	-117.27735	40.93117	1340
49	-117.16232	41.08410	1360
95	-117.04928	41.13012	1420
96	-116.95985	41.14575	1420
97	-117.17020	40.79370	1400

MAGNETOTELLURIC DATA

Frequencies sampled for profiles MT5 to MT9 ranged from 0.002 to 200 Hz using single station recordings of both orthogonal horizontal components of the electric and magnetic fields, along with the vertical magnetic field at stations 37, 48, 49, 53, 59, 63 to 69, 73 to 76, and 90 to 97 (Williams and Rodriguez, 2001b; 2001c; 2001d). The single station recordings for profiles MT1 to MT4 are reported in Williams and Rodriguez (2000; 2001a) and Williams and others (2001a; 2001b; 2001c) along

with the vertical magnetic field recordings at stations 12A to 28A, 1, 11, 14, 71, 77, 79 to 89, 98, 108, and 109. Sampling this frequency range in other areas of widely varying geology has allowed us to probe the crust from depths of hundreds of meters to depths of tens of kilometers (Eberhart-Phillips and others, 1990; Stanley and others, 1991; 1997; Rodriguez and others, 1996a; 1996b). The recorded time-series data were transformed to the frequency domain and processed to determine a two-dimensional apparent resistivity and phase tensor at each site. Rotation of the impedance tensor to maximum and minimum directions allows for decoupling into the TE and TM modes.

A measure of the dimensionality (2- or 3-D) of MT data is provided by the impedance skew of the impedance tensor (Vozoff, 1972) and the impedance polar plots (Reddy and others, 1977). By examining the tensor impedances, the dimensionality of electrical structures and the general strikes of 2-D structures were estimated for different frequencies. MT stations whose impedances were 3-D in the lower frequencies (Williams and Rodriguez, 2001; Williams and others, 2001a; 2001b; 2001c) are indicated with triangle symbols in Figure 1. Predicted values of the electric field can be computed from the measured values of the magnetic field (Vozoff, 1991). The coherence of the predicted electric field with the measured electric field is a measure of the signal-to-noise ratio provided in the multiple coherency plot. Values are normalized between 0 and 1, where values at 0.5 signify signal levels equal to noise levels. For this data set, coherencies were generally at an acceptable level, except at times in the "dead band" (0.1 to 1 Hz) and at times in the lower frequencies (0.002 to 0.1). Overall data quality was fair to good for profiles MT6, MT7, MT8, and MT9, and fair to poor for MT5 (Williams and Rodriguez, 2001; Williams and others, 2001a; 2001b; 2001c). The worst data points were ignored and the data used in the modeling generally had predicted coherencies above 90% and 60% for the higher and lower quality data, respectively.

In the Appendix, observed data of each MT sounding for each profile (MT5 to MT9) are represented by descrete values (circle and x symbols) of the TE and TM modes from the raw data curves (Williams and Rodriguez, 2001; Williams and others, 2001a; 2001b; 2001c). Calculated data for each profile are represented by solid (TE mode) and dashed (TM mode) lines interpolated from the descrete values (0.003, 0.01, 0.03, 0.1, 0.3, 1, 3, 10, 30, 100) output from the 2-D finite element models (Figures 2 and 3).

RESISTIVITY MODELS

Wannamaker (1983) found that MT responses in the northern Basin and Range are fundamentally 3-D in nature. However, for elongated structures, 2-D modeling can be used to construct reasonable estimates of the resistivity cross-sections along each profile (Figures 2 and 3). Wannamaker and others (1984)

demonstrated that approximating 3-D structure beneath a centrally located profile with 2-D modeling is best achieved when fitting the TM curve even at the expense of a poor fit of the TE curve. However, because TM data are relatively insensitive to the depth extent of a subsurface body (Eberhart-Phillips and others, 1995), the depths to the base of the bodies in the model are not well constrained. Hence, clarifying the model limits with 3-D resistivity modeling may be necessary.

The 2-D resistivity models of Figures 2 and 3 were constructed for each profile using the forward modeling finite element algorithm of Wannamaker and others (1987). The resistivity models generally fit the TM data better than the TE data (see Appendix A, B, C, D, and E), although fits to the TE data were satisfactory for stations where 2-D structure was indicated (Figure 1). However, because of the widespread 3-D character of the results, we focus only on the gross structure determined by the models.

The variable-dimension finite-element grid cells used for our models had 127 horizontal and 38 vertical nodes (plus 9 more vertical nodes used for the air layer). The edges of the model were extended to over 800-km horizontally and 450-km vertically, so as to minimize edge effects. The resolution of the resistivity boundaries used for each model is somewhat subjective. If different resistivities are used, then boundary positions and layer depths would have to be adjusted to achieve similar fits to the observed data. The extreme case would be to use a model with a "continuous" resistivity gradient from low to high resistivities. The resolution of the resistivity boundaries is also, in part, a function of our model grid mesh design. We have attempted to keep each model simple. The MT profile model (Figures 2 and 3) depths are relative to the surface.

DISCUSSION

The deeper section of the 2-D resistivity model for profile MT4 (Figure 2) was reported previously in (Rodriguez and Williams, 2001), but did not include a description of the upper 2 km, which is important for gold endowment estimates in the Humboldt River Basin. We, therefore, present our interpretation of the upper 2 km here, following a summary of the deeper section. The sub-vertical, 2-D, north trending (Figure 4) conductor (1 to 10 ohm-m) beneath stations 22A to 24A that penetrates to mid-crustal depths (from 5 to 20 km depth) is hard to explain other than by a major crustal-dimension fault or fracture zone (Eberhart-Phillips and others, 1995). The low resistivities (conductors) are likely caused by material associated with faulting or fracture filling, such as mylonitic breccia, brine-filled fractures, argillaceous alteration from hydrothermal fluids, substantial graphitic carbon associated with shearing, or a combination of these (Eberhart-Phillips and others, 1995). Additional support for a fault zone

interpretation is the 2-D electrical structure. In the upper 8 km, the resistive (30 to 300 ohm-m) crustal blocks near Battle Mountain appear to be broken by a separate northeast trending (Figure 4) conductor (10 ohm-m beneath station 16A, Figure 2) that is characteristic of a crustal fault zone. A separate northeast trending conductor (3 ohm-m) beneath station 12A (Figure 2) is also characteristic of a crustal fault zone. Each of these inferred crustal faults occur within the BME gold trend. A north trending (Figure 4) conductor (1 to 10 ohm-m) within the Carlin gold trend beneath station 25A (Figure 2) is also characteristic of a crustal fault zone. The large 3-D conductive (1 ohm-m) zone from 1 to 12 km depth between stations 27A and 28A (between the BME and Carlin trends) is characteristic of a geothermal system or a thick section of carbonaceous rocks. The upper 2 km is characterized primarily by conductive (1 to 30 ohm-m) basin fill (Reese River Valley and Boulder Valley basins). The resistive (100 to 1,000 ohm-m) crustal blocks within the northern Nevada rift (Zoback and others, 1994) between stations 25A and 26A are characteristic of lower Paleozoic rocks and intruded lower Paleozoics reported by Rodriguez and Williams (2001). The northwest trending (Figure 5) conductor (3 to 10 ohm-m) near the Good Hope fault within the Carlin trend beneath station 27 appears to be a local fault zone (Figure 6) and not a crustal fault zone, because its electrical character at lower depths is 3-D.

The deeper southwestern half of the 2-D resistivity model for profile MT8 (Figure 2) is dominated by conductive (10 ohm-m) rocks we interpret to be part of the Battle Mountain Heat-Flow High (Sass and others, 1981). The entire profile lies within the BME trend. The northeastern half is characterized by a northwest trending (Figure 4) conductor (1 to 10 ohm-m) beneath stations 73 and 74 that is characteristic of a crustal fault zone, which also continues in the upper 2 km (Figure 2). The southwestern half of the shallow section appears to be characterized by resistive (30 to 300 ohm-m) rocks that are characteristic of lower Paleozoics or other unknown volcanic and/or clastic sedimentary rocks at depth (Grauch and others, 1998).

The 2-D resistivity model for profile MT6 (Figure 2) shows a northeast trending (Figure 4) conductor (3 to 10 ohm-m) between the BME and Carlin trends beneath station 65 that is characteristic of a crustal fault zone, which also continues in the upper 2 km. The large 3-D conductive (1 ohm-m) zone from about 1.5 to 15 km depth also between the BME and Carlin trends beneath stations 64 and 28A (Figure 2) is characteristic of a geothermal system or a thick section of carbonaceous rocks. The western edge of the deeper section beneath station 72 shows resistive (30 to 100 ohm-m) rocks that are characteristic of intruded lower Paleozoics in the northern Nevada rift (NNR). Other conductive (3 to 10 ohm-m) zones in this model that are 3-D

in the their deeper character are not interpreted as crustal fault zones.

The 2-D resistivity model for profile MT7 (Figure 2) shows a northeast trending (Figure 4) conductor (3 to 10 ohm-m) near the southwestern edge of the Carlin trend beneath stations 68 and 69 that is characteristic of a crustal fault zone, which also continues in the upper 2 km. The large 3-D conductive (1 ohm-m) zone from about 0.5 to 15 km depth between the BME and Carlin trends beneath stations 63, 64 and 28A (Figure 2) is characteristic of a geothermal system or a thick section of carbonaceous rocks. The northern edge of the deeper section beneath station 70 within the Carlin trend shows resistive (100 ohm-m) rocks that are characteristic of lower Paleozoics.

The 2-D resistivity model for profile MT5 (Figure 3) shows a northeast trending (Figure 4) conductor (1 to 10 ohm-m) within the BME trend beneath stations 48 and 62 that is characteristic of a crustal fault zone. The western end of the model, within the BME trend, beneath stations 53 and 61 shows resistive (300 ohm-m) rocks that are characteristic of Precambrian rocks that outcrop nearby (Stewart and Carlson, 1976). The central half of the deeper section between the BME and Carlin trends beneath stations 43, 42, and 59 shows resistive (300 ohm-m) rocks that are characteristic of intruded lower Paleozoics in the NNR. Other resistive (30 to 300 ohm-m) rocks beneath stations 60, 58, and 57 are also characteristic of lower Paleozoic rocks. The eastern half of the model shows a northeast trending conductor (10 to 30 ohm-m) within the Carlin trend beneath station 34 and a north-northeast (Figure 4) trending conductor (3 to 30 ohm-m) on the northeastern edge of the Carlin trend beneath station 56 (Figure 3). Both of these conductors, characteristic of crustal fault zones, continue in the upper 2 km. Resistive (30 to 1,000 ohm-m) rocks within the Carlin trend beneath stations 37, 33, 32, and 35 are characteristic of lower Paleozoic rocks. The upper 2 km of section over the entire profile length is dominated by resistive (30 to 1,000 ohm-m) rocks that are characteristic of lower Paleozoic rocks, but also includes shallow conductive (3 to 30 ohm-m) basin fill for Paradise Valley (0.5 km), Kelly Creek basin (1 km) and Boulder Valley (0.5 to 1 km).

The 2-D resistivity model for profile MT9 (Figure 3) shows a north trending (Figure 4) conductor (1 to 10 ohm-m) within the BME trend beneath station 94 that is characteristic of a crustal fault zone. The northeastern half of the model shows two northeast trending (Figure 4) conductors (1 to 30 ohm-m) on the northeast edge of the BME trend beneath stations 48, 49, and 95 (Figure 3). Since the model profile is also trending northeast, these northeast trending conductors are characteristic of and probably sub-parallel to a single crustal fault zone (Figure 7). Resistive (30 to 1,000 ohm-m) rocks within the BME trend beneath stations 90 and 91, in the upper 8 km beneath station 93, northeast of station 49, and in the upper 5 km beneath station 95

(Figure 3), are characteristic of lower Paleozoic rocks. Other conductive (1 to 10 ohm-m) zones in this model that are 3-D in the their deeper character are not interpreted as crustal fault zones. The upper 2 km of section over the entire profile length is dominated by resistive (30 to 1,000 ohm-m) rocks that are characteristic of lower Paleozoic rocks, but also includes shallow conductive (3 to 30 ohm-m) basin fill for Pumpernickel Valley (about 0.4 km) and Kelly Creek basin (about 0.3 to 1 km).

The crustal conductors, in general, are not well constrained laterally due to wide station spacing, giving 2 to 15 km as the overall range of widths (Figures 2, 3, and 7). The shallow (at about 1-km depth) conductors are even less well constrained laterally because the recording frequency is higher. Thus, the shallow conductive inferred fault zones are shown in Figure 6 with narrow and uniform widths. The interpreted electrical property sections also show regional changes in the resistive crust from south to north. Most of the subsurface in the upper 20 km beneath Reese River Valley and southern Boulder Valley (Figure 2) are underlain by rock that is generally more conductive than the subsurface beneath Pumpernickel Valley and northern Boulder Valley (Figure 3). This suggests that either elevated-temperature or high-salinity fluids, alteration, or carbonaceous rocks are more pervasive in the more conductive area (Battle Mountain Heat-Flow High, Figure 2). This implies that the crust beneath these valleys is either more fractured or has more carbonaceous rocks than in the area surveyed along the 41st parallel.

SUMMARY

Strengthening the suggestion of Shawe (1991), MT data collected along five profiles show deep resistivity structures beneath the Battle Mountain-Eureka (BME) and Carlin gold trends in north-central Nevada. These appear consistent with tectonic breaks in the crust that possibly served as channels for hydrothermal fluids. It seems likely that gold deposits along these linear trends were, therefore, controlled by deep regional crustal fault systems.

Two-dimensional resistivity modeling of the magnetotelluric data generally show resistive (30 to 1,000 ohm-m) crustal blocks broken by sub-vertical, two-dimensional, conductive (1 to 10 ohm-m) zones that are indicative of large-scale crustal fault zones. These inferred fault zones are regional in scale, trend northeast-southwest, north-south, and northwest-southeast (Figure 7), and extend to mid-crustal (20 km) depths. The individual conductors are about 2- to 15-km wide, extend from about 1 to 4 km below the surface to about 20 km depth, and show two-dimensional electrical structure. By connecting the locations of similar trending (Figure 4) conductors together, individual regional crustal fault zones within the upper crust can be inferred that range from about 4- to 10-km wide and about 30- to

150-km long (Figure 7). One of these crustal fault zones coincides with the Battle Mountain-Eureka mineral trend.

The interpreted structure from these profiles provide constraints for future geologic interpretations of the genesis of gold deposits along the Carlin and BME trends. The deep regional resistivity structure across the Carlin and BME trends has direct implications for large gold resources in northeastern Nevada. The resistivity structure reveals major crustal structures that are probably related to the deformation and shattering of upper crustal rocks that provided local permeable zones favorable for fluid flow and precipitation of gold ores. This implies that the potential for additional undiscovered deeper-level deposits in the Carlin trend is large.

Acknowledgments. We thank Bruce D. Smith of the U.S. Geological Survey for his helpful comments and suggestions to this report.

REFERENCES CITED

Arehart, G.B., Foland, K.A., Naeser, C.W., and Kesler, S.E., 1993, 40Ar/39Ar, K/Ar, and fission track geochronology of sediment-hosted disseminated gold deposits at Post-Betze, Carlin Trend, northeastern Nevada: Economic Geology, vol. 88, no. 3, p. 622-646.

Bendat, J.S., and Piersol, A.G., 1971, Random Data: Analysis and Measurement Procedures: New York, Wiley Interscience, 407 p.

Dobrin, M.D., and Savit, C.H., 1988, Introduction to Geophysical Prospecting (4th ed.): New York, McGraw-Hill, 867 p.

Eberhart-Phillips, D., Labson, V. F., Stanley, W. D., Michael, A. J. and Rodriguez, B. D., 1990, Preliminary velocity and resistivity models of the Loma Prieta Earthquake region: Geophysical Research Letters, vol. 17, no. 8, pp. 1235-1238.

Eberhart-Phillips, D., Stanley, W. D., Rodriguez, B. D. and Lutter, W. J., 1995, Surface seismic and electrical methods to detect fluids related to faulting: Journal of Geophysical Research, vol. 100, no. B7, pp. 12,919-12,936.

Grauch, V.J.S., Klein, D.P., and Rodriguez, B.D., 1998, Progress on understanding the crustal structure near the Battle Mountain-Eureka mineral trend from geophysical constraints, in Tosdal, R.M., ed., 1998, Contributions to the gold metallogeny of northern Nevada: U.S. Geological Survey Open-File Report 98-338, p. 8-14.

Ilchik, R.P. and Barton, M.D., 1997, An amagmatic origin of Carlin-type gold deposits: Economic Geology, vol. 92, no. 3, p. 269-288.

Keller, G.V., 1987, Rock and mineral properties, in Electromagnetic Methods in Applied Geophysics Theory: M.N. Nabighian, Ed., Society of Exploration Geophysicists, Tulsa, Oklahoma, v. 1, p. 13 51.

Keller, G.V., 1989, Electrical properties, in Carmichael, R.S., Ed., Practical handbook of physical properties of rocks and minerals: CRC Press, Boca Raton, Florida, p. 359-427.

Nelson, P.H. and Anderson, L.A., 1992, Physical properties of ash flow tuff from Yucca Mountain, Nevada: Journal of Geophysical Research, vol. 97, no. B5, p. 6823-6841.

Palacky, G.J., 1987, Resistivity characteristics of geologic targets, in Electromagnetic Methods in Applied Geophysics Theory: M.N. Nabighian, Ed., Society of Exploration Geophysicists, Tulsa, Oklahoma, vol. 1, p. 53 129.

Radtke, A.S., 1985, Geology of the Carlin gold deposit, Nevada: U.S. Geological Survey Professional Paper 1267, 124 p.

Reddy, I.K., Rankin, D., and Phillips, R.J., 1977, Three-dimensional modelling in magnetotelluric and magnetic variational sounding: Geophysics Journal of the Royal Astronomical Society, vol. 51, p. 313-325.

Rodriguez, B. D., Stanley, W. D., and Heran, W. D., 1996a, Deep geoelectric structure for mineral resource assessment in the Payette National Forest, Idaho: U. S. Geological Survey Open-File Report 96-666, 16p.

Rodriguez, B.D., Stanley, W.D., and Williams, J.M., 1996b, Axial structures within the Reelfoot rift delineated with magnetotelluric surveys: U.S. Geological Survey Professional Paper 1538-K, 30 p.

Rodriguez, B.D. and Williams, J.M., 2001, Deep regional resistivity structure across the Battle Mountain-Eureka and Carlin trends, north-central Nevada: U. S. Geological Survey Open-File Report 01-346, 165p.

Sass, J.H., D.D. Blackwell, D.S. Chapman, J.K. Costain, E.R. Decker, L.A. Lawver, and C.A. Swanberg, Heat flow from the crust of the United States, in Physical properties of rocks and minerals, edited by Y.S. Touloukian, W.R. Judd, and R.F. Roy, McGraw-Hill, 503-548, 1981.

Shawe, D.R., 1991, Structurally controlled gold trends imply large gold resources in Nevada, in Geology and ore deposits of the Great Basin, Symposium Proceedings: Raines, G.L., Lisle, R.E., Schafe, R.W., Wilkinson, W.H., Eds., Geological Society of Nevada, Reno, vol. 1, p. 199-212.

Sillitoe, R.H. and Bonham, H.F., 1990, Sediment-hosted gold deposits; distal products of magmatic-hydrothermal systems: Geology, vol. 18, no. 2, p. 157-161.

Stanley, W. D., Hoover, D. B., Sorey, M. L., Rodriguez, B. D. and Heran, W. D., 1991, Electrical geophysical investigations in the Norris-Mammoth corridor, Yellowstone National Park, and the adjacent Corwin Springs Known Geothermal Resources Area, in Sorey, M., ed., Effects of Potential Geothermal Development in the Corwin Springs KGRA, Montana, on the Thermal Features of Yellowstone National Park: Water Resources Division Report on Investigations No. 91-4052, pp. D1-D18, 205 p.

Stanley, W. D., Benz, H. M., Walters, M. A., and Rodriguez, B. D., 1997, Tectonic controls on magmatism and geothermal resources in The Geysers-Clear Lake region, California: integration of new geologic, earthquake tomography, seismicity, gravity and magnetotelluric data: U.S. Geological Survey Open-File Report 97-95, 40 p.

Stewart, J.H. and Carlson, J.E., 1976, Geologic map of north-central Nevada: Nevada Bureau of Mines and Geology Map 50, 250000 scale.

Struhsacker, E.M., Jones, E., and Green, S.M., 1996, Roadside geology and precious-metal mineralization along the I-80 corridor, Reno to Elko, Nevada, in Struhsacker, E.M. and Green, S.M., eds., Geology and ore deposits of the American Cordillera - Field Trip Guidebook Compendium: Geological Society of Nevada, Reno, Nevada, p. 3.

Tosdal, R.M., 1998, Contributions to the gold metallogeny of northern Nevada: U.S. Geological Survey Open-File Report 98-338, 290 p.

Vozoff, K., 1972, The magnetotelluric method in the exploration of sedimentary basins: Geophysics, vol. 37, p. 98-141.

Vozoff, K., 1991, The magnetotelluric method, in Electromagnetic methods in applied geophysics: M.N. Nabighian, Ed., Society of Exploration Geophysicists, Tulsa, Oklahoma, vol. 2, part B, p. 641-711.

Wannamaker, P.E., 1983, Resistivity structure of the northern Basin and Range: Geothermal Resources Council, Special Report No. 13, p. 345-361.

Wannamaker, P.E., Hohmann, G.W. and Ward, S.H., 1984, Magnetotelluric responses of three-dimensional bodies in layered earths: Geophysics, vol. 49, no. 9, p. 1517-1533.

Wannamaker, P.E., Stodt, J. A. and Rijo, L., 1987, PW2D: finite element program for solution of magnetotelluric responses of two-dimensional earth resistivity structure, (User documentation): Earth Science Laboratory, University of Utah Research Institute, Salt Lake City, Utah, 40 p.

Williams, J.M. and Rodriguez, B.D., 2000, Deep electrical geophysical measurements across the Carlin trend, Nevada: U.S. Geological Survey Open-File Report 00-419, 141 p.

Williams, J.M. and Rodriguez, B.D., 2001a, Magnetotelluric data across the Battle Mountain-Eureka and Carlin trends, north of Eureka, Nevada: U.S. Geological Survey Open-File Report 01-168, 135 p.

Williams, J.M. and Rodriguez, B.D., 2001b, Magnetotelluric data across the Battle Mountain-Eureka and Carlin trends, near the 41st parallel, Nevada: U.S. Geological Survey Open-File Report 01-278, 127 p.

Williams, J.M. and Rodriguez, B.D., 2001c, Magnetotelluric data across Boulder Valley and the Humboldt River, Nevada: U.S. Geological Survey Open-File Report 01-279, 124 p.

Williams, J.M. and Rodriguez, B.D., 2001d, Magnetotelluric data across the Battle Mountain-Eureka trend in Pumpernickel Valley and Kelly Creek Basin, Nevada: U.S. Geological Survey Open-File Report 01-316, 94 p.

Williams, J.M. Rodriguez, B.D., and Klein, D.P., 2001a, Magnetotelluric data across the Battle Mountain-Eureka and Carlin trends, north of Cortez, Nevada: U.S. Geological Survey Open-File Report 01-117, 154 p.

Williams, J.M. Rodriguez, B.D., and Klein, D.P., 2001b, Magnetotelluric data across the Battle Mountain-Eureka and Carlin trends, south of Cortez, Nevada: U.S. Geological Survey Open-File Report 01-118, 109 p.

Williams, J.M. Rodriguez, B.D., and Klein, D.P., 2001c, Magnetotelluric data across the Battle Mountain-Eureka and Carlin trends, near Battle Mountain, Nevada: U.S. Geological Survey Open-File Report 01-228, 205 p.

Zoback, M.L., McKee, E.H., Blakely, R.J. and Thompson, G.A., 1994, The northern Nevada rift: Regional tectonomagmatic relations and middle Miocene stress direction: Geological Society of America Bulletin, vol. 106, p. 371-382.

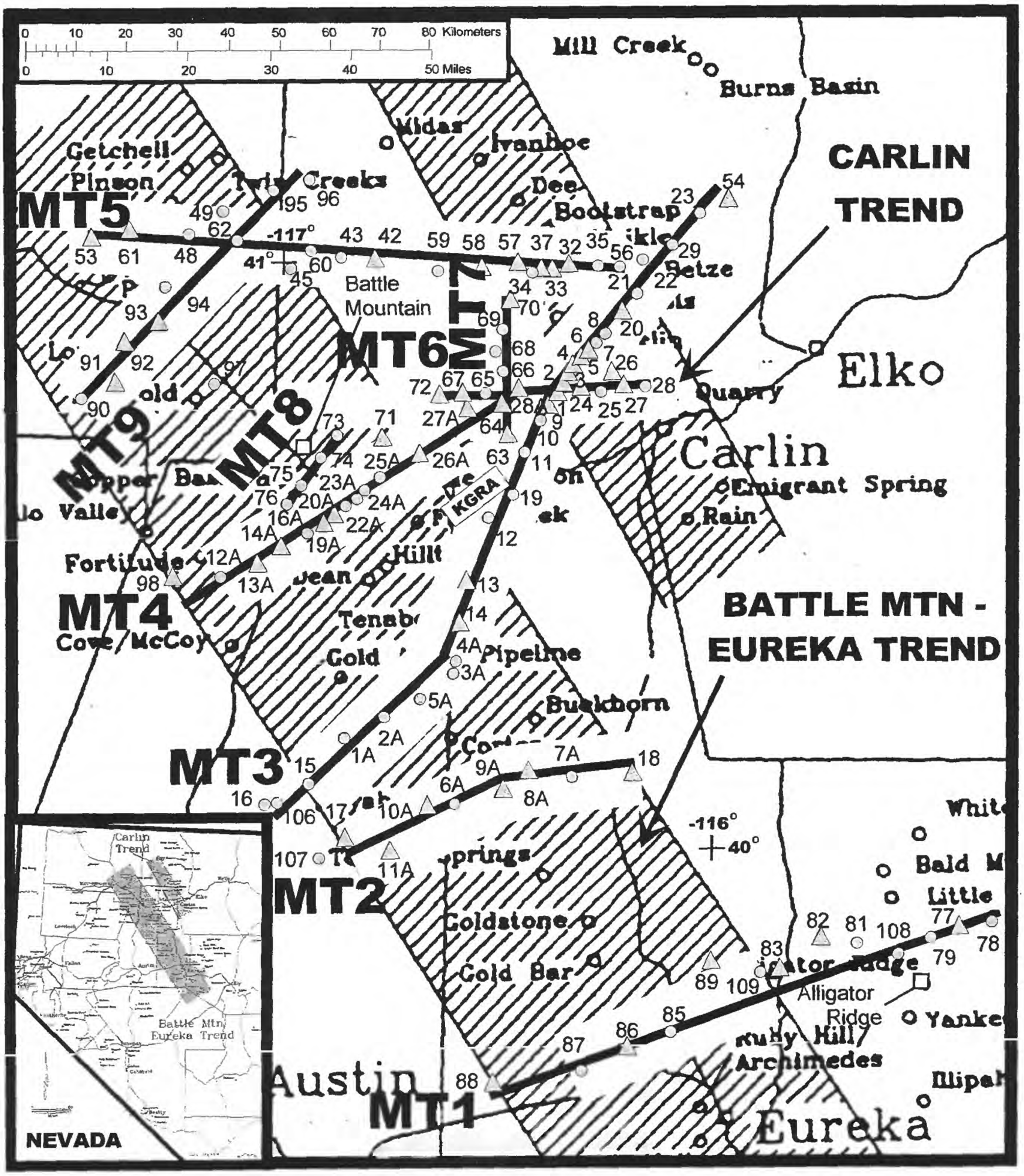

Figure 1. Index map. Magnetotelluric (MT) transects (MT5 to MT9) acquired in 1998, 1999, and 2000. Hatched zones represent two northwest-trending mineralized belts in north-central Nevada, the well-known Carlin trend and the less well-defined Battle Mountain-Eureka trend. The MT stations are shown as gray circles (for data that is 2-D in character) and triangles (for data that is three-dimensional character in the lower frequencies). KGRA is Beowawe Known Geothermal Resource Area. The base map is adapted from Struhsacker and others (1996).

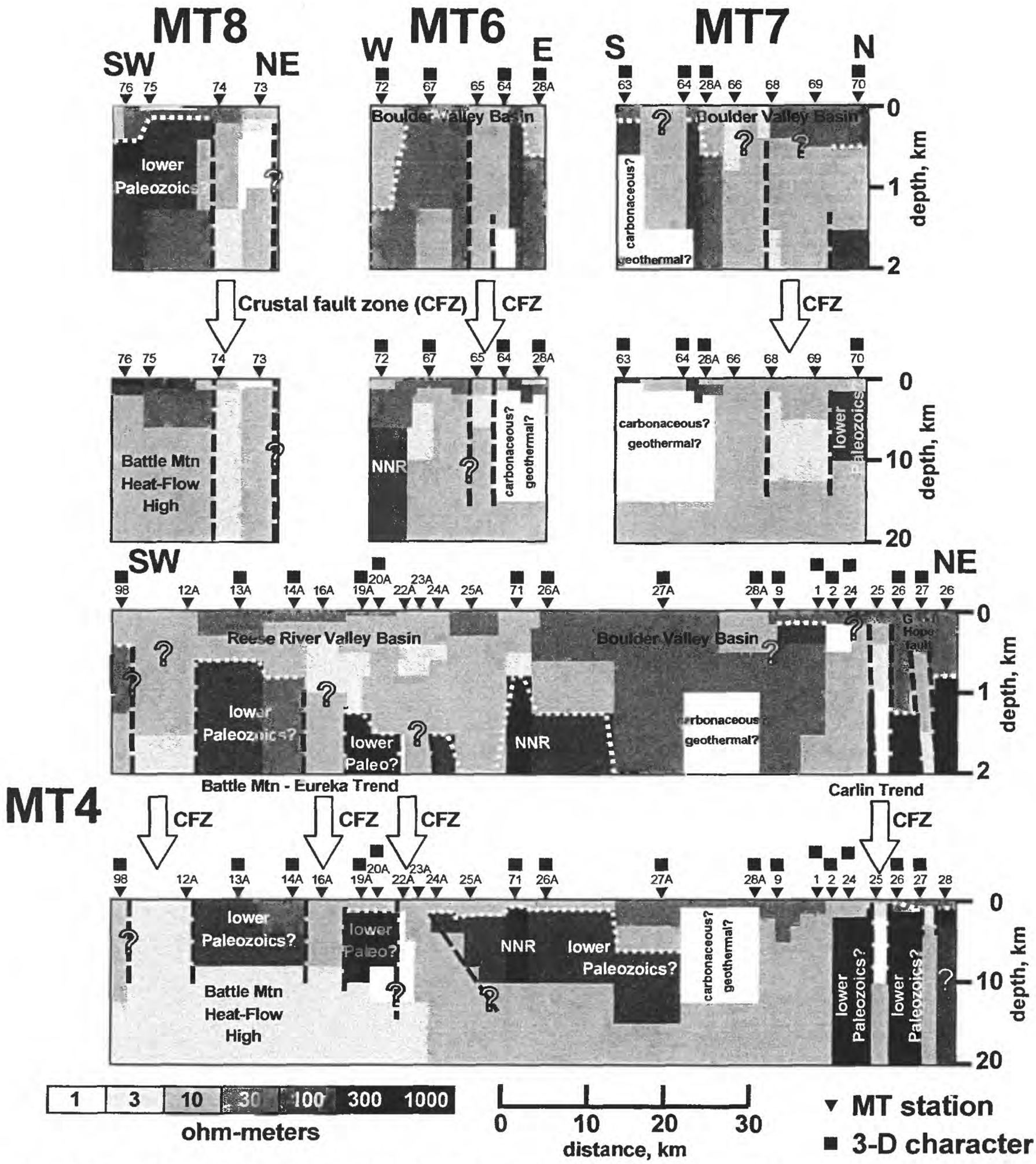

Figure 2. Two-dimensional, resistivity models at 10 times and no vertical exaggeration of MT profiles MT4, MT6, MT7 and MT8. Depths are from ground surface. White arrows mark interpreted crustal fault zones. Black squares show stations whose MT data indicated three-dimensional character at the lower frequencies. Dashed white lines in the upper few kilometers represent estimated basin basement. Dashed black lines outline estimated crustal fault zone (CFZ) boundaries. Question marks indicate less certain definition of fault zone boundaries or basin basement. NNR is Northern Nevada Rift.

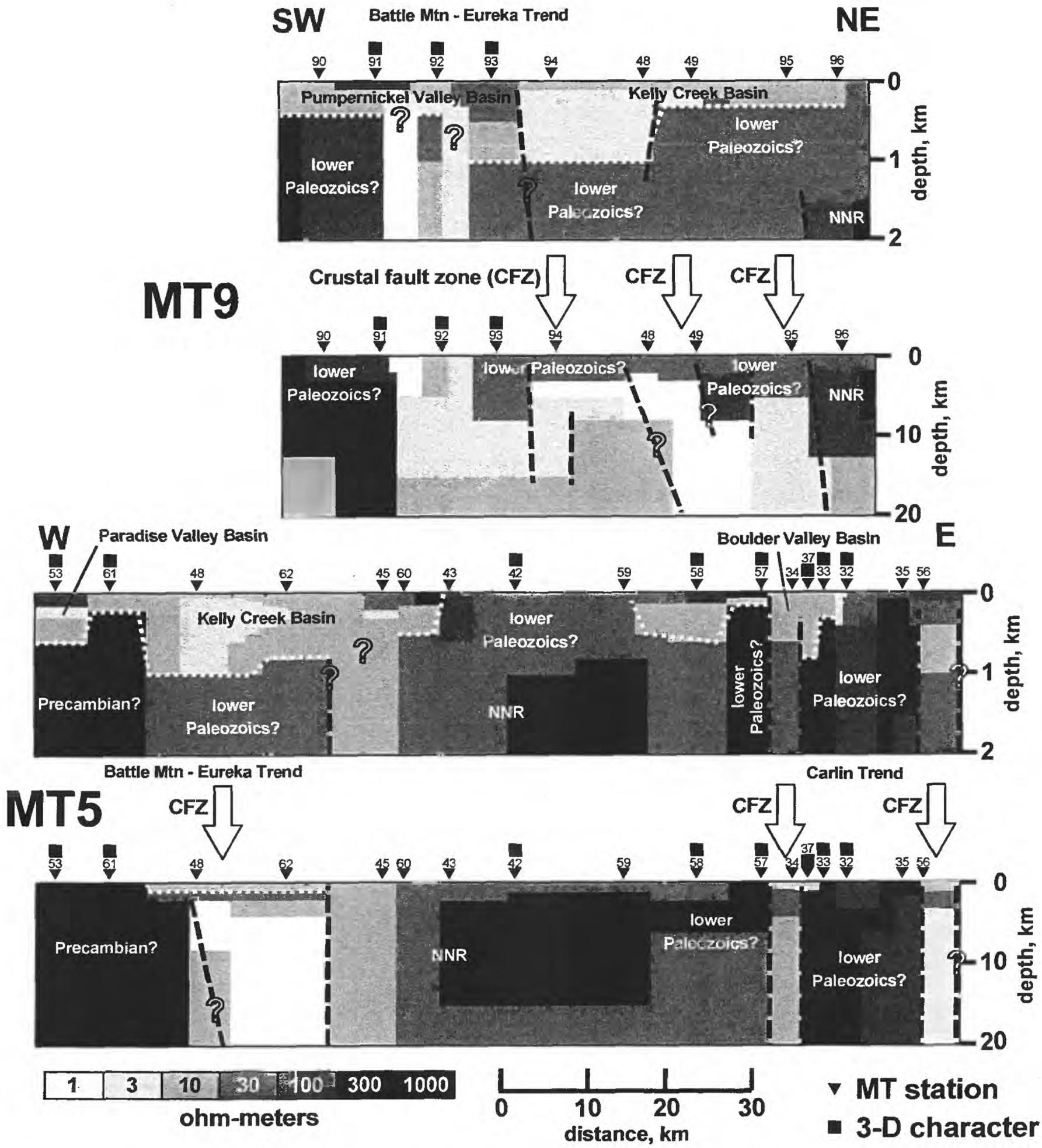

Figure 3. Two-dimensional, resistivity models at 10 times and no vertical exaggeration of MT profiles MT5 and MT9. Depths are from ground surface. White arrows mark interpreted crustal fault zones. Black squares show stations whose MT data indicated three-dimensional character at the lower frequencies. Dashed white lines in the upper few kilometers represent estimated basin basement. Dashed black lines outline estimated crustal fault zone (CFZ) boundaries. Question marks indicate less certain definition of fault zone boundaries or basin basement. NNR is Northern Nevada Rift.

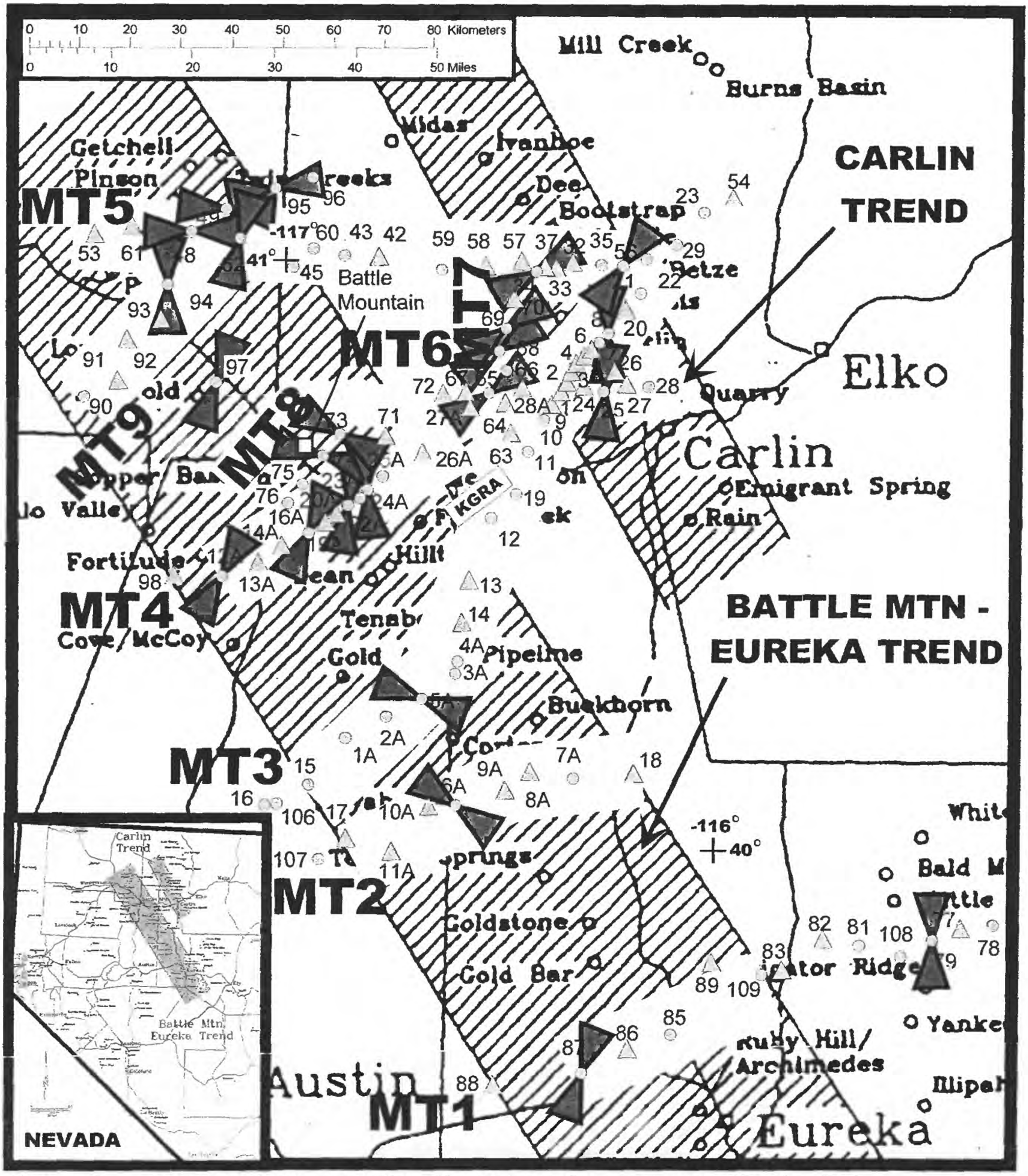

Figure 4. Deep conductor strike directions for magnetotelluric (MT) transects MT1 to MT9 acquired from 1994 to 2000. Hatched zones represent two northwest-trending mineralized belts in north-central Nevada, the well-known Carlin trend and the less well-defined Battle Mountain-Eureka trend. The MT stations are shown as gray circles (for data that is 2-D in character) and triangles (for data that is three-dimensional character in the lower frequencies). Bow-tie symbols show estimated 2-D strike directions for 2-D conductors at about 10-km below the ground surface. MT strike resolution is about ±20 degrees. The base map is adapted from Struhsacker and others (1996).

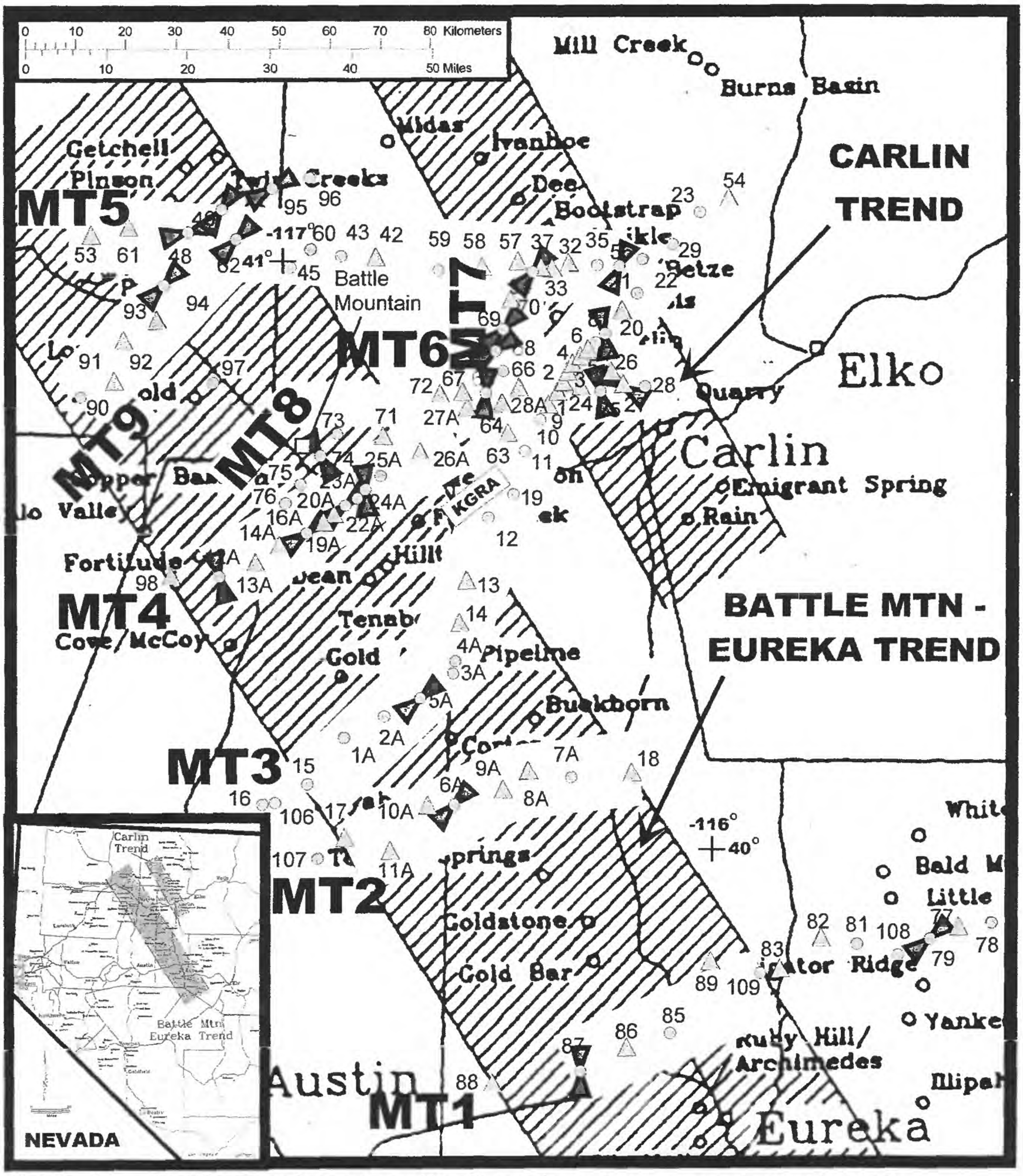

Figure 5. Shallow conductor strike directions for magnetotelluric (MT) transects MT1 to MT9 acquired from 1994 to 2000. Hatched zones represent two northwest-trending mineralized belts in north-central Nevada, the well-known Carlin trend and the less well-defined Battle Mountain-Eureka trend. The MT stations are shown as gray circles (for data that is 2-D in character) and triangles (for data that is three-dimensional character in the lower frequencies). Bow-tie symbols show estimated 2-D strike directions for 2-D conductors at about 1-km below the ground surface. MT strike resolution is about ±20 degrees. The base map is adapted from Struhsacker and others (1996).

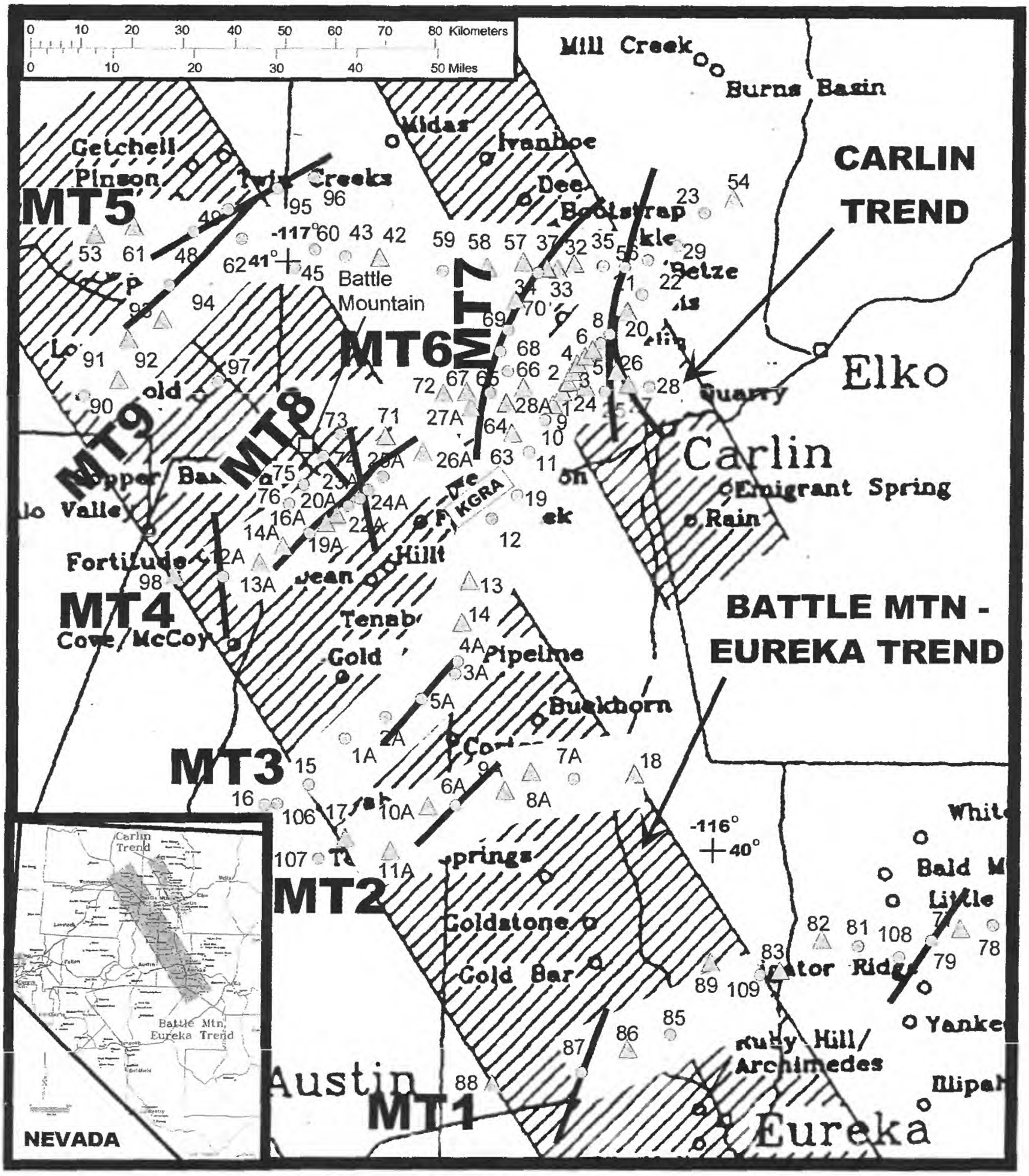

Figure 6. Shallow fault zones defined by magnetotelluric (MT) transects MT1 to MT9 acquired from 1994 to 2000. Hatched zones represent two northwest-trending mineralized belts in north-central Nevada, the well-known Carlin trend and the less well-defined Battle Mountain-Eureka trend. The MT stations are shown as gray circles (for data that is 2-D in character) and triangles (for data that is three-dimensional character in the lower frequencies). Interpreted fault zones, shown by black lines are based on the locations of the shallow sub-vertical 2-D conductors at about 1-km below the ground surface. The base map is adapted from Struhsacker and others (1996).

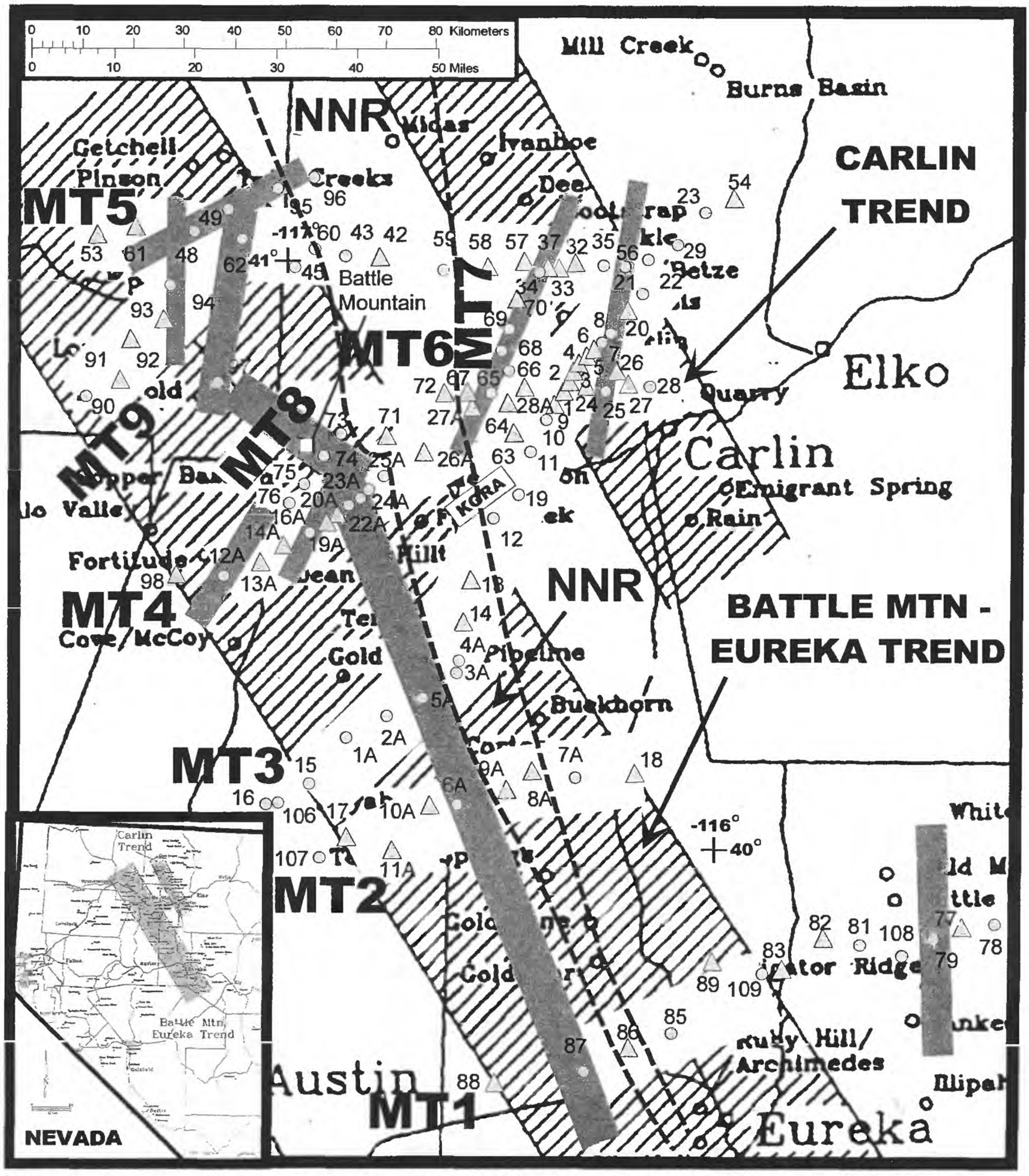

Figure 7. Deep crustal fault zones defined by magnetotelluric (MT) transects MT1 to MT9 acquired from 1994 to 2000. Hatched zones represent two northwest-trending mineralized belts in north-central Nevada, the well-known Carlin trend and the less well-defined Battle Mountain-Eureka trend. The MT stations are shown as gray circles (for data that is 2-D in character) and triangles (for data that is three-dimensional character in the lower frequencies). Interpreted crustal fault zones, shown by 4- to 10-km wide gray swaths are based on the locations and lateral extents of the deep sub-vertical 2-D conductors (see Figures 2 and 3. Dashed black line is outline of northern Nevada rift (Zoback and others, 1994). The base map is adapted from Struhsacker and others (1996).

APPENDIX A

OBSERVED AND CALCULATED DATA - PROFILE MT5

Magnetotelluric (MT) observed (circle and x symbols) and calculated (solid and dashed lines are TE and TM modes, respectively) resistivity and phase data for profile MT5. See the "Magnetotelluric Data" section of this report for a description of the observed data and the "Resistivity Models" section for a description of the calculated data.

Station 53

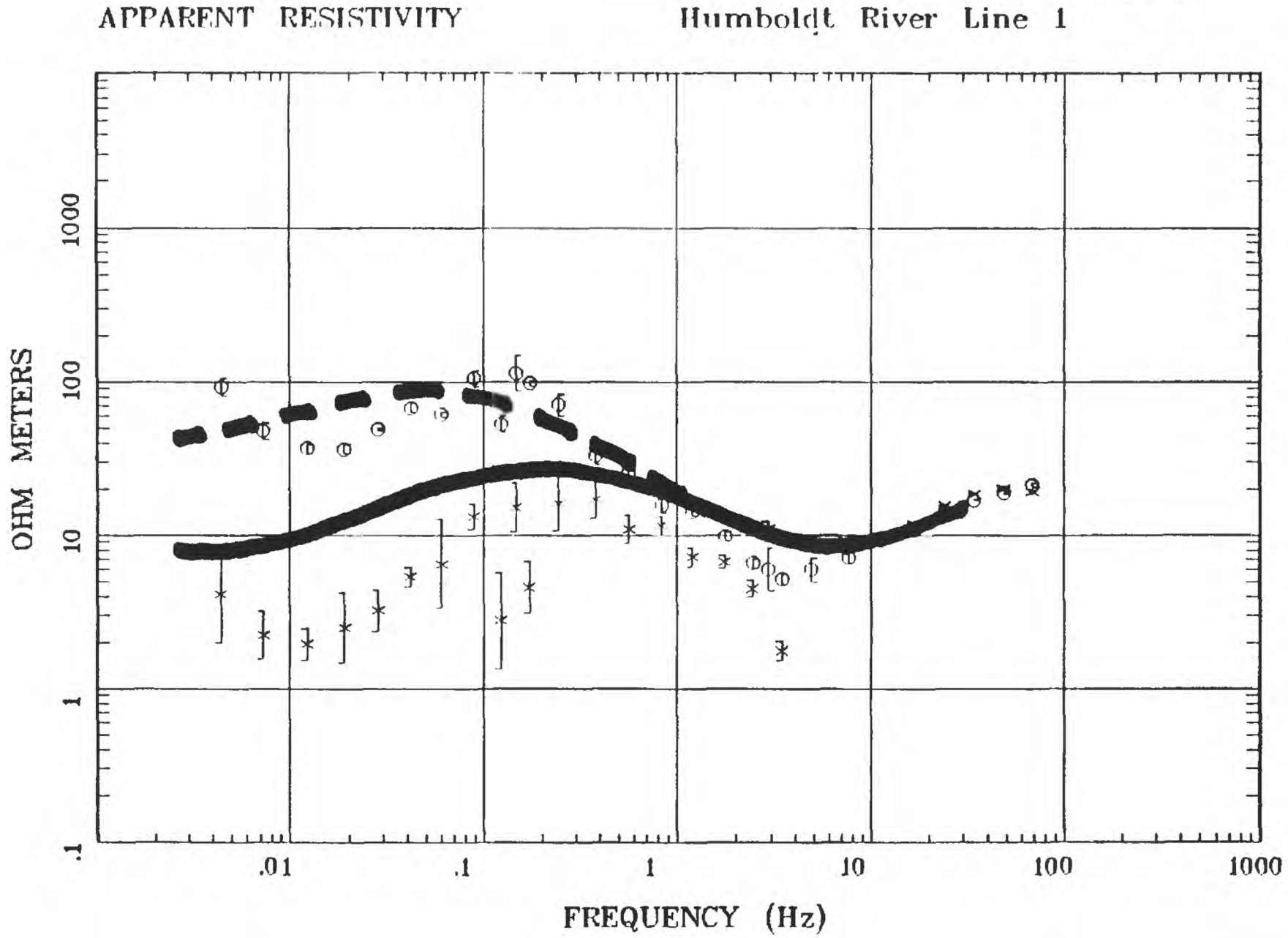

Client:
Remote: Local B
Acquired: 10:1 Jul 30, 1998
Survey Co:USGS GD-MRP Denver

Rotation:
Filename: hr53all.avg
Channels: Ch1 Ch2 Ch3 Ch4 Ch5 Ch8 Ch9
Plotted: 13:55 Dec 07, 2000
< EMI - ElectroMagnetic Instruments >

Station 53

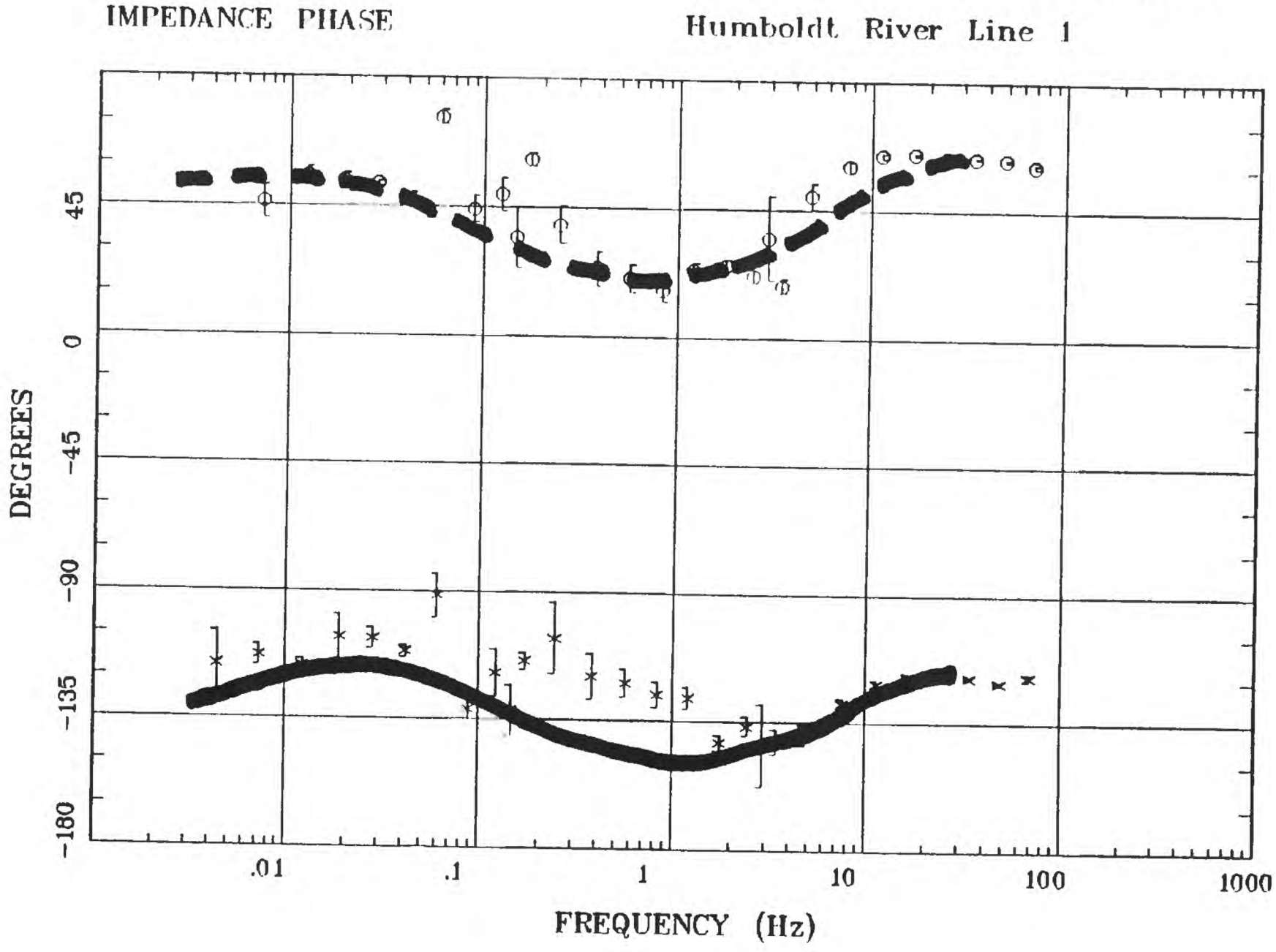

Client:
Remote: Local B
Acquired: 10:1 Jul 30, 1998
Survey Co:USGS GD-MRP Denver

Rotation:
Filename: hr53all.avg
Channels: Ch1 Ch2 Ch3 Ch4 Ch5 Ch8 Ch9
Plotted: 13:55 Dec 07, 2000
< EMI - ElectroMagnetic Instruments >

Station 61

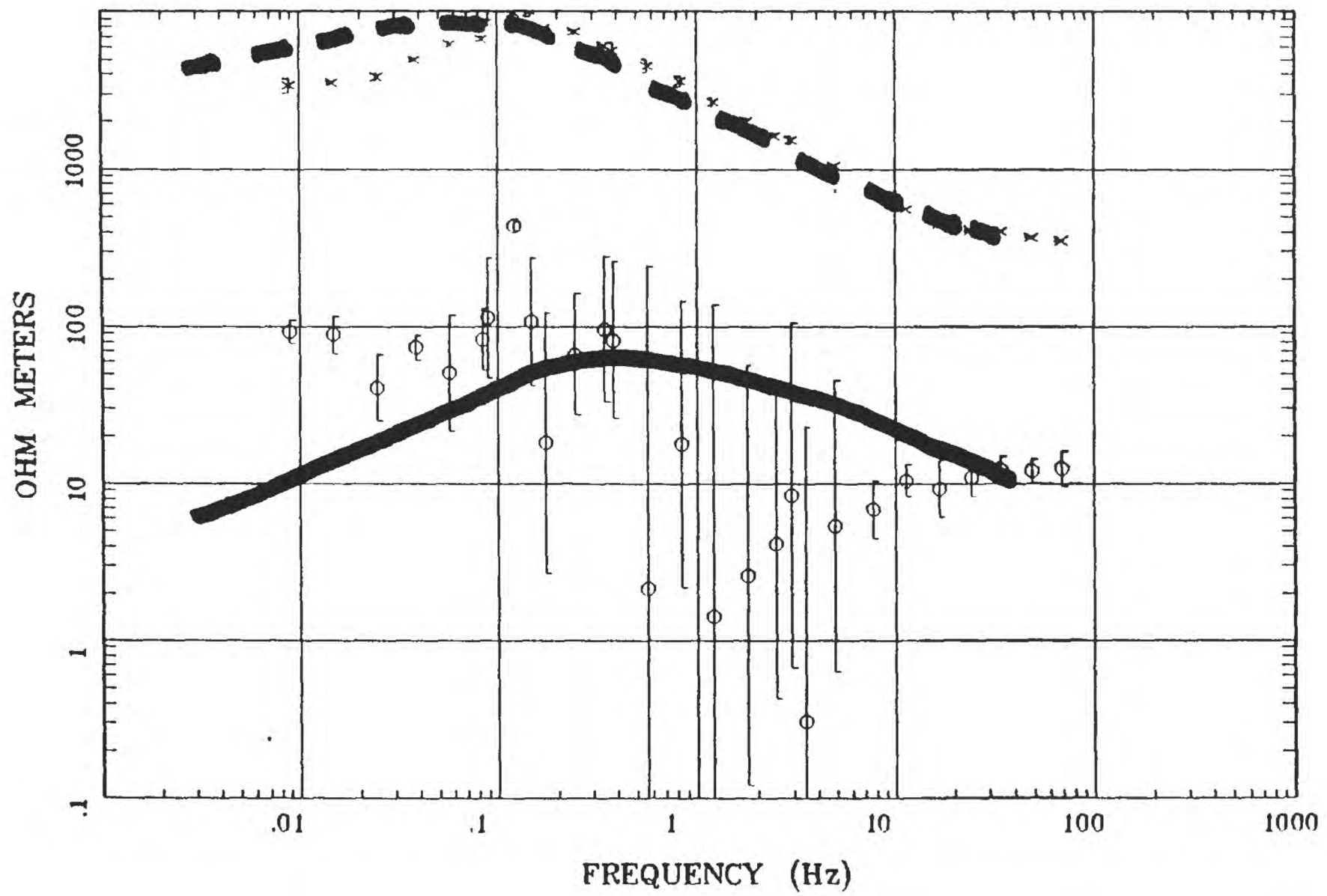

Client:
Remote: Local B
Acquired: 09:5 Aug 07, 1998
Survey Co:USGS GD-MRP Denver

Rotation:
Filename: hr61.avg
Channels: Ch1 Ch2 Ch3 Ch4 Ch5 Ch8 Ch9
Plotted: 14:04 Dec 07, 2000
< EMI - ElectroMagnetic Instruments >

Station 61

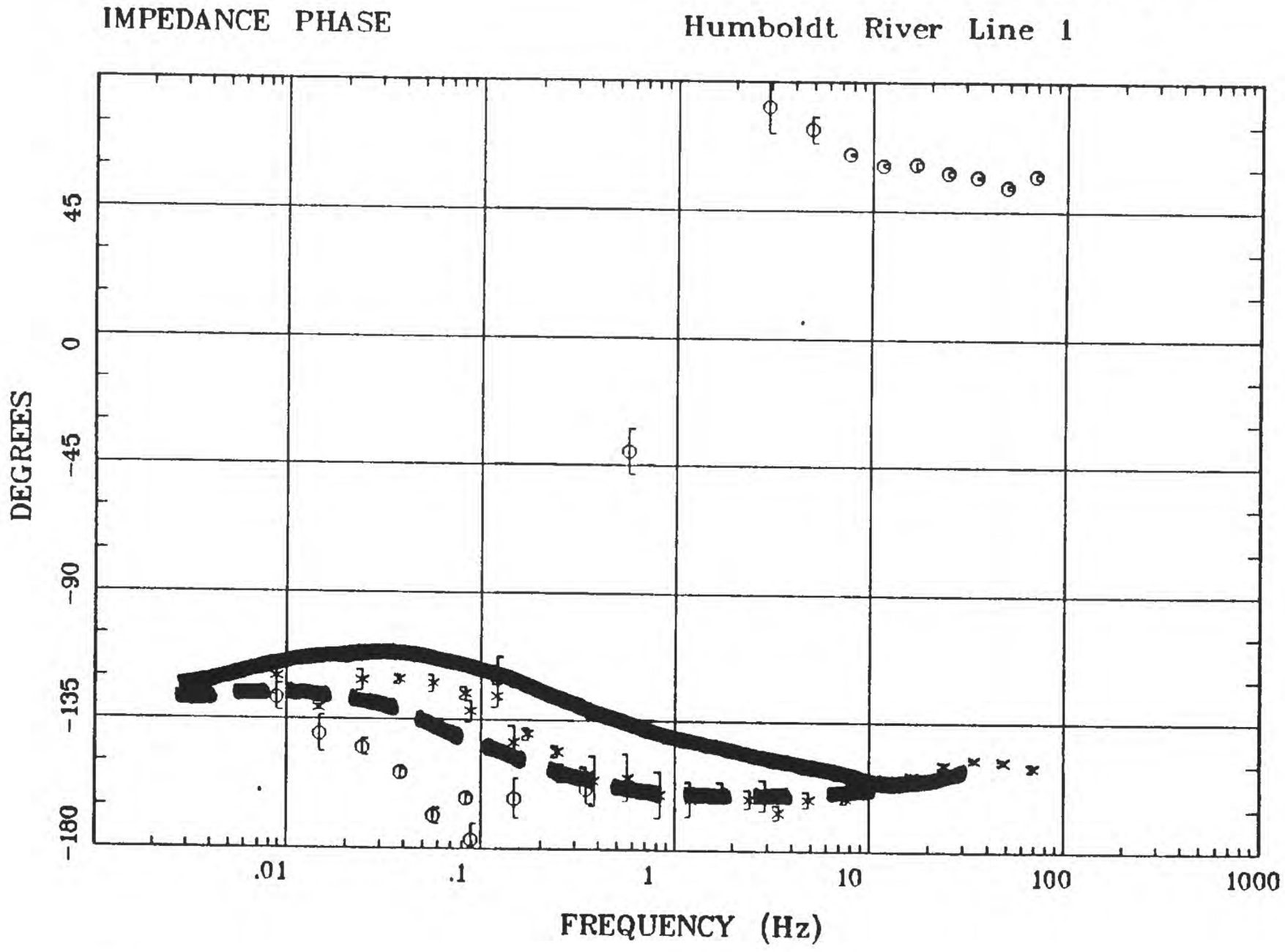

Client:
Remote: Local B
Acquired: 09:5 Aug 07, 1998
Survey Co:USGS GD-MRP Denver

Rotation:
Filename: hr61.avg
Channels: Ch1 Ch2 Ch3 Ch4 Ch5 Ch8 Ch9
Plotted: 14:04 Dec 07, 2000
< EMI - ElectroMagnetic Instruments >

Station 48

APPARENT RESISTIVITY Osgood Mtns, NV 100K

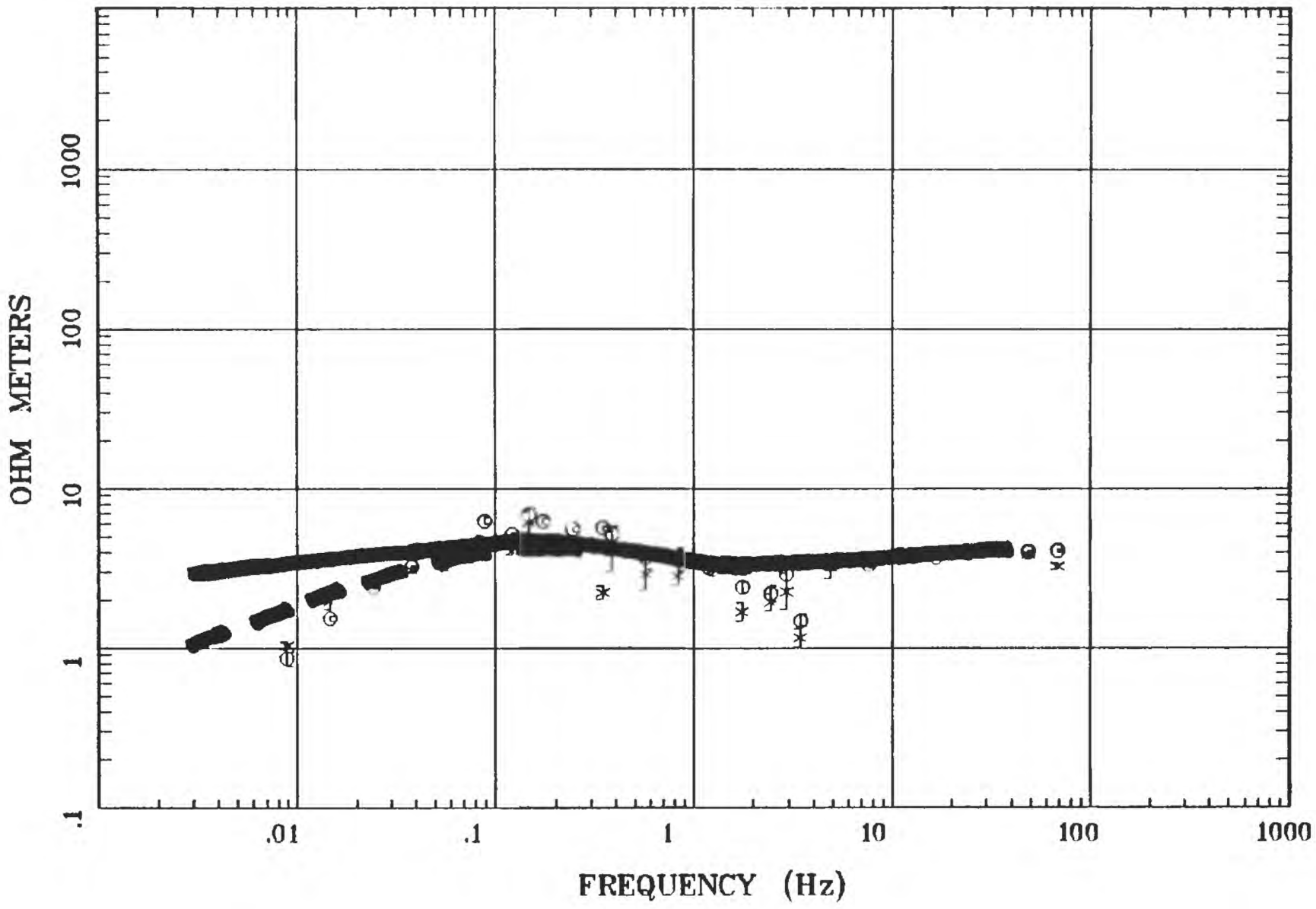

Client:
Remote: none
Acquired: 10:4 Jul 22, 2000
Survey Co:USGS

Rotation:
Filename: hr48c.avg
Channels: Ch1 Ch2 Ch3 Ch4 Ch5 Ch3 Ch4
Plotted: 11:05 Feb 06, 2001
< EMI - ElectroMagnetic Instruments >

Station 48

IMPEDANCE PHASE Osgood Mtns, NV 100K

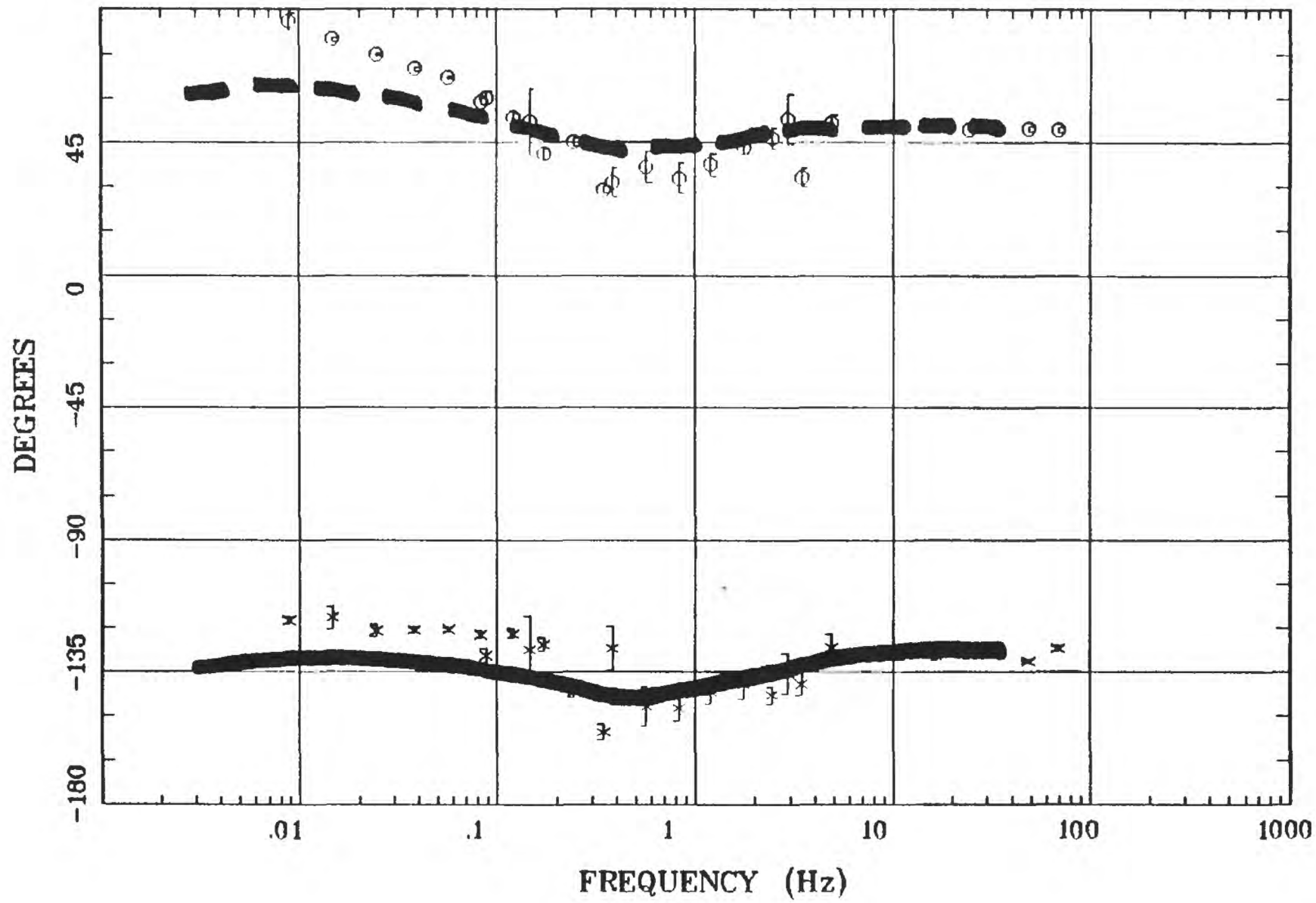

Client:
Remote: none
Acquired: 10:4 Jul 22, 2000
Survey Co:USGS

Rotation:
Filename: hr48c.avg
Channels: Ch1 Ch2 Ch3 Ch4 Ch5 Ch3 Ch4
Plotted: 11:05 Feb 06, 2001
< EMI - ElectroMagnetic Instruments >

Station 62

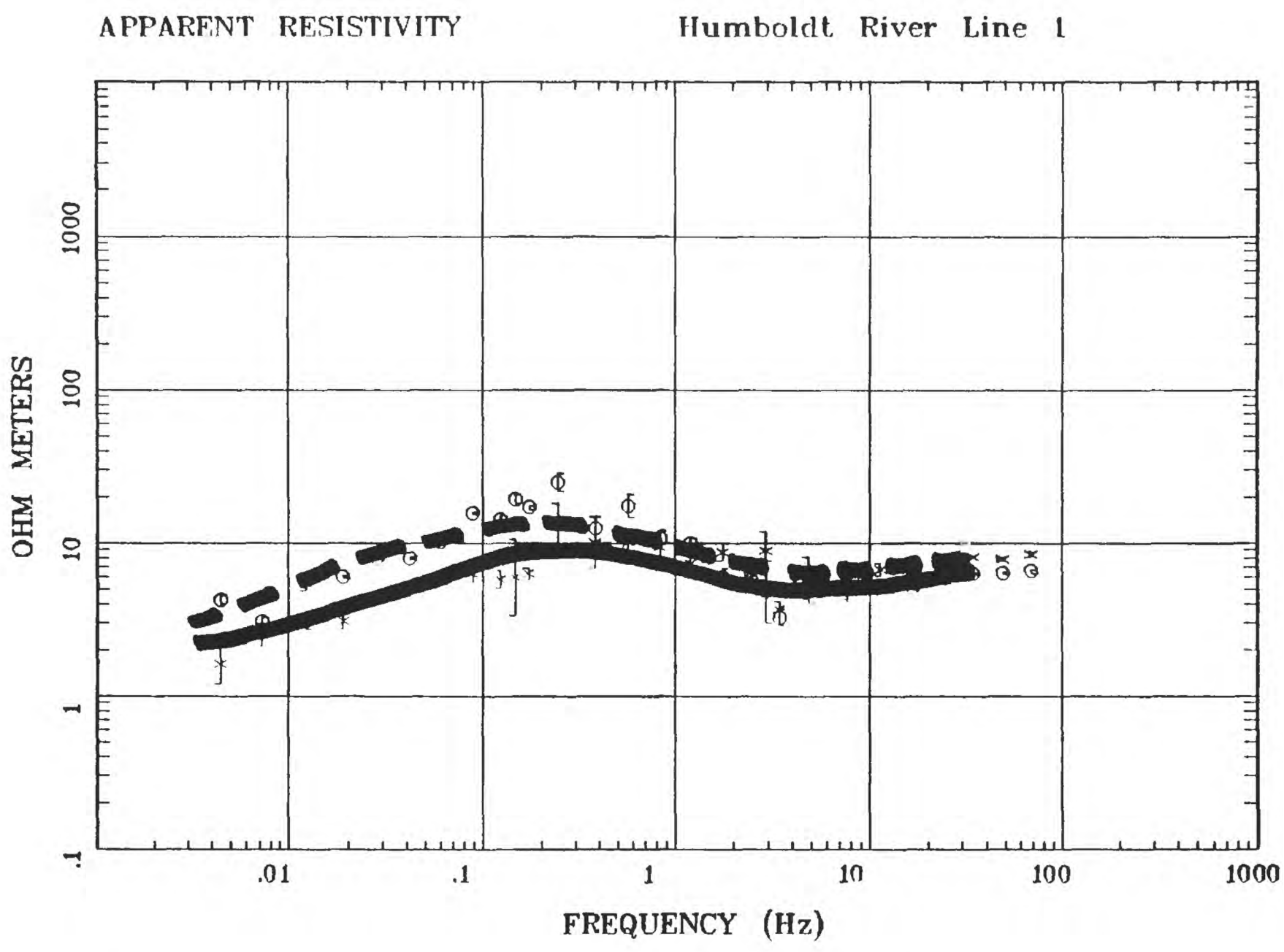

Client:
Remote: Local B
Acquired: 14:5 Aug 07, 1998
Survey Co:USGS GD-MRP Denver

Rotation:
Filename: hr62.avg
Channels: Ch1 Ch2 Ch3 Ch4 Ch5 Ch8 Ch9
Plotted: 14:04 Dec 07, 2000
< EMI - ElectroMagnetic Instruments >

Station 62

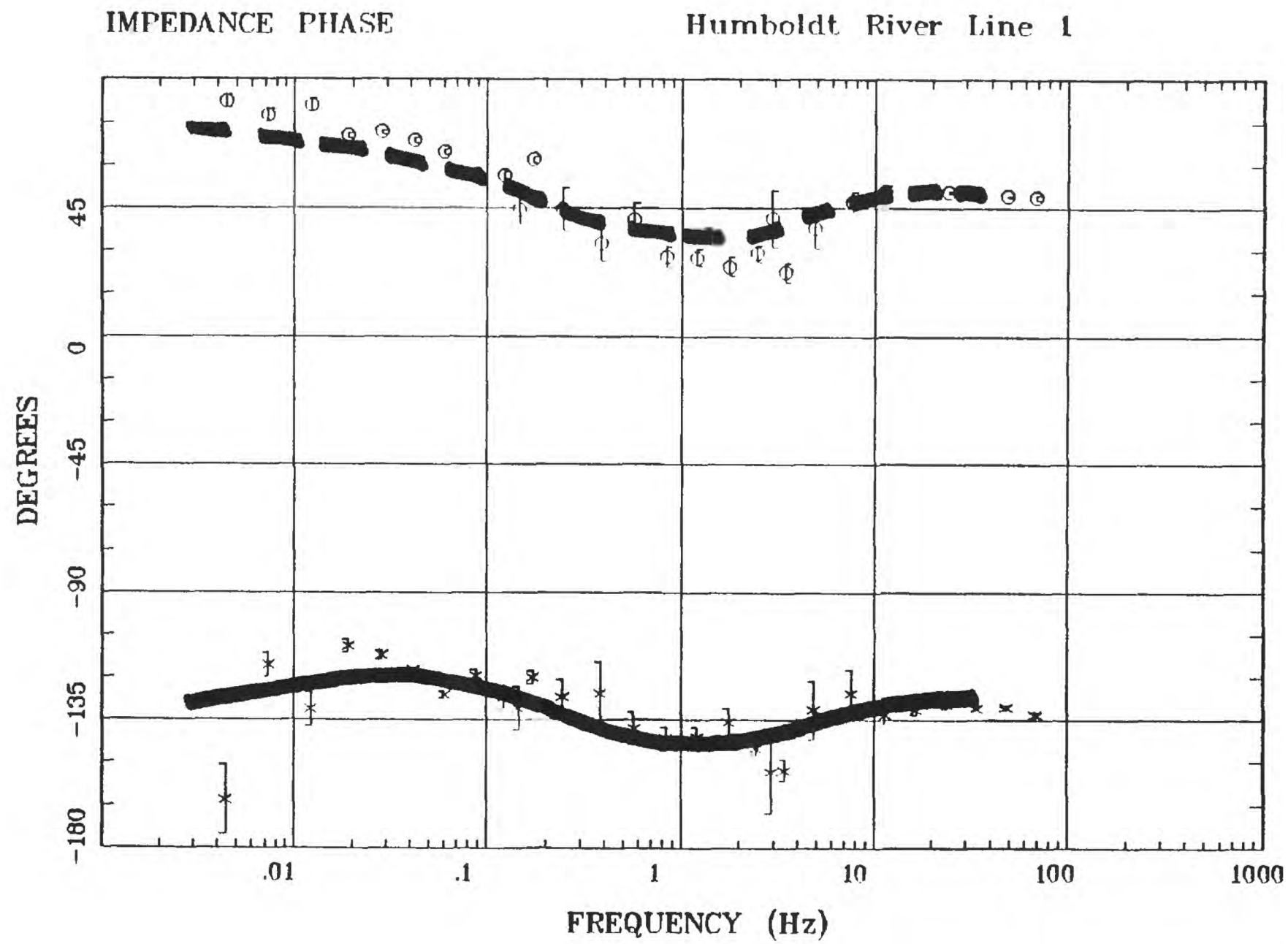

Client:
Remote: Local B
Acquired: 14:5 Aug 07, 1998
Survey Co:USGS GD-MRP Denver

Rotation:
Filename: hr62.avg
Channels: Ch1 Ch2 Ch3 Ch4 Ch5 Ch8 Ch9
Plotted: 14:04 Dec 07, 2000
< EMI - ElectroMagnetic Instruments >

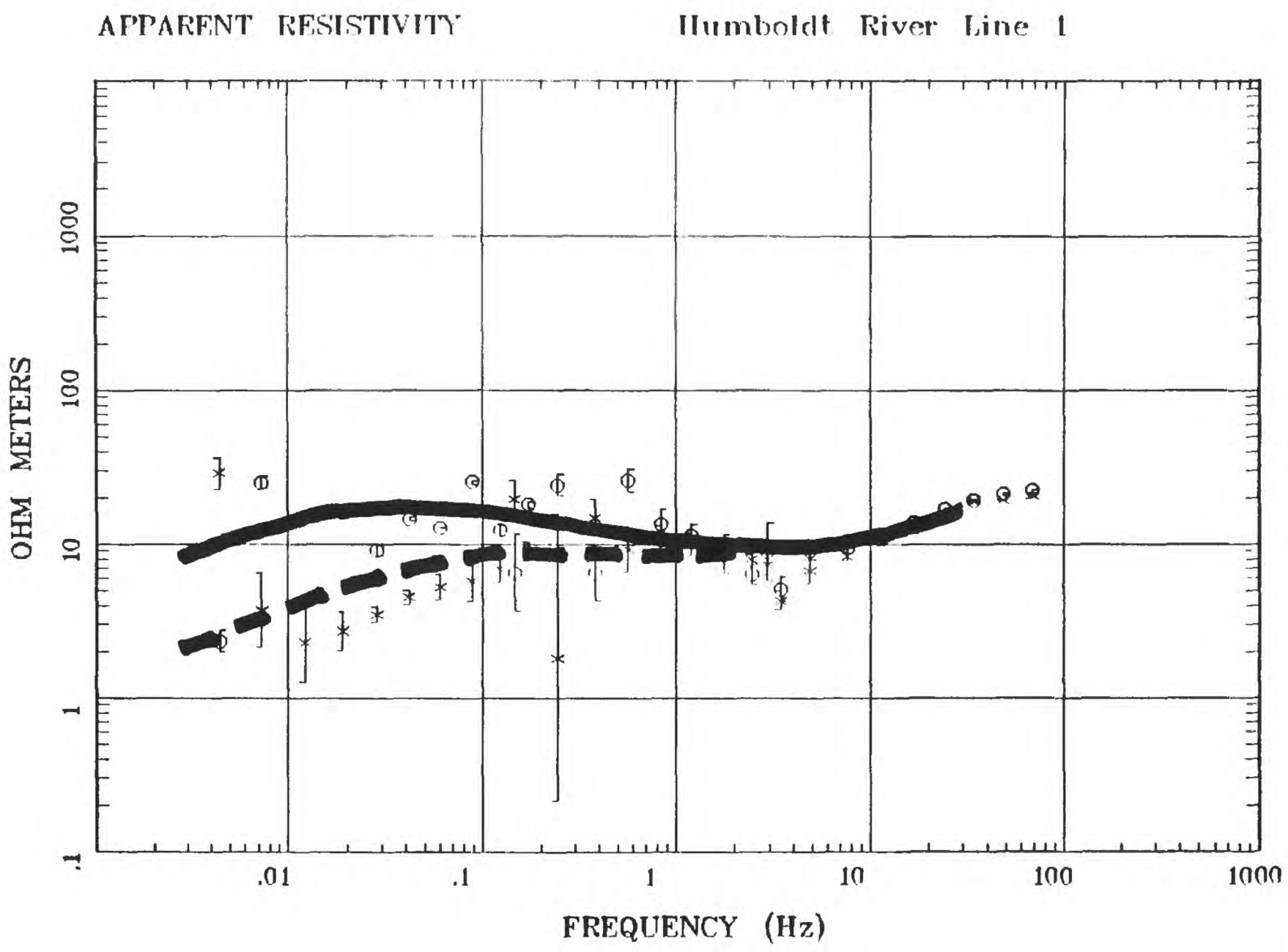

Client:
Remote: Local B
Acquired: 14:5 Aug 05, 1998
Survey Co:USGS GD-MRP Denver

Rotation:
Filename: hr45.avg
Channels: Ch1 Ch2 Ch3 Ch4 Ch5 Ch8 Ch9
Plotted: 13:53 Dec 07, 2000
< EMI - ElectroMagnetic Instruments >

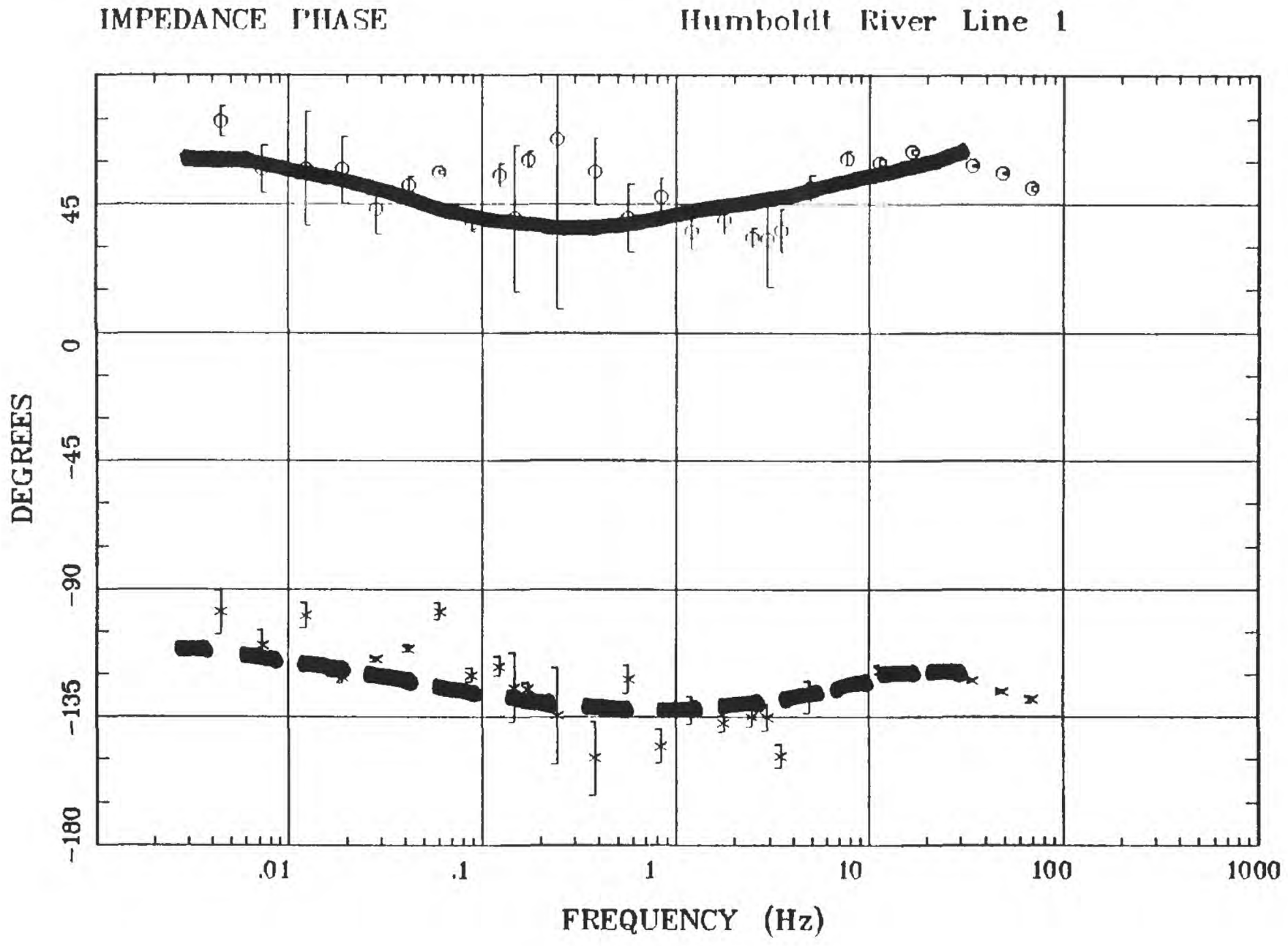

Client:
Remote: Local B
Acquired: 14:5 Aug 05, 1998
Survey Co:USGS GD-MRP Denver

Rotation:
Filename: hr45.avg
Channels: Ch1 Ch2 Ch3 Ch4 Ch5 Ch8 Ch9
Plotted: 13:53 Dec 07, 2000
< EMI - ElectroMagnetic Instruments >

Station 60

APPARENT RESISTIVITY Humboldt River Line 1

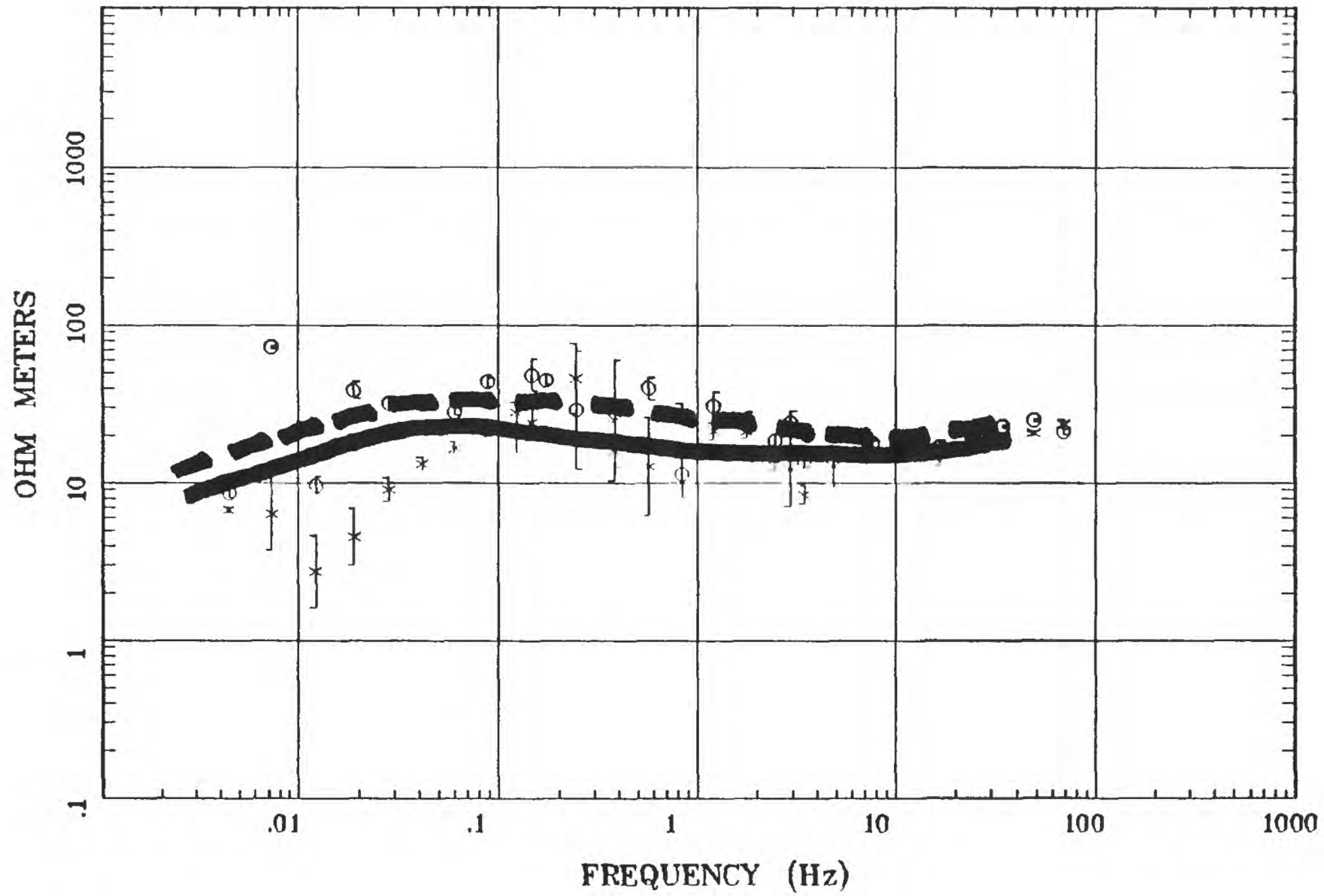

Client:
Remote: Local B
Acquired: 11:0 Aug 06, 1998
Survey Co:USGS GD-MRP Denver

Rotation:
Filename: hr60.avg
Channels: Ch1 Ch2 Ch3 Ch4 Ch5 Ch8 Ch9
Plotted: 14:03 Dec 07, 2000
< EMI - ElectroMagnetic Instruments >

Station 60

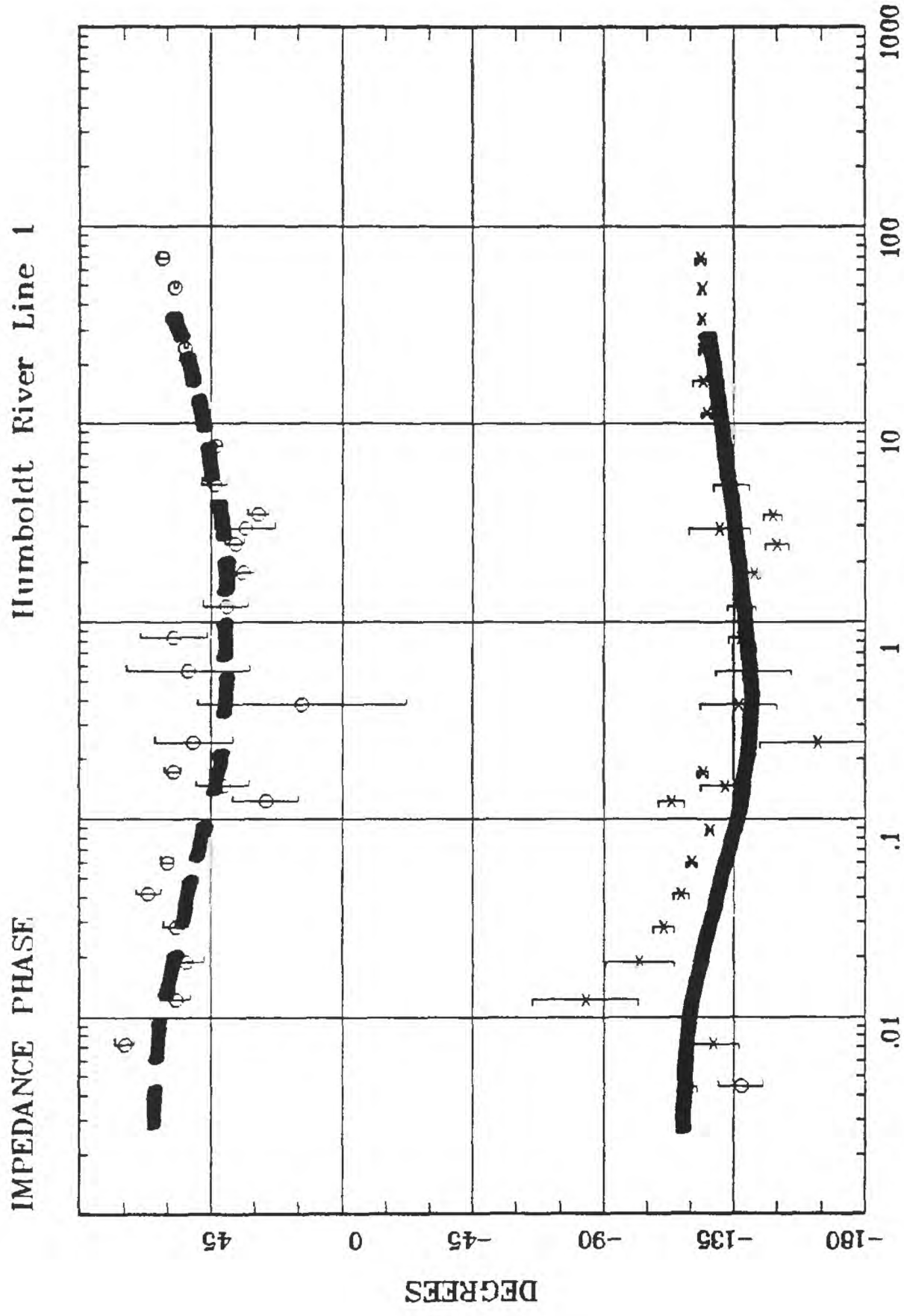
Humboldt River Line 1
IMPEDANCE PHASE
DEGREES
45
0
-45
-90
-135
-180
.01
.1
1
10
100
1000
FREQUENCY (Hz)
Rotation:
Filename: hr60.avg
Channels: Ch1 Ch2 Ch3 Ch4 Ch5 Ch8 Ch9
Plotted: 14:03 Dec 07, 2000
< EMI - ElectroMagnetic Instruments >
Client:
Remote: Local B
Acquired: 11:0 Aug 06, 1998
Survey Co:USGS GD-MRP Denver

Station 43

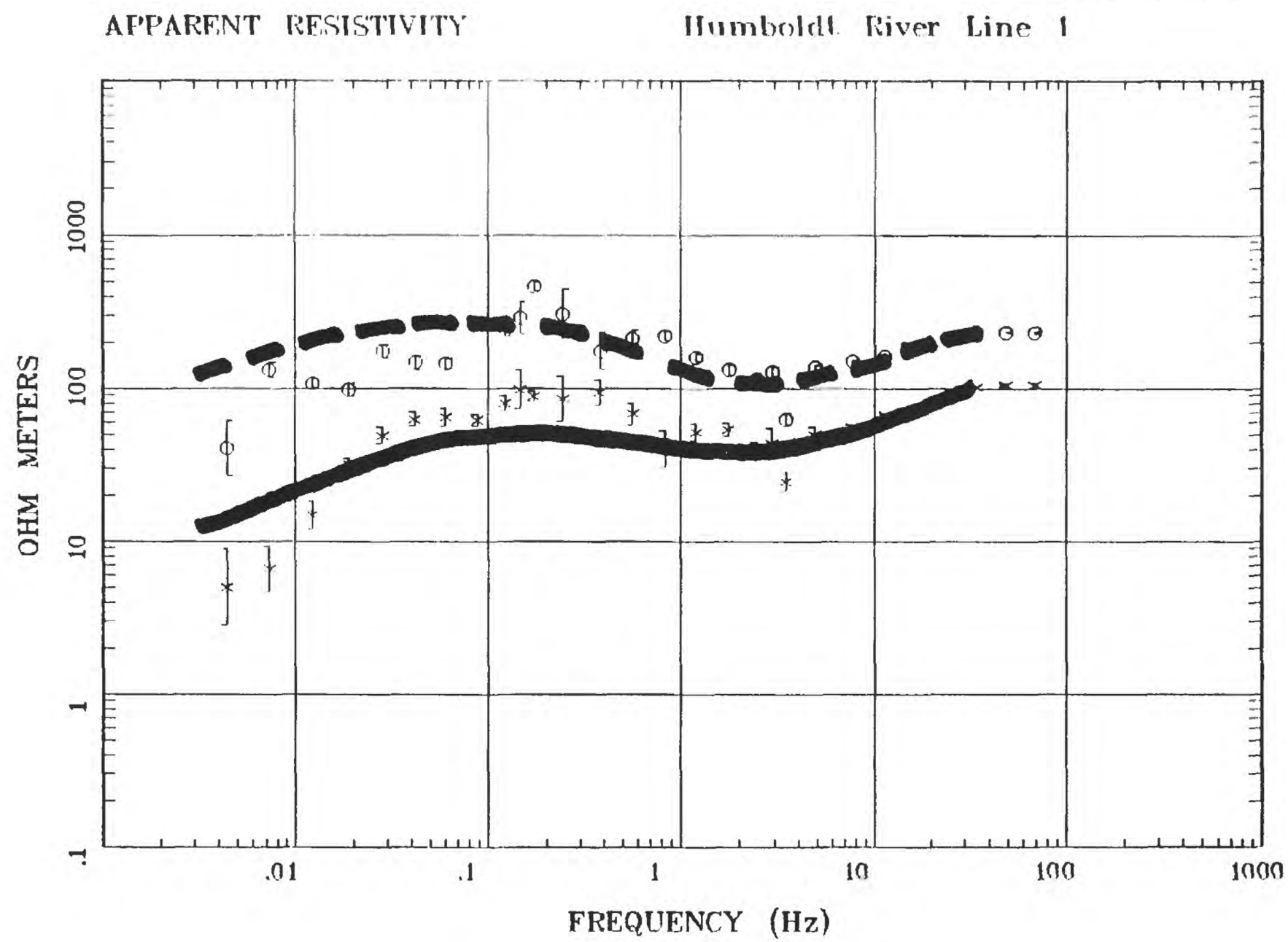

Client:
Remote: Local B
Acquired: 10:2 Aug 05, 1998
Survey Co:USGS GD-MRP Denver

Rotation:
Filename: hr43.avg
Channels: Ch1 Ch2 Ch3 Ch4 Ch5 Ch8 Ch9
Plotted: 13:52 Dec 07, 2000
< EMI - ElectroMagnetic Instruments >

Station 43

IMPEDANCE PHASE — Humboldt River Line 1

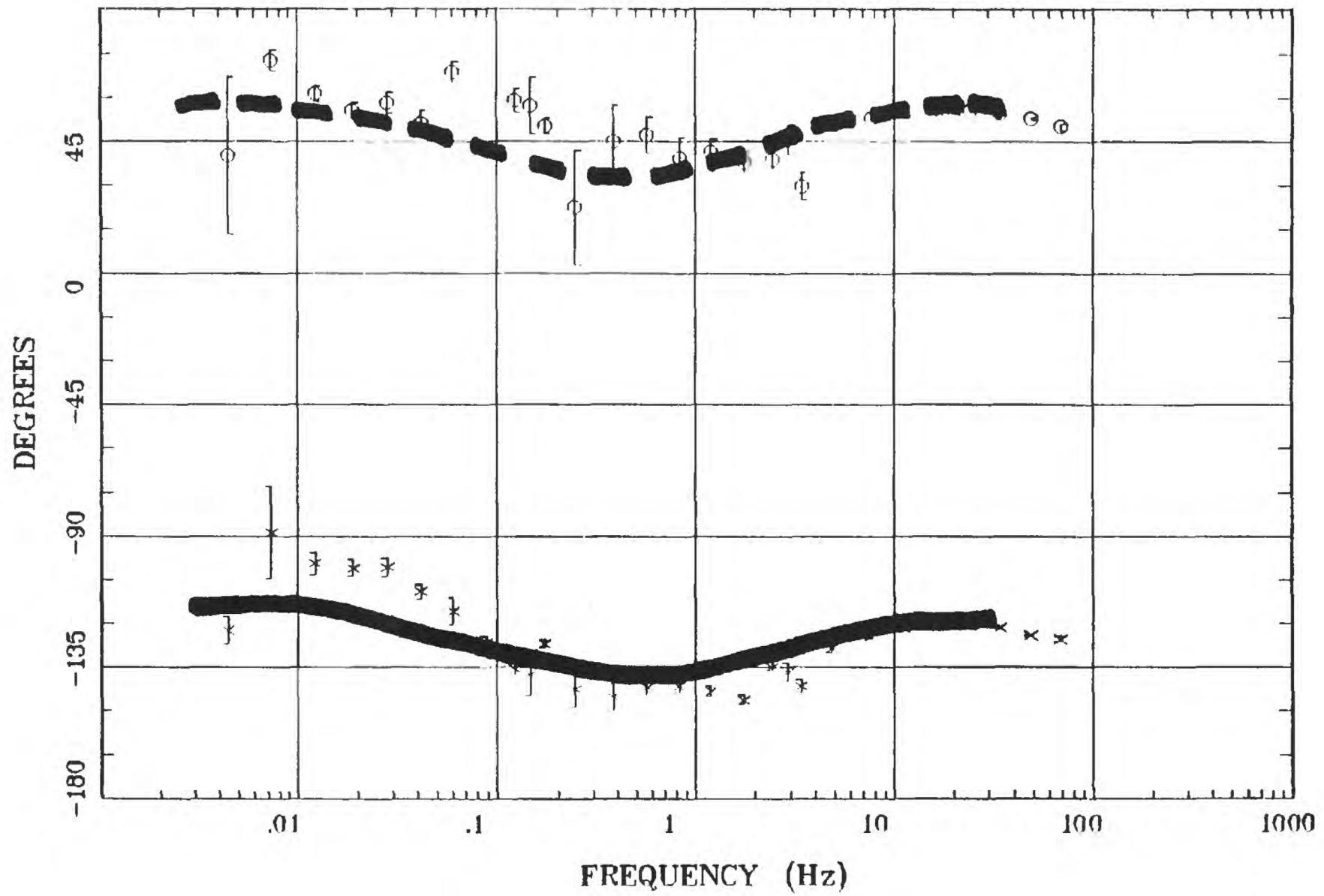

Client:
Remote: Local B
Acquired: 10:2 Aug 05, 1998
Survey Co:USGS GD-MRP Denver

Rotation:
Filename: hr43.avg
Channels: Ch1 Ch2 Ch3 Ch4 Ch5 Ch8 Ch9
Plotted: 13:52 Dec 07, 2000
< EMI - ElectroMagnetic Instruments >

Station 42

APPARENT RESISTIVITY Humboldt River Line 1

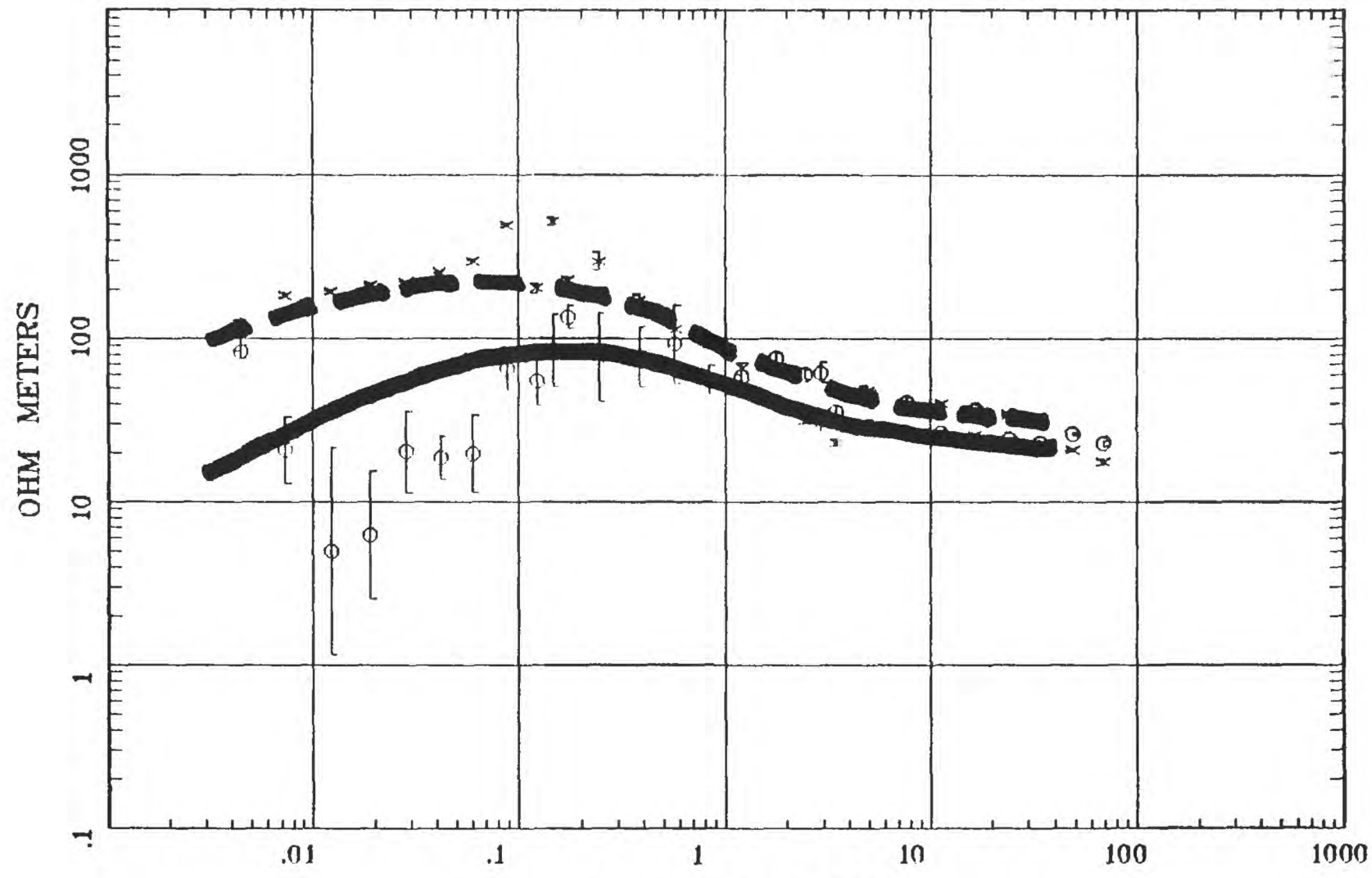

Client:
Remote: Local B
Acquired: 13:4 Aug 04, 1998
Survey Co:USGS GD-MRP Denver

Rotation:
Filename: hr42.avg
Channels: Ch1 Ch2 Ch3 Ch4 Ch5 Ch8 Ch9
Plotted: 13:50 Dec 07, 2000
< EMI - ElectroMagnetic Instruments >

Station 42

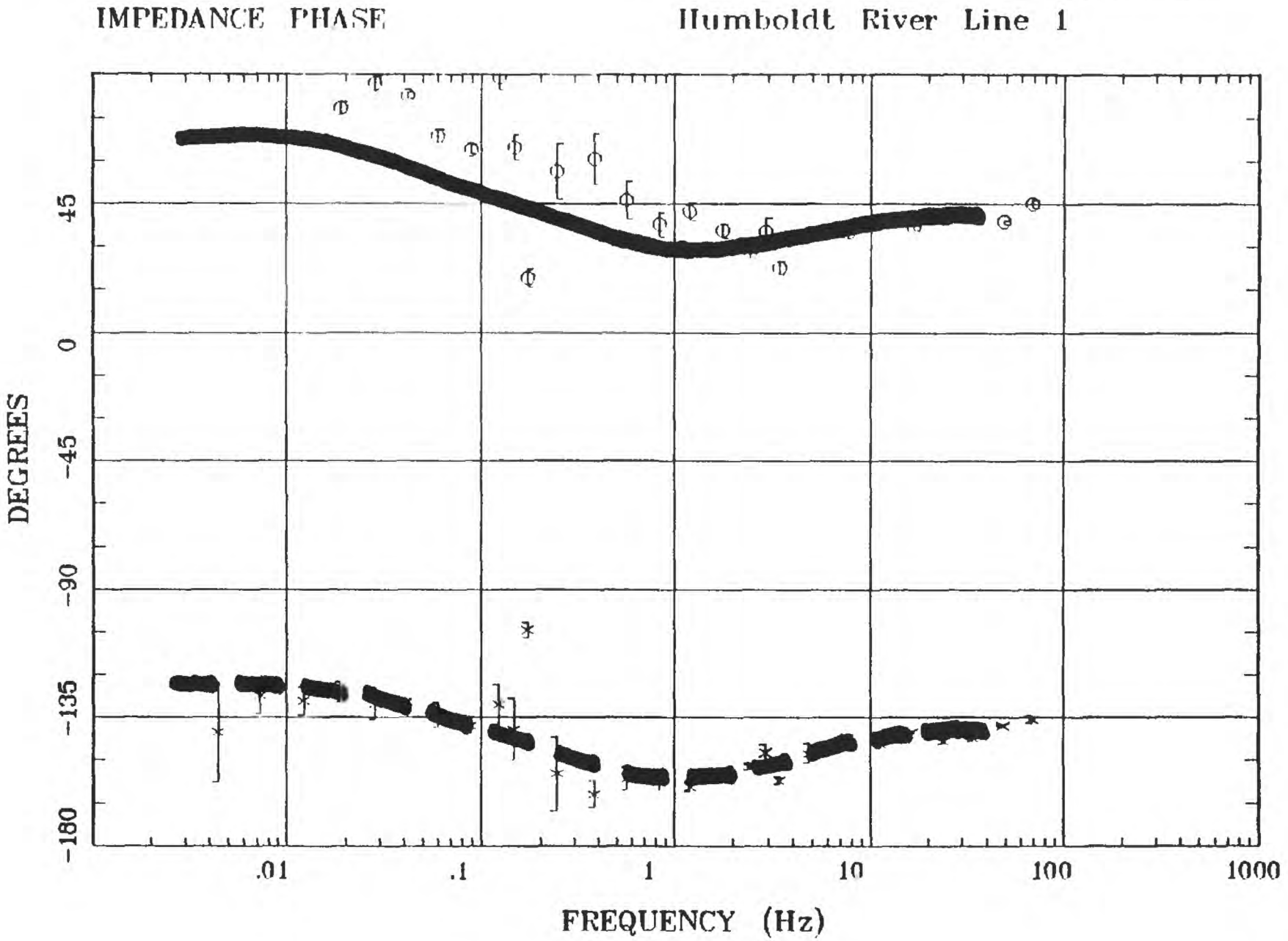

Client:
Remote: Local B
Acquired: 13:4 Aug 04, 1998
Survey Co:USGS GD-MRP Denver

Rotation:
Filename: hr42.avg
Channels: Ch1 Ch2 Ch3 Ch4 Ch5 Ch8 Ch9
Plotted: 13:50 Dec 07, 2000
< EMI - ElectroMagnetic Instruments >

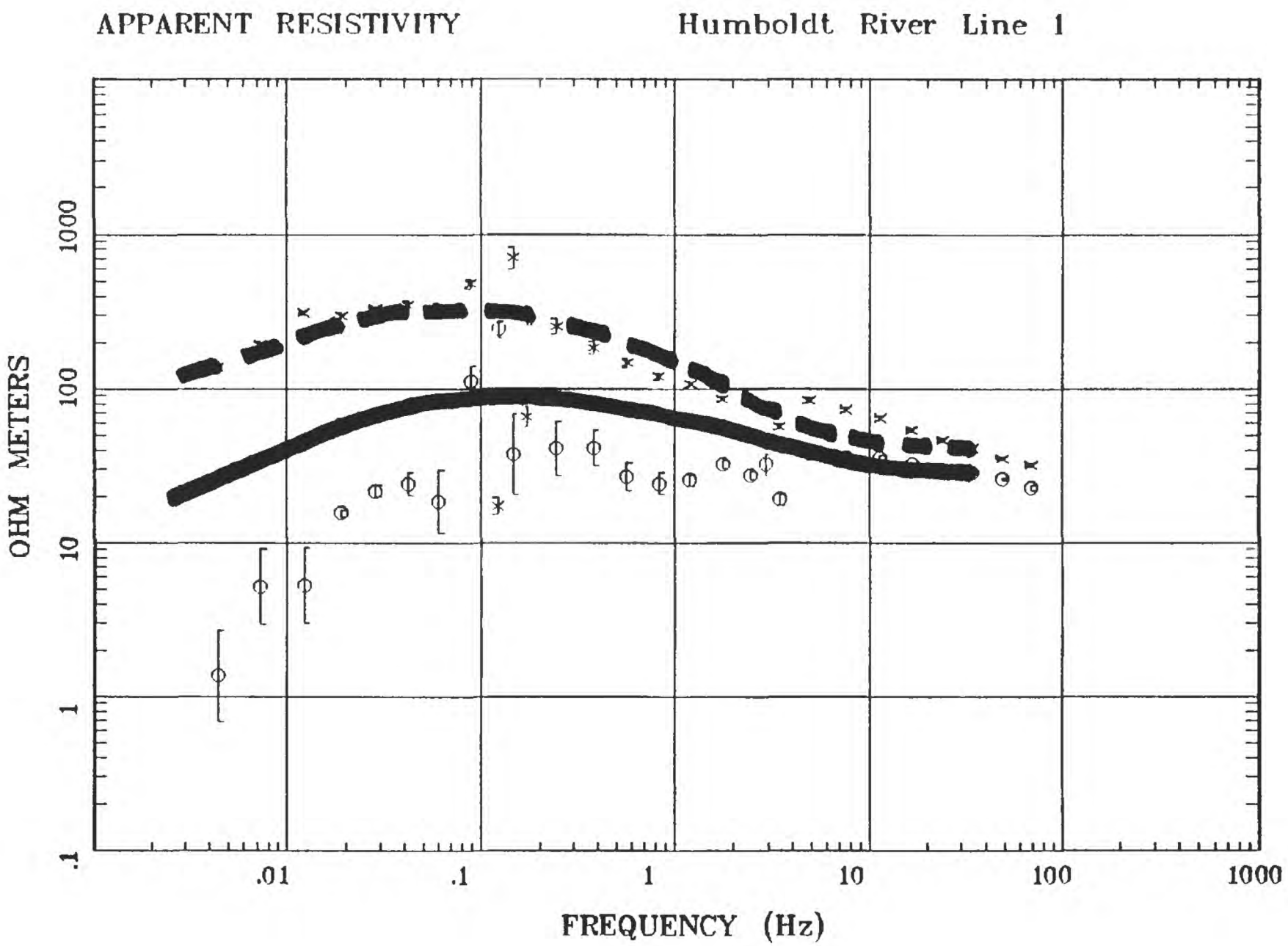

Client:
Remote: Local B
Acquired: 09:4 Aug 04, 1998
Survey Co:USGS GD-MRP Denver

Rotation:
Filename: hr59.avg
Channels: Ch1 Ch2 Ch3 Ch4 Ch5 Ch8 Ch9
Plotted: 13:59 Dec 07, 2000
< EMI - ElectroMagnetic Instruments >

Station 59

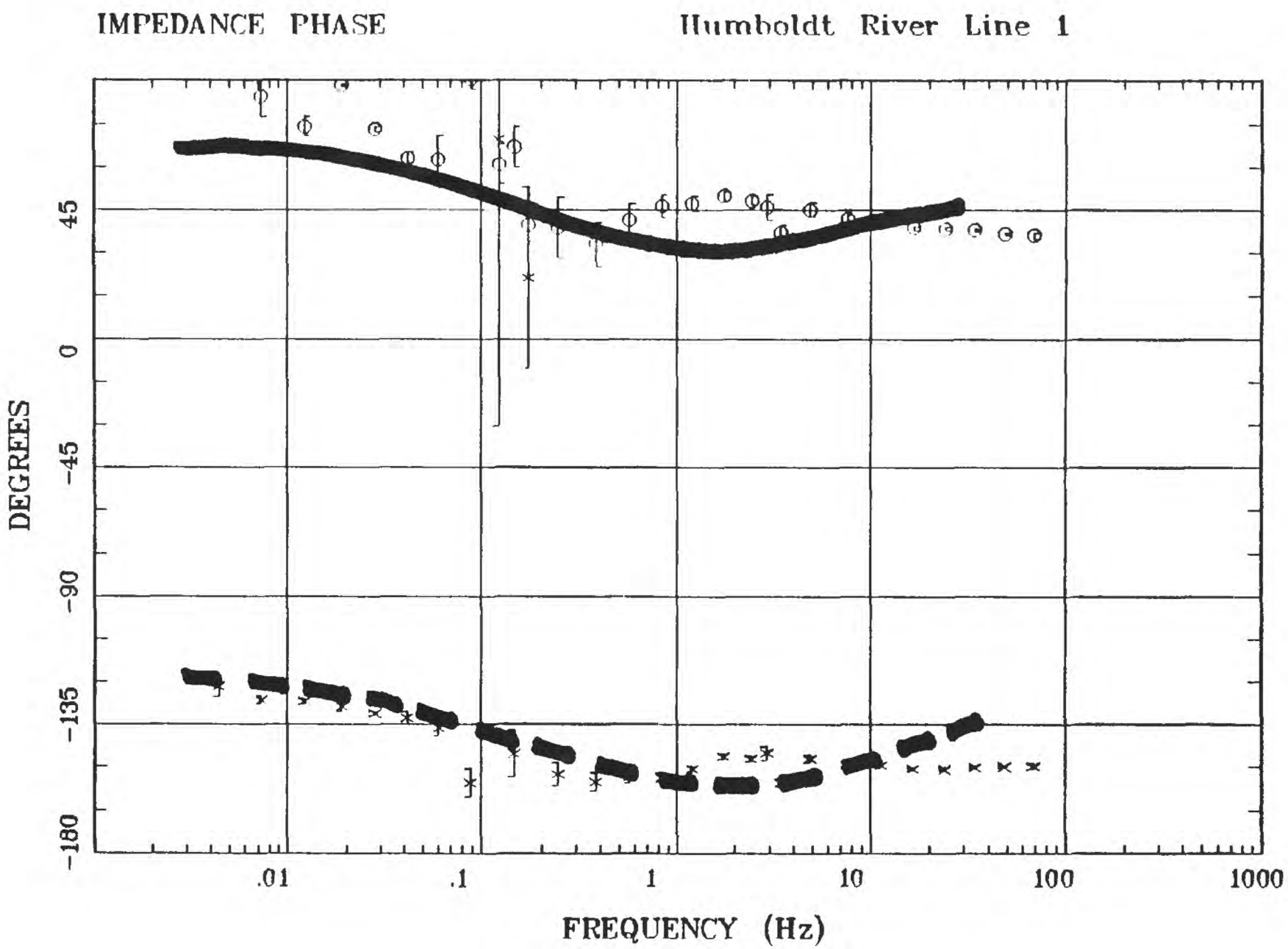

Client:
Remote: Local B
Acquired: 09:4 Aug 04, 1998
Survey Co:USGS GD-MRP Denver

Rotation:
Filename: hr59.avg
Channels: Ch1 Ch2 Ch3 Ch4 Ch5 Ch8 Ch9
Plotted: 13:59 Dec 07, 2000
< EMI - ElectroMagnetic Instruments >

Station 58

APPARENT RESISTIVITY Humboldt River Line 1

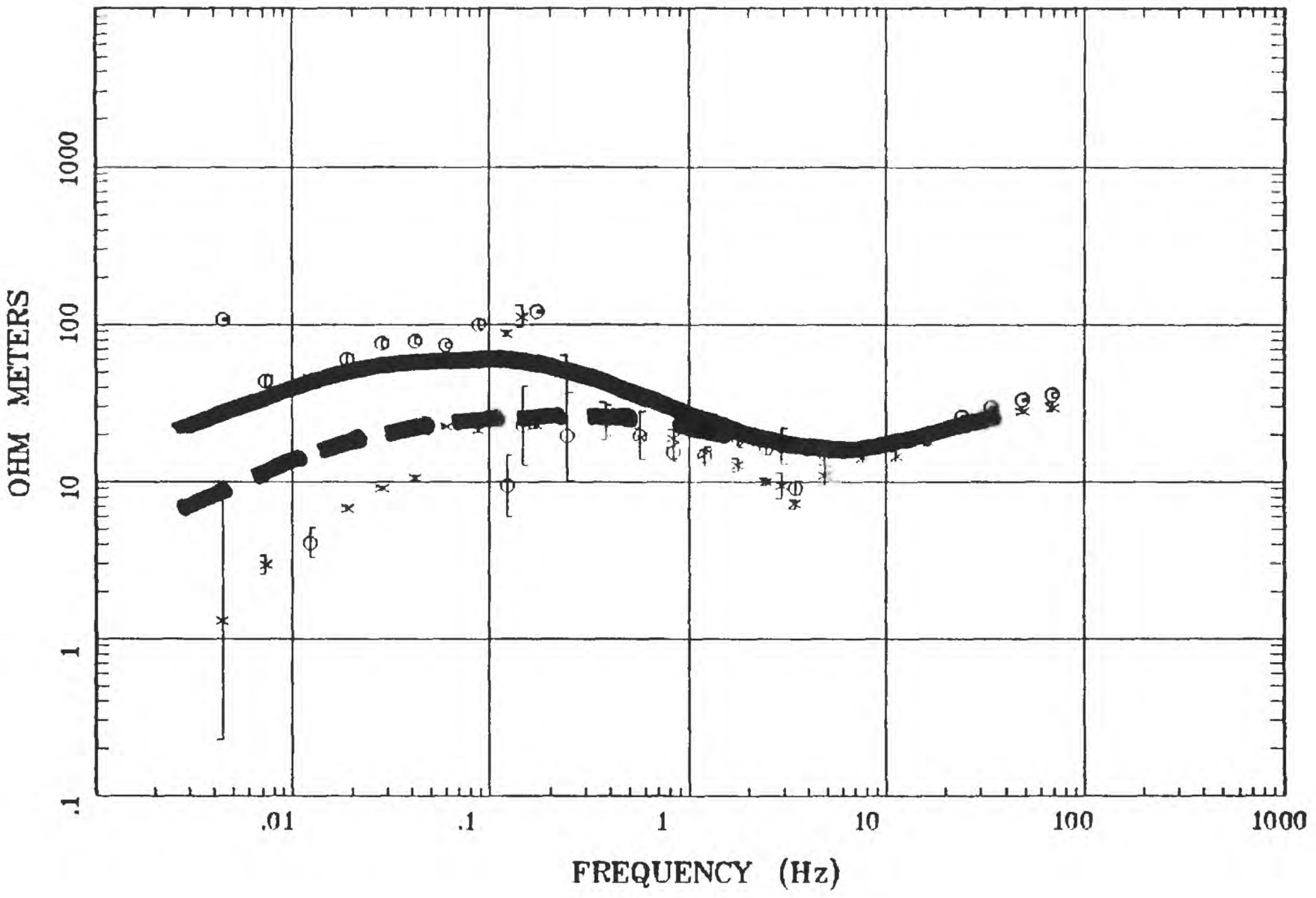

Client:
Remote: Local B
Acquired: 16:2 Aug 03, 1998
Survey Co:USGS GD-MRP Denver

Rotation:
Filename: hr58.avg
Channels: Ch1 Ch2 Ch3 Ch4 Ch5 Ch8 Ch9
Plotted: 13:58 Dec 07, 2000
< EMI - ElectroMagnetic Instruments >

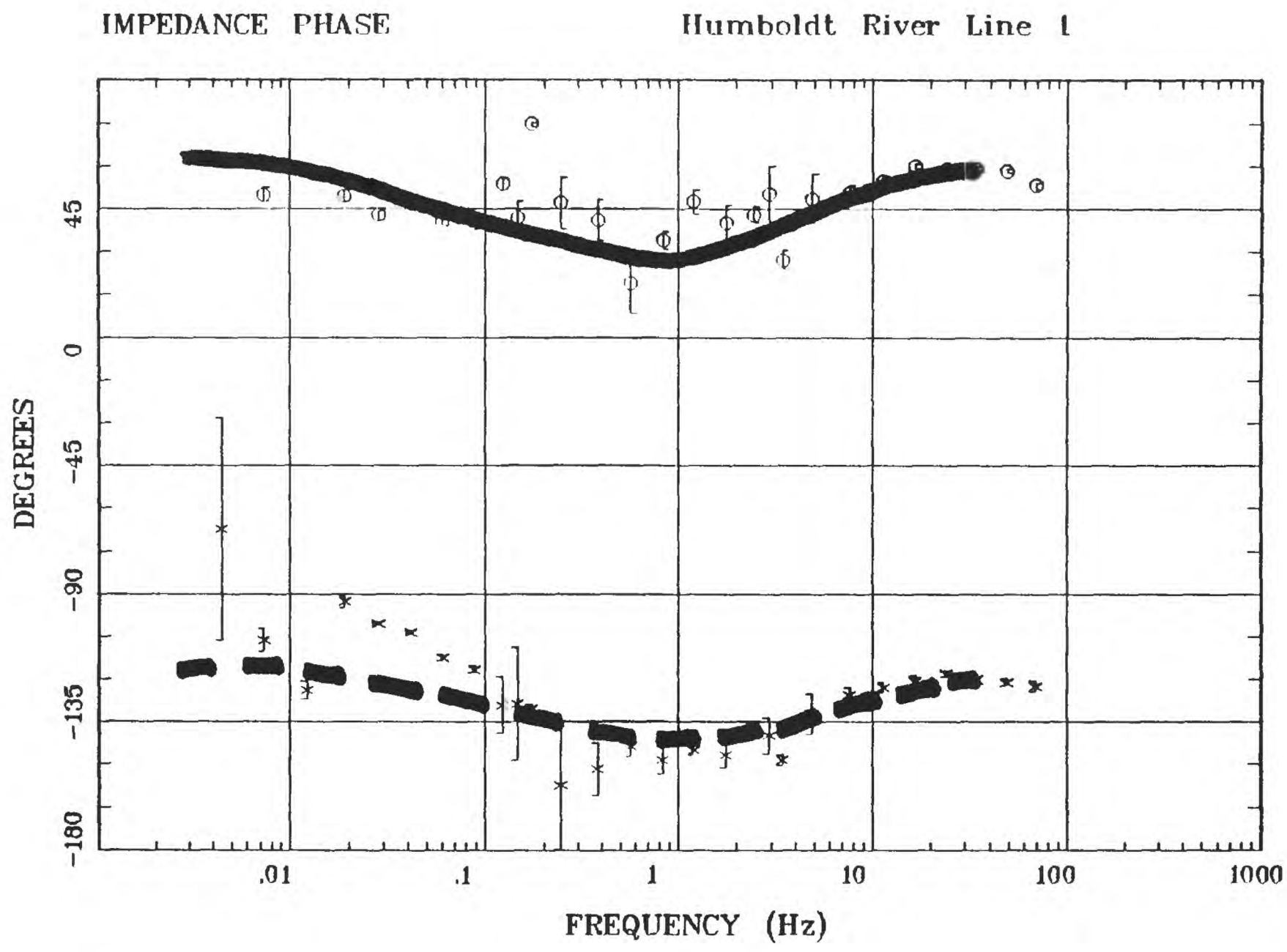

Client:
Remote: Local B
Acquired: 16:2 Aug 03, 1998
Survey Co:USGS GD-MRP Denver

Rotation:
Filename: hr58.avg
Channels: Ch1 Ch2 Ch3 Ch4 Ch5 Ch8 Ch9
Plotted: 13:58 Dec 07, 2000
< EMI - ElectroMagnetic Instruments >

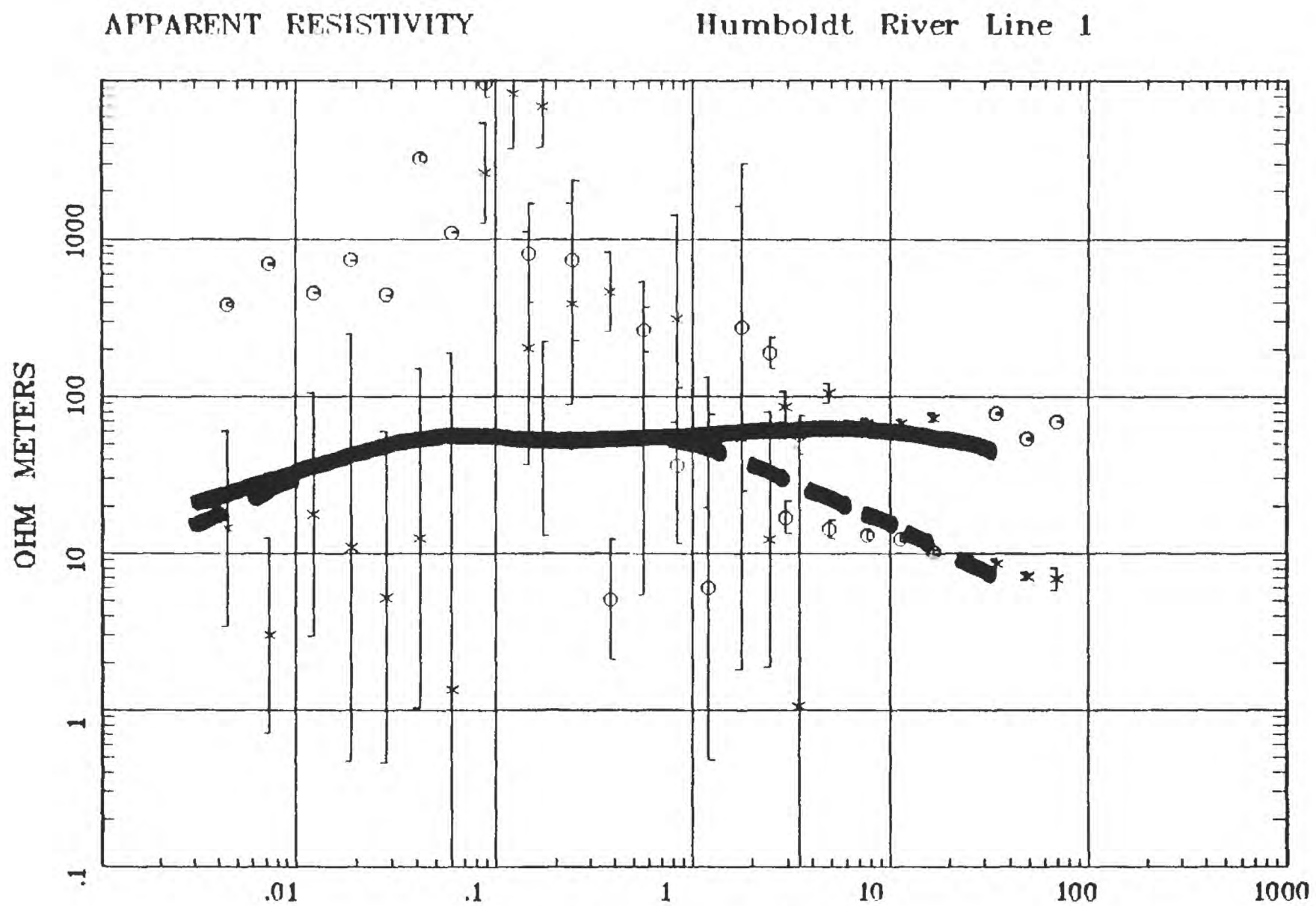

Client:
Remote: Local E
Acquired: 11:1 Aug 03, 1998
Survey Co:USGS GD-MRP Denver

Rotation:
Filename: hr57.avg
Channels: Ch1 Ch2 Ch3 Ch4 Ch5 Ch6 Ch7
Plotted: 13:57 Dec 07, 2000
< EMI - ElectroMagnetic Instruments >

Station 57

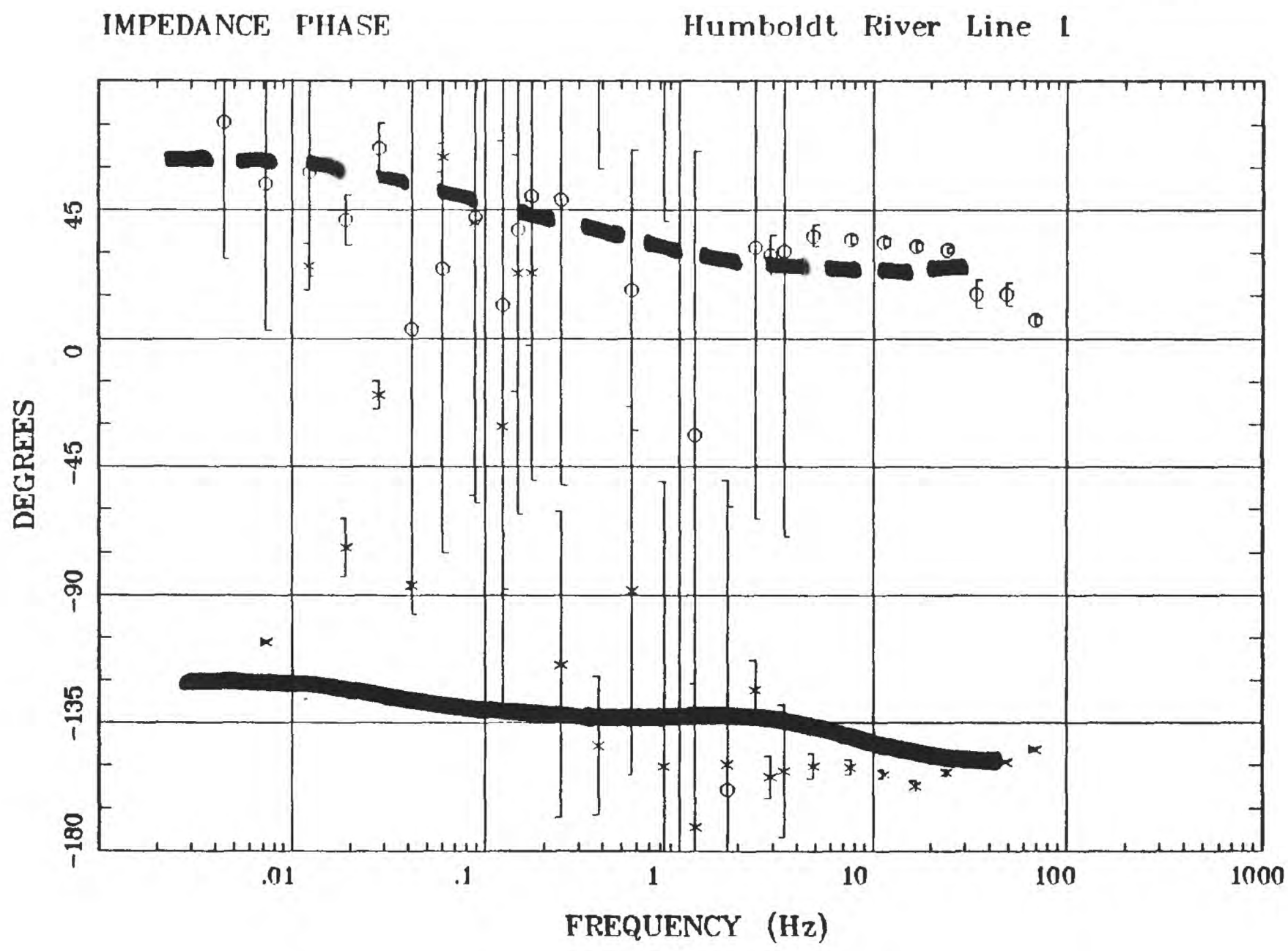

Client:
Remote: Local E
Acquired: 11:1 Aug 03, 1998
Survey Co:USGS GD-MRP Denver

Rotation:
Filename: hr57.avg
Channels: Ch1 Ch2 Ch3 Ch4 Ch5 Ch6 Ch7
Plotted: 13:57 Dec 07, 2000
< EMI - ElectroMagnetic Instruments >

APPARENT RESISTIVITY Humboldt River Line **Station 34**

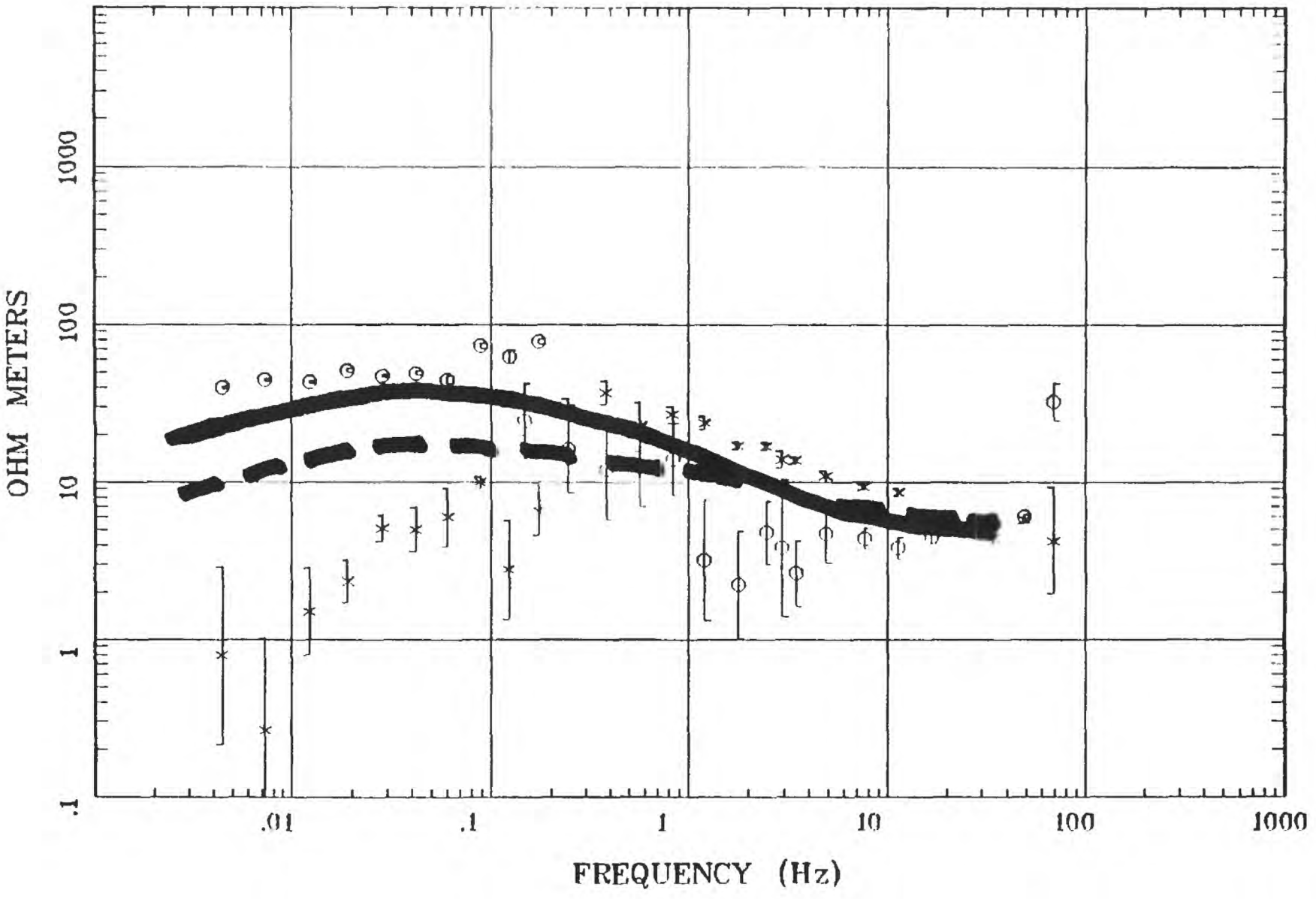

Client:
Remote: Local B
Acquired: 10:1 Aug 01, 1998
Survey Co:USGS GD-MRP Denver

Rotation:
Filename: hr34.avg
Channels: Ch1 Ch2 Ch3 Ch4 Ch5 Ch8 Ch9
Plotted: 13:43 Dec 07, 2000
< EMI - ElectroMagnetic Instruments >

IMPEDANCE PHASE

Humboldt River Line 1

Station 34

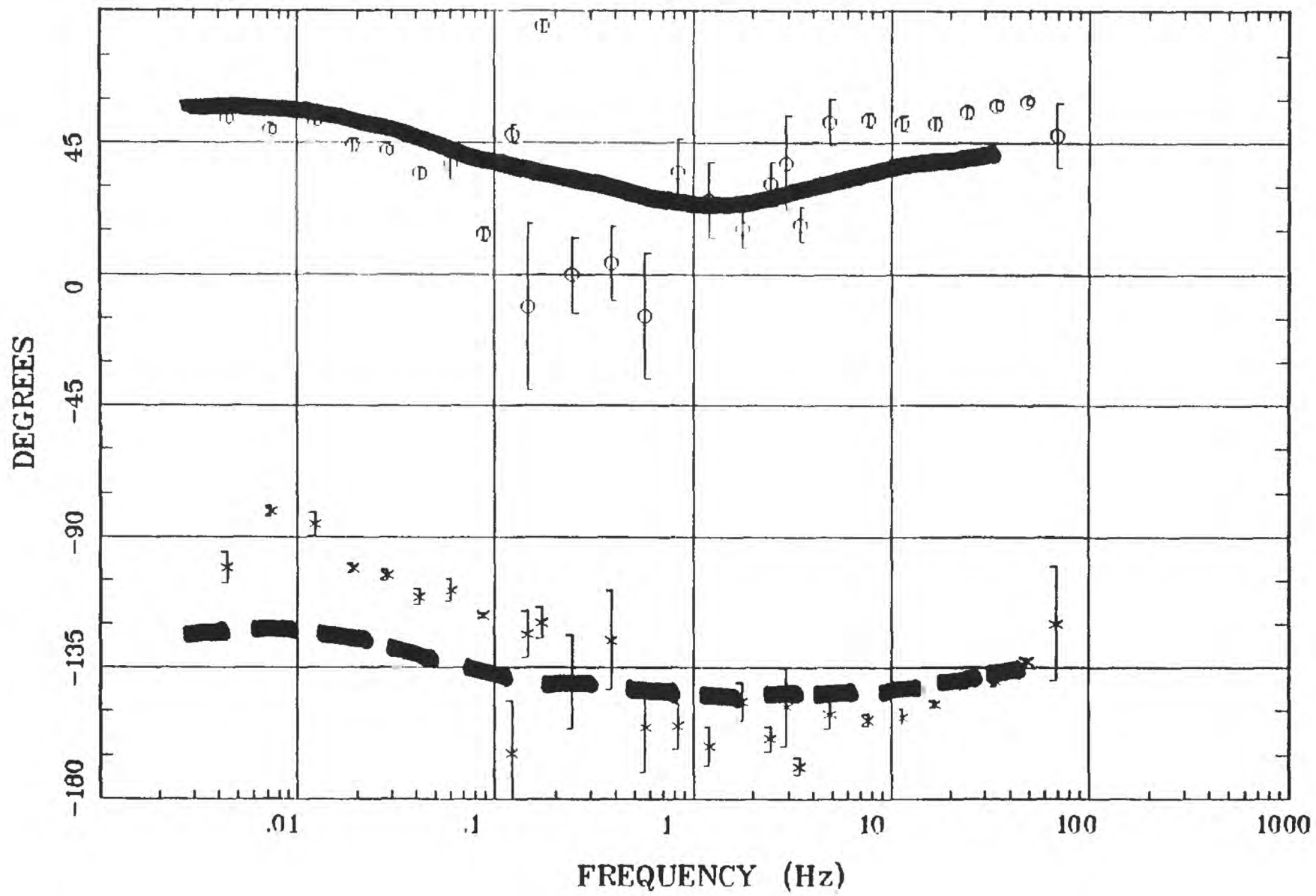

Client:
Remote: Local B
Acquired: 10:1 Aug 01, 1998
Survey Co:USGS GD-MRP Denver

Rotation:
Filename: hr34.avg
Channels: Ch1 Ch2 Ch3 Ch4 Ch5 Ch8 Ch9
Plotted: 13:43 Dec 07, 2000
< EMI - ElectroMagnetic Instruments >

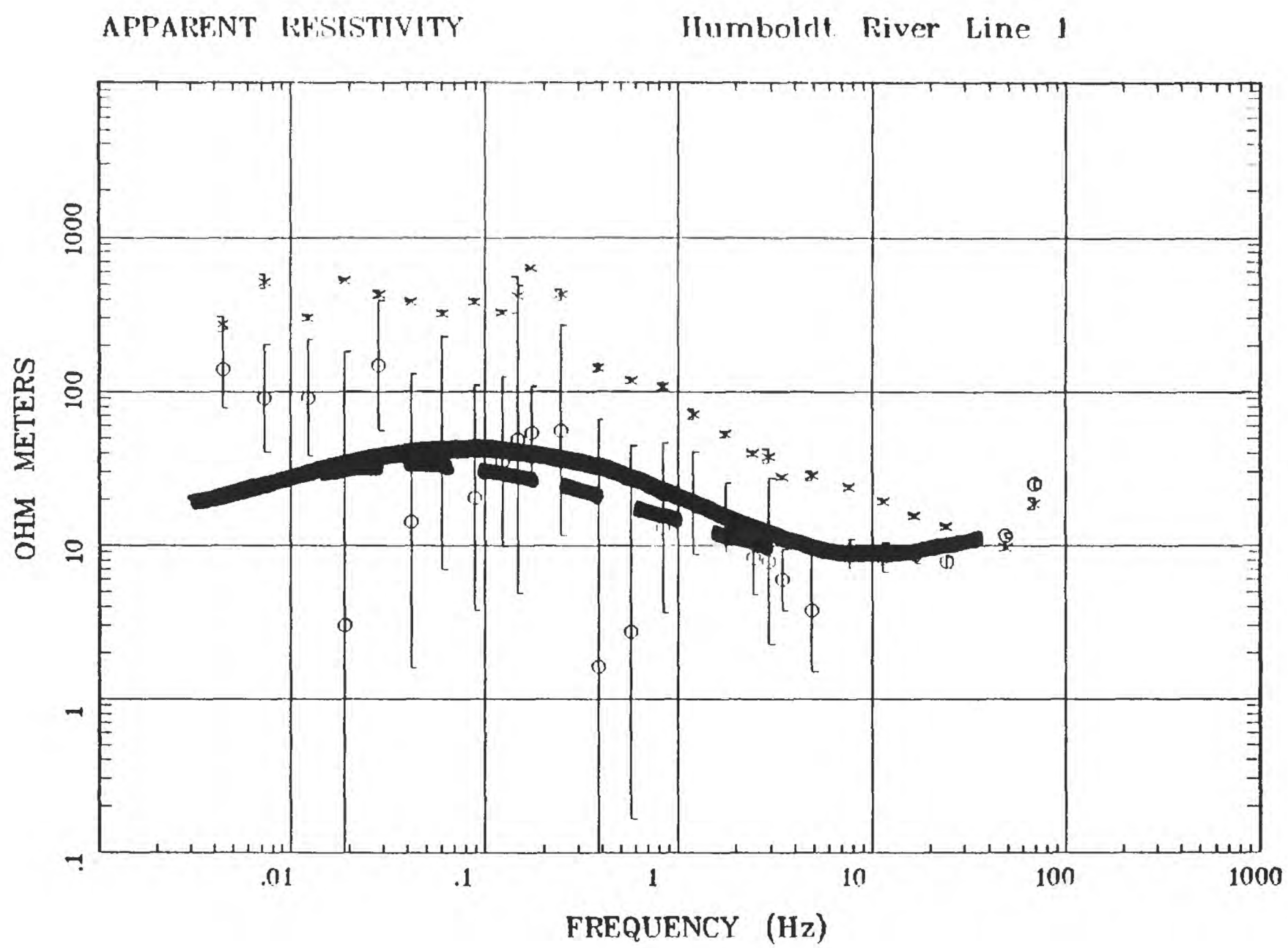

Client:
Remote: none
Acquired: 13:4 Aug 01, 1998
Survey Co:USGS GD-MRP Denver

Rotation:
Filename: hr37a.avg
Channels: Ch1 Ch2 Ch3 Ch4 Ch5 Ch3 Ch4
Plotted: 13:49 Dec 07, 2000
< EMI - ElectroMagnetic Instruments >

Station 37

IMPEDANCE PHASE Humboldt River Line 1

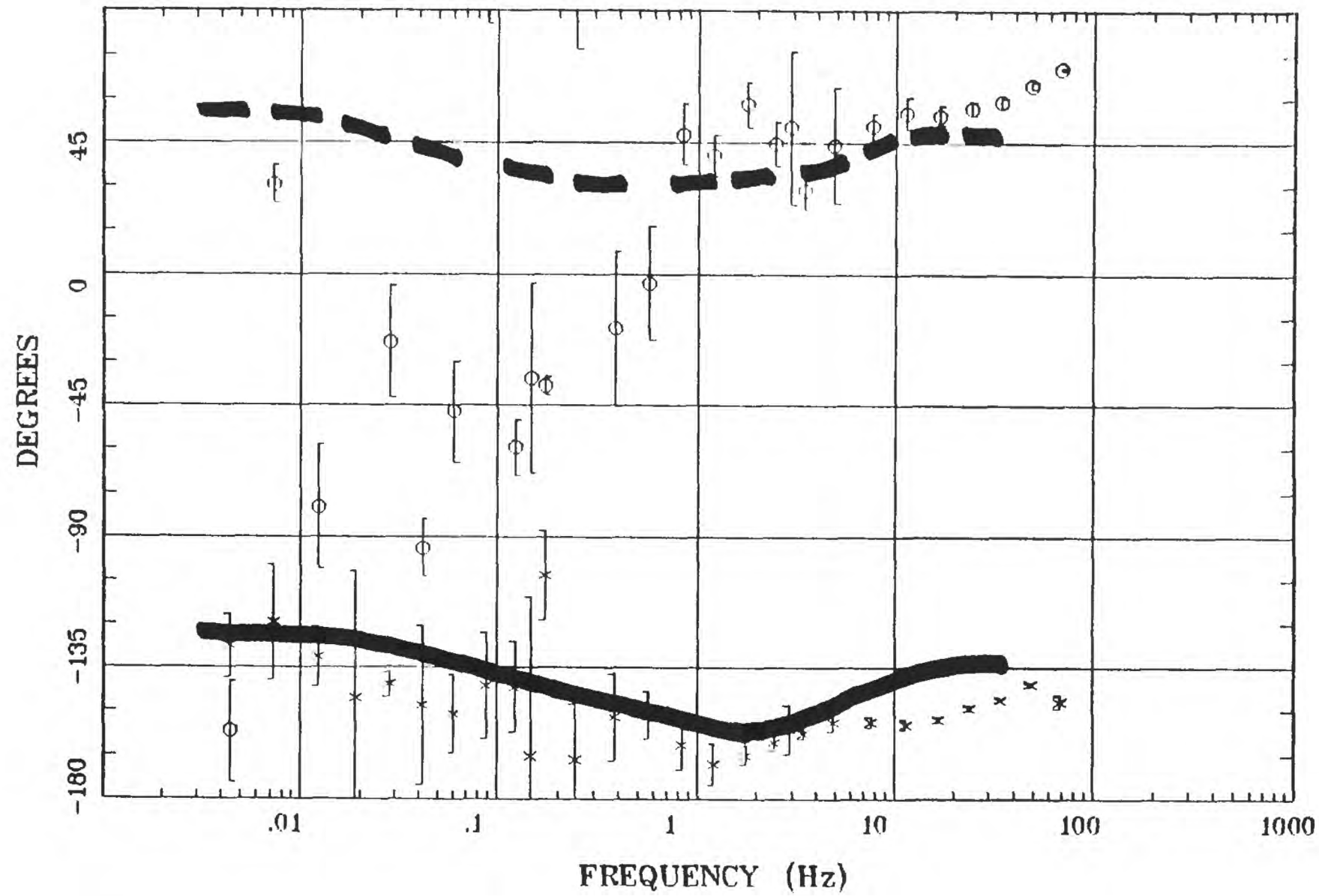

Client:
Remote: none
Acquired: 13:4 Aug 01, 1998
Survey Co:USGS GD-MRP Denver

Rotation:
Filename: hr37a.avg
Channels: Ch1 Ch2 Ch3 Ch4 Ch5 Ch3 Ch4
Plotted: 13:49 Dec 07, 2000
< EMI - ElectroMagnetic Instruments >

Station 33

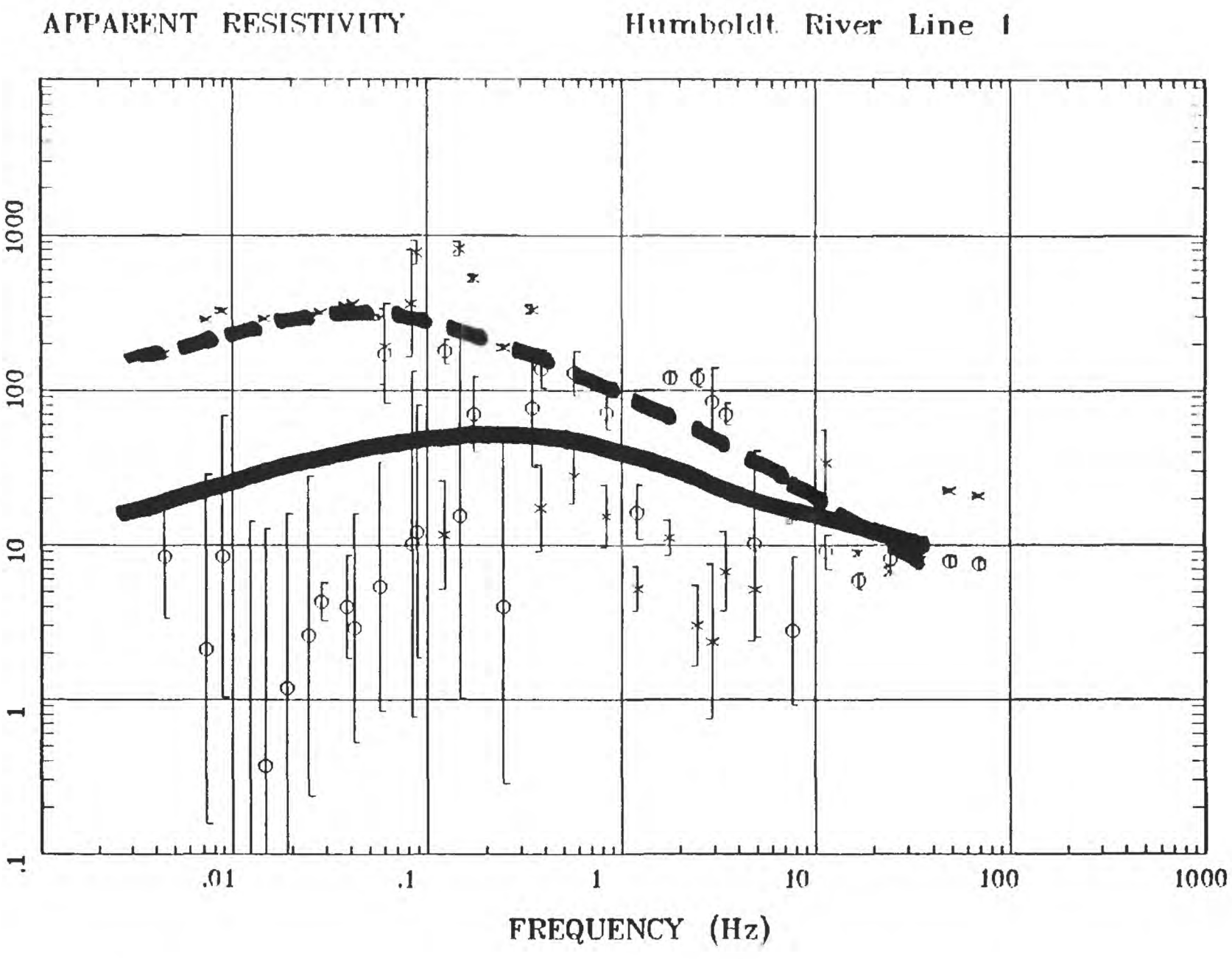

Client:
Remote: Local B
Acquired: 10:0 Aug 02, 1998
Survey Co:USGS GD--MRP Denver

Rotation:
Filename: HR33.avg
Channels: Ch1 Ch2 Ch3 Ch4 Ch5 Ch8 Ch9
Plotted: 13:28 Dec 07, 2000
< EMI - ElectroMagnetic Instruments >

Station 33

IMPEDANCE PHASE — Humboldt River Line 1

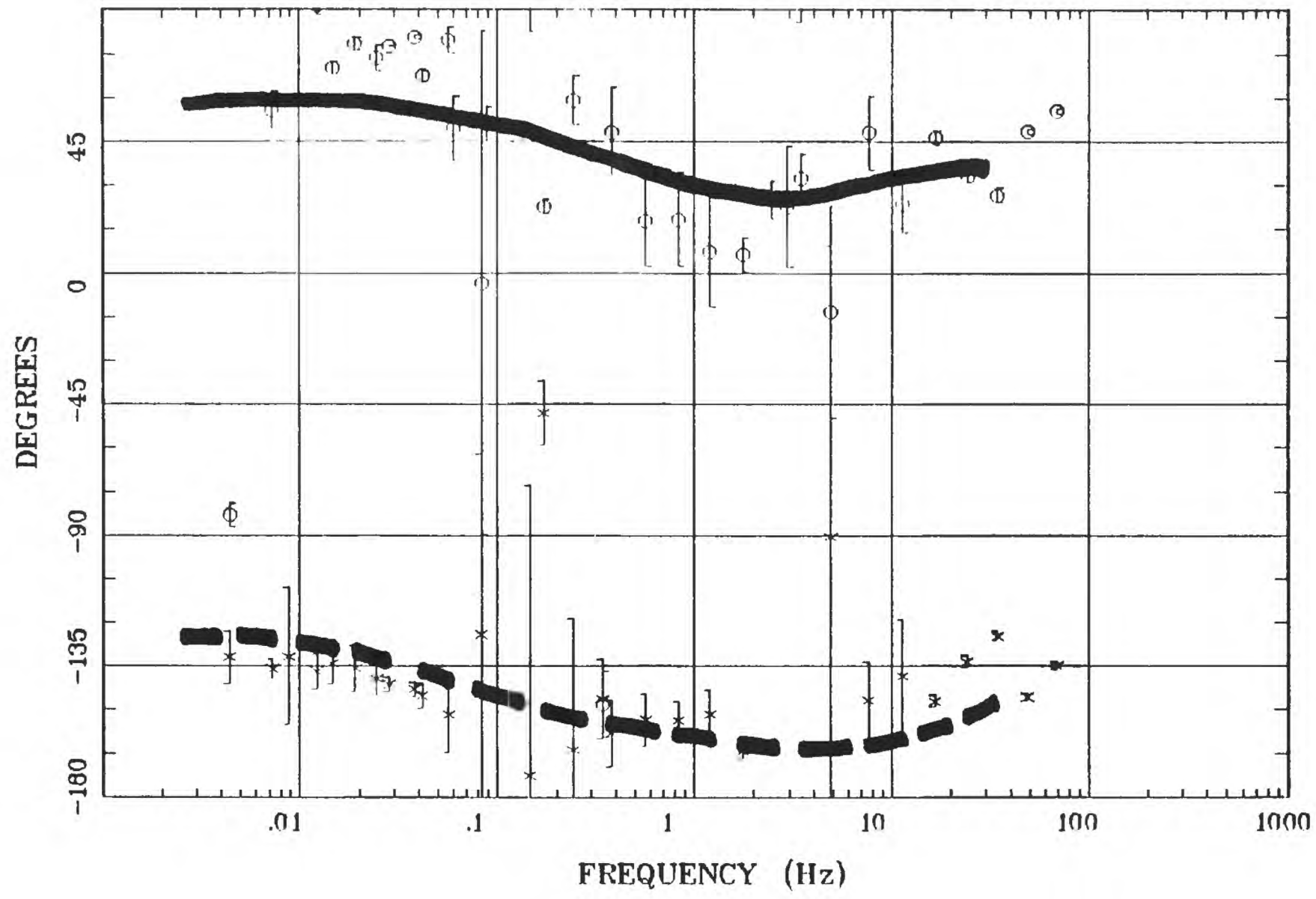

Client:
Remote: Local B
Acquired: 10:0 Aug 02, 1998
Survey Co:USGS GD-MRP Denver

Rotation:
Filename: HR33.avg
Channels: Ch1 Ch2 Ch3 Ch4 Ch5 Ch8 Ch9
Plotted: 13:28 Dec 07, 2000
< EMI - ElectroMagnetic Instruments >

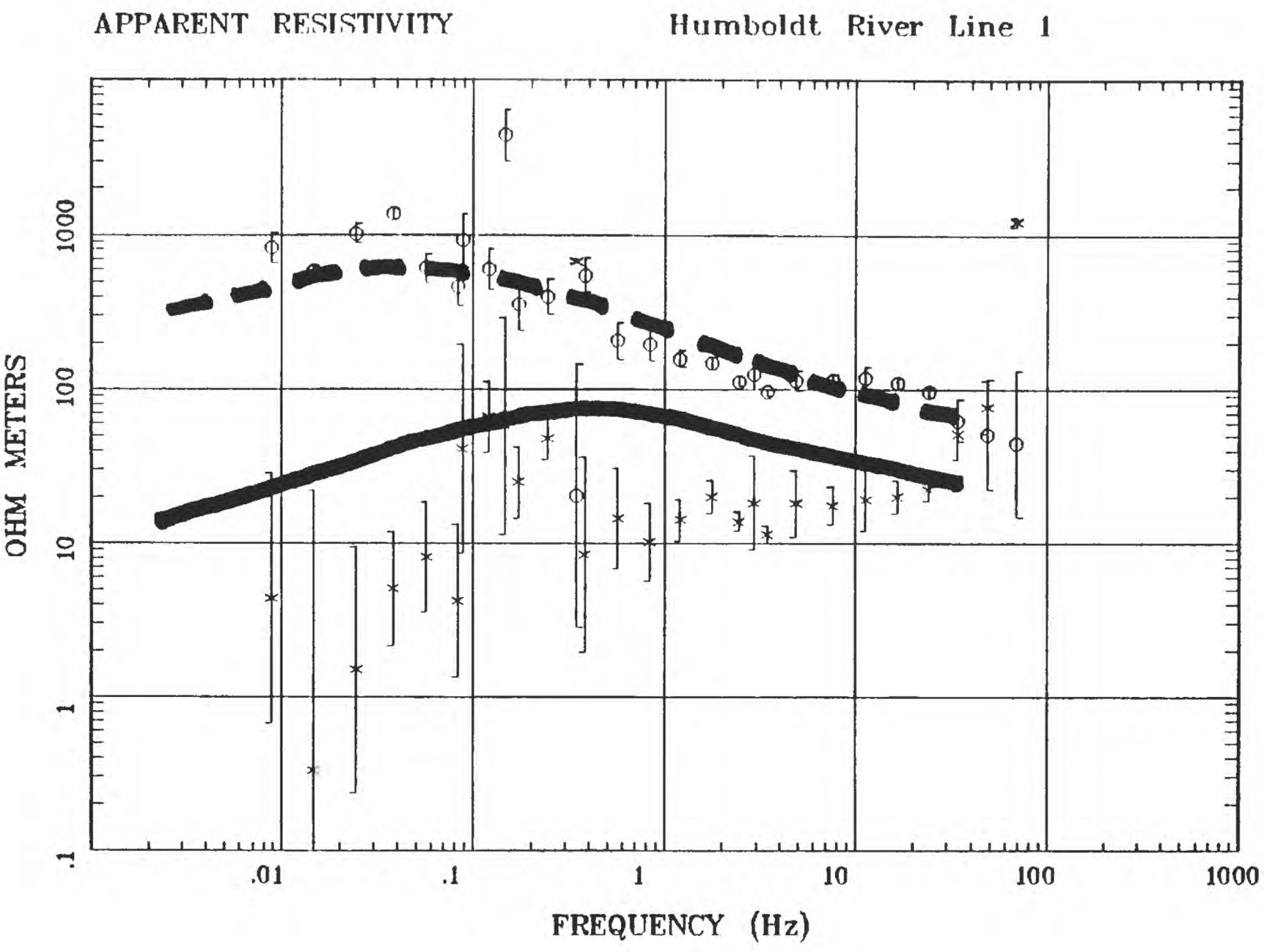

Client:
Remote: Local B
Acquired: 14:1 Aug 02, 1998
Survey Co:USGS GD-MRP Denver

Rotation:
Filename: HR32.avg
Channels: Ch1 Ch2 Ch3 Ch4 Ch5 Ch8 Ch9
Plotted: 13:22 Dec 07, 2000
< EMI - ElectroMagnetic Instruments >

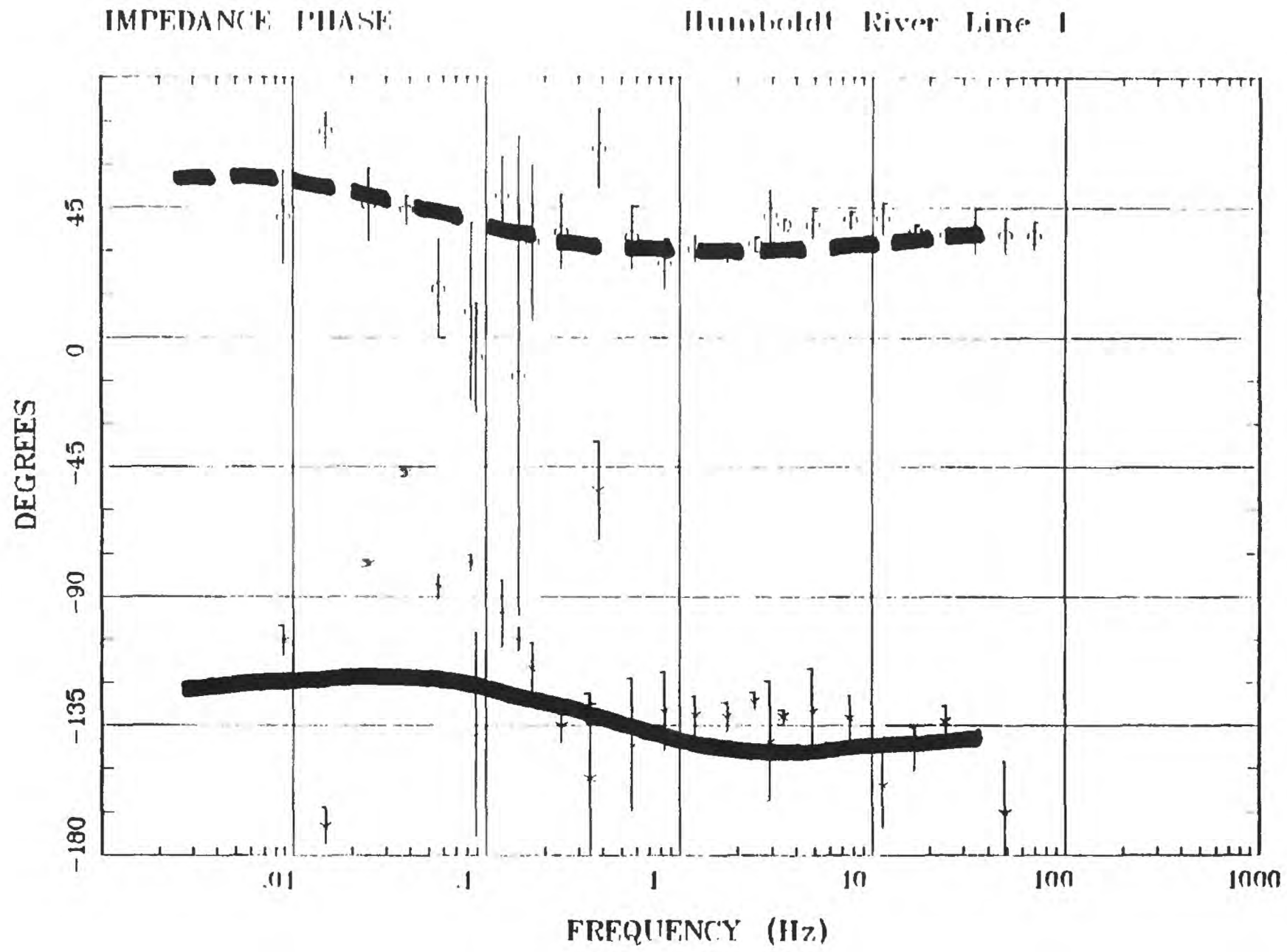

Client:
Remote: Local B
Acquired: 14:1 Aug 02, 1998
Survey Co:USGS GD MRP Denver

Rotation:
Filename: HR32.avg
Channels: Ch1 Ch2 Ch3 Ch4 Ch5 Ch8 Ch9
Plotted: 13:22 Dec 07, 2000
EMI ElectroMagnetic Instruments

Station 35

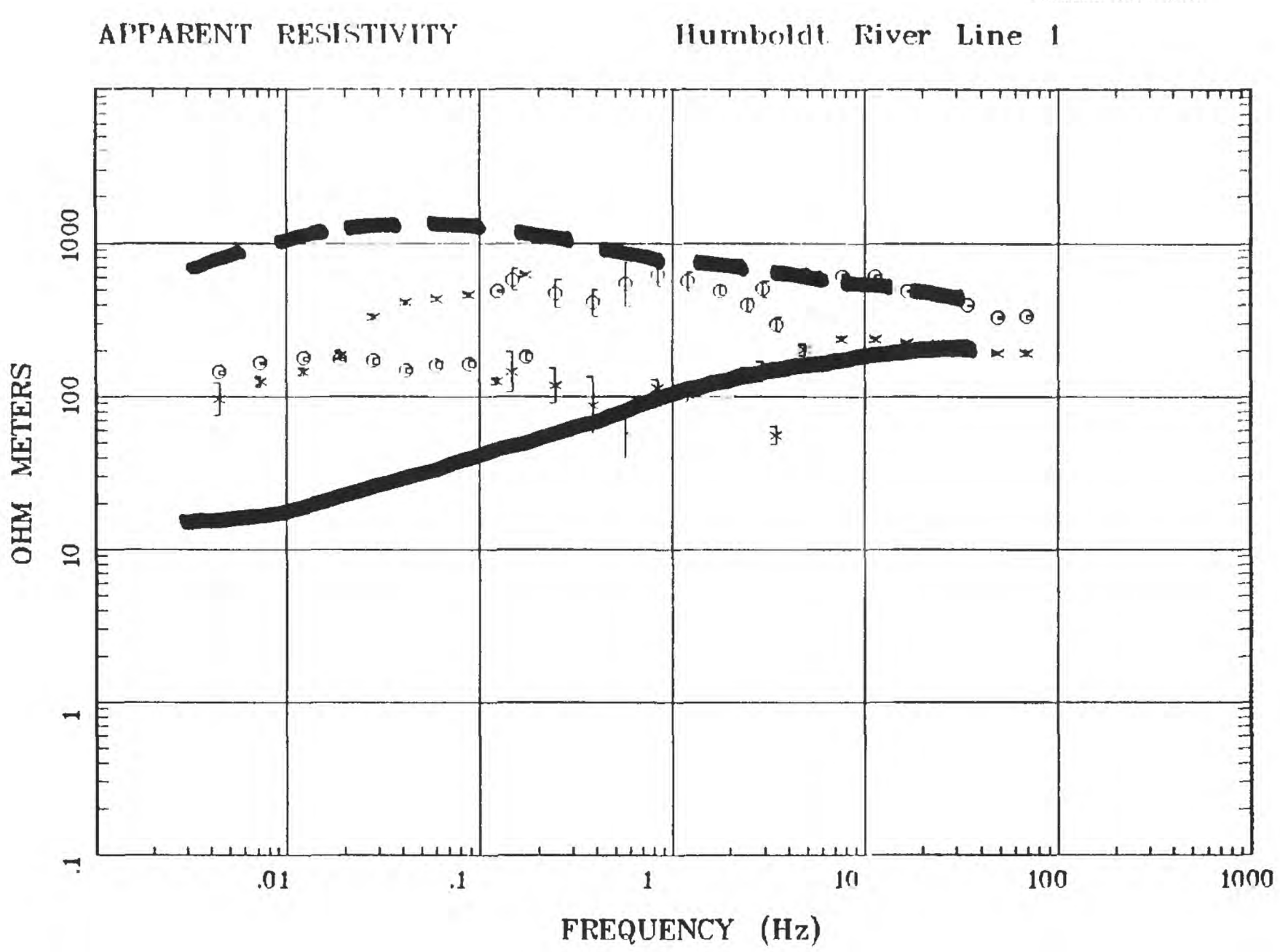

Client:
Remote: Local B
Acquired: 10:2 Jul 31, 1998
Survey Co:USGS GD-MRP Denver

Rotation:
Filename: hr35.avg
Channels: Ch1 Ch2 Ch3 Ch4 Ch5 Ch8 Ch9
Plotted: 13:44 Dec 07, 2000
< EMI - ElectroMagnetic Instruments >

Station 35

IMPEDANCE PHASE

Humboldt River Line 1

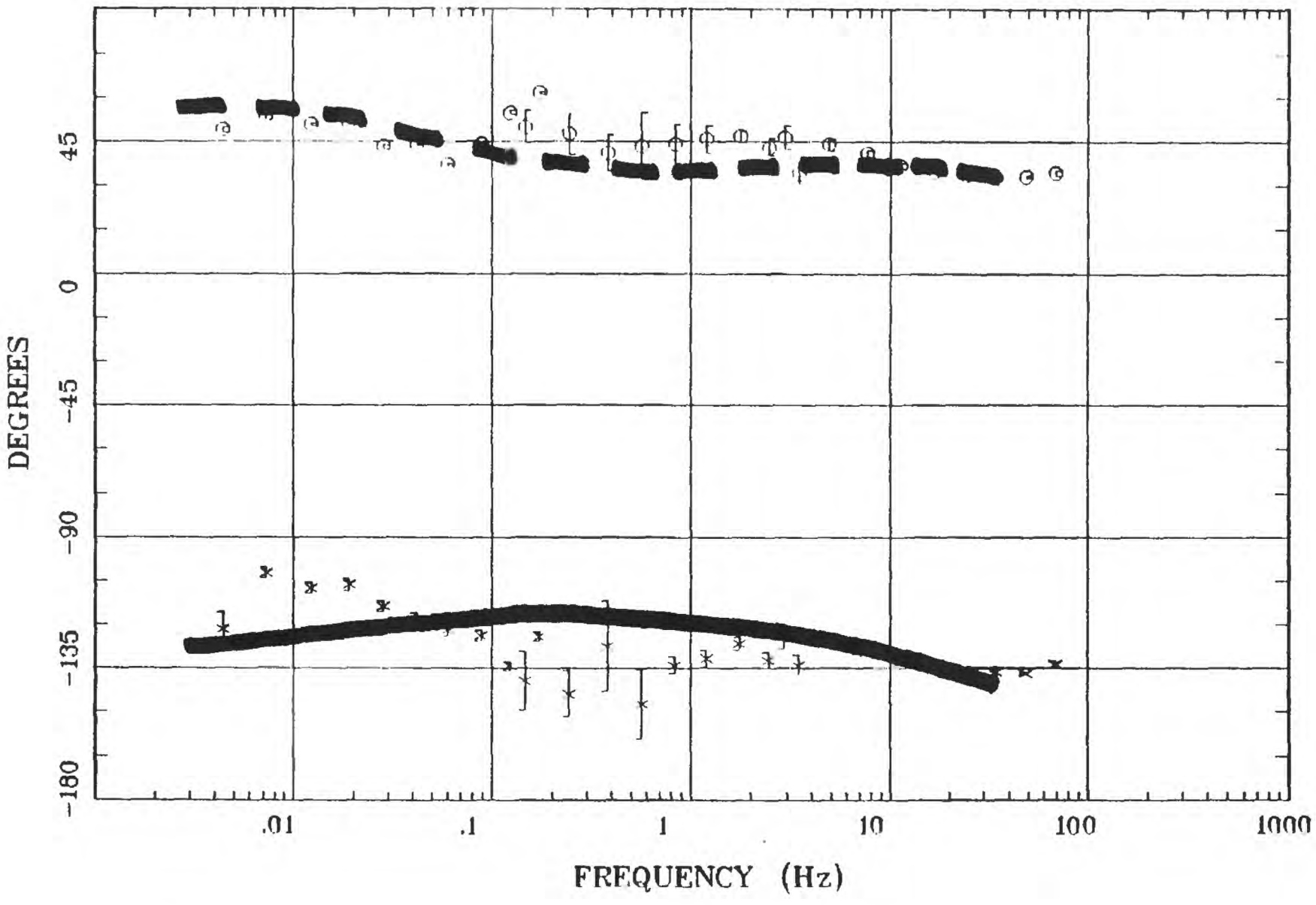

Client:
Remote: Local B
Acquired: 10:2 Jul 31, 1998
Survey Co:USGS GD-MRP Denver

Rotation:
Filename: hr35.avg
Channels: Ch1 Ch2 Ch3 Ch4 Ch5 Ch8 Ch9
Plotted: 13:44 Dec 07, 2000
< EMI - ElectroMagnetic Instruments >

Station 56

APPARENT RESISTIVITY — Humboldt River Line 1

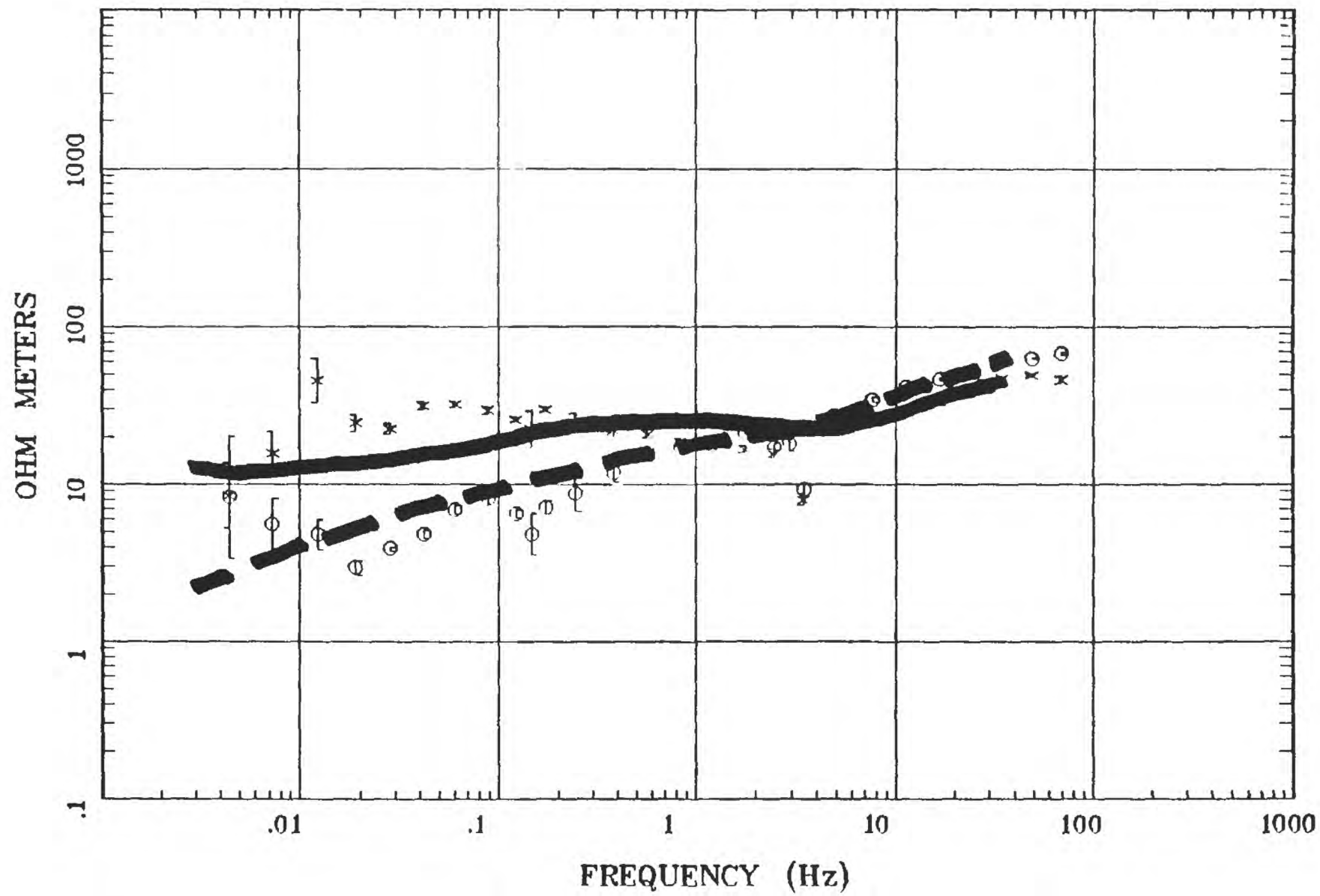

Client:
Remote: Local B
Acquired: 15:1 Jul 31, 1998
Survey Co:USGS GD-MRP Denver

Rotation:
Filename: hr56.avg
Channels: Ch1 Ch2 Ch3 Ch4 Ch5 Ch8 Ch9
Plotted: 13:56 Dec 07, 2000
< EMI - ElectroMagnetic Instruments >

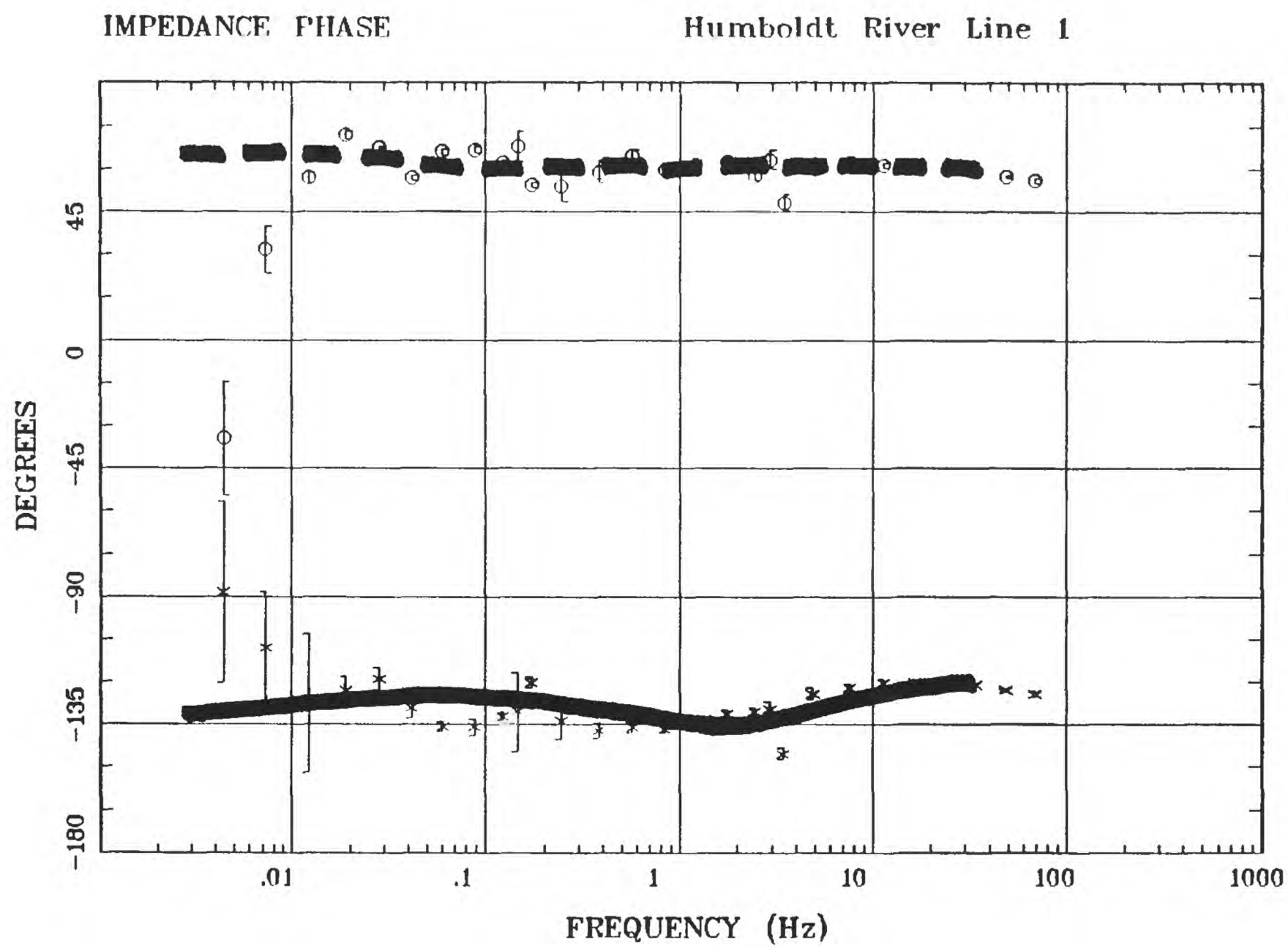

Client:
Remote: Local B
Acquired: 15:1 Jul 31, 1998
Survey Co:USGS GD-MRP Denver

Rotation:
Filename: hr56.avg
Channels: Ch1 Ch2 Ch3 Ch4 Ch5 Ch8 Ch9
Plotted: 13:56 Dec 07, 2000
< EMI - ElectroMagnetic Instruments >

APPENDIX B

OBSERVED AND CALCULATED DATA - PROFILE MT6

Magnetotelluric (MT) observed (circle and x symbols) and calculated (solid and dashed lines are TE and TM modes, respectively) resistivity and phase data for profile MT6. See the "Magnetotelluric Data" section of this report for a description of the observed data and the "Resistivity Models" section for a description of the calculated data.

APPARENT RESISTIVITY Boulder Valley, NV

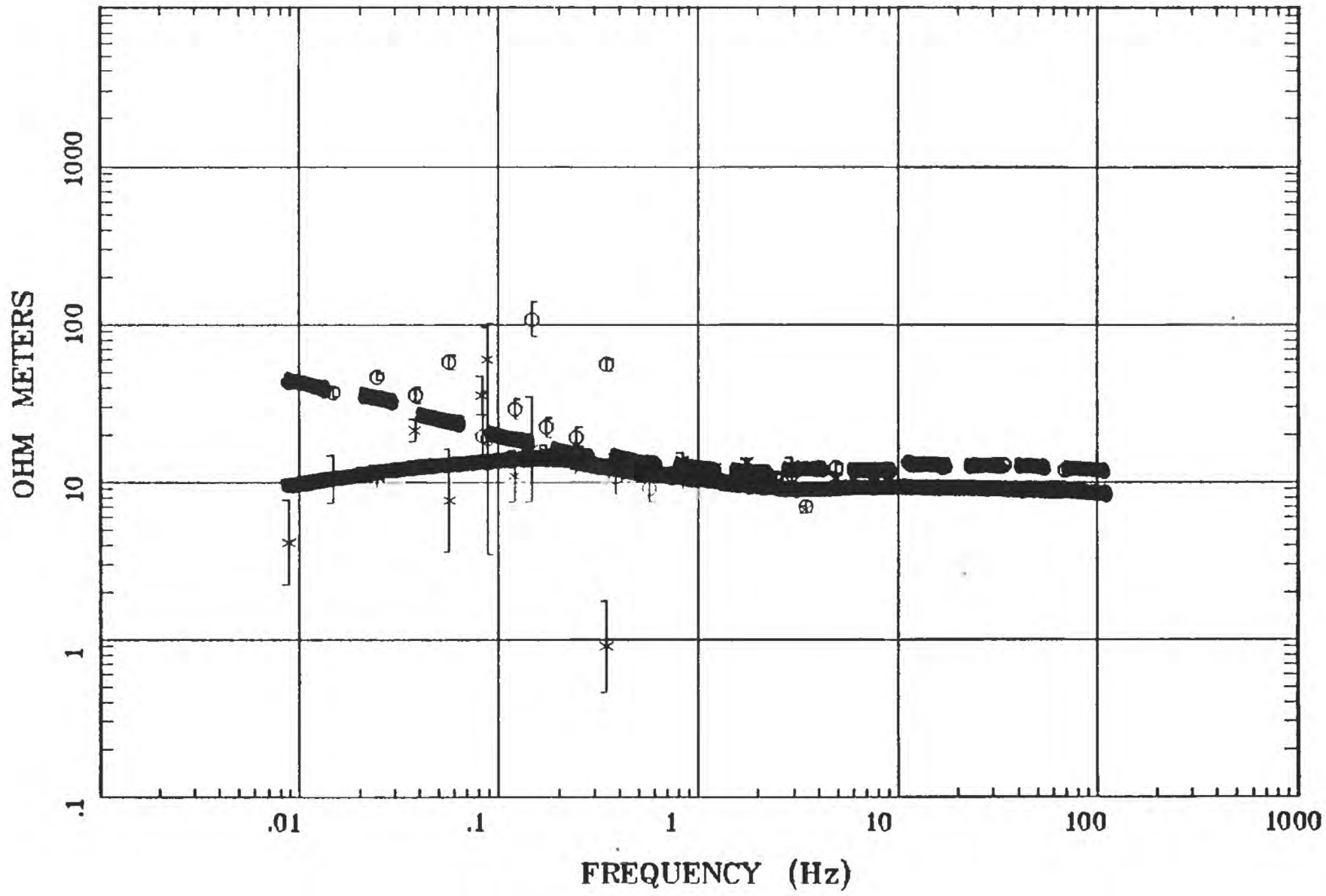

Client:
Remote: local
Acquired: 14:5 Jul 31, 1999
Survey Co:USGS

Rotation:
Filename: hr72.avg
Channels: Ch1 Ch2 Ch3 Ch4 Ch5 Ch3 Ch4
Plotted: 14:56 Feb 06, 2001
< EMI - ElectroMagnetic Instruments >

Station 72

IMPEDANCE PHASE — Boulder Valley, NV

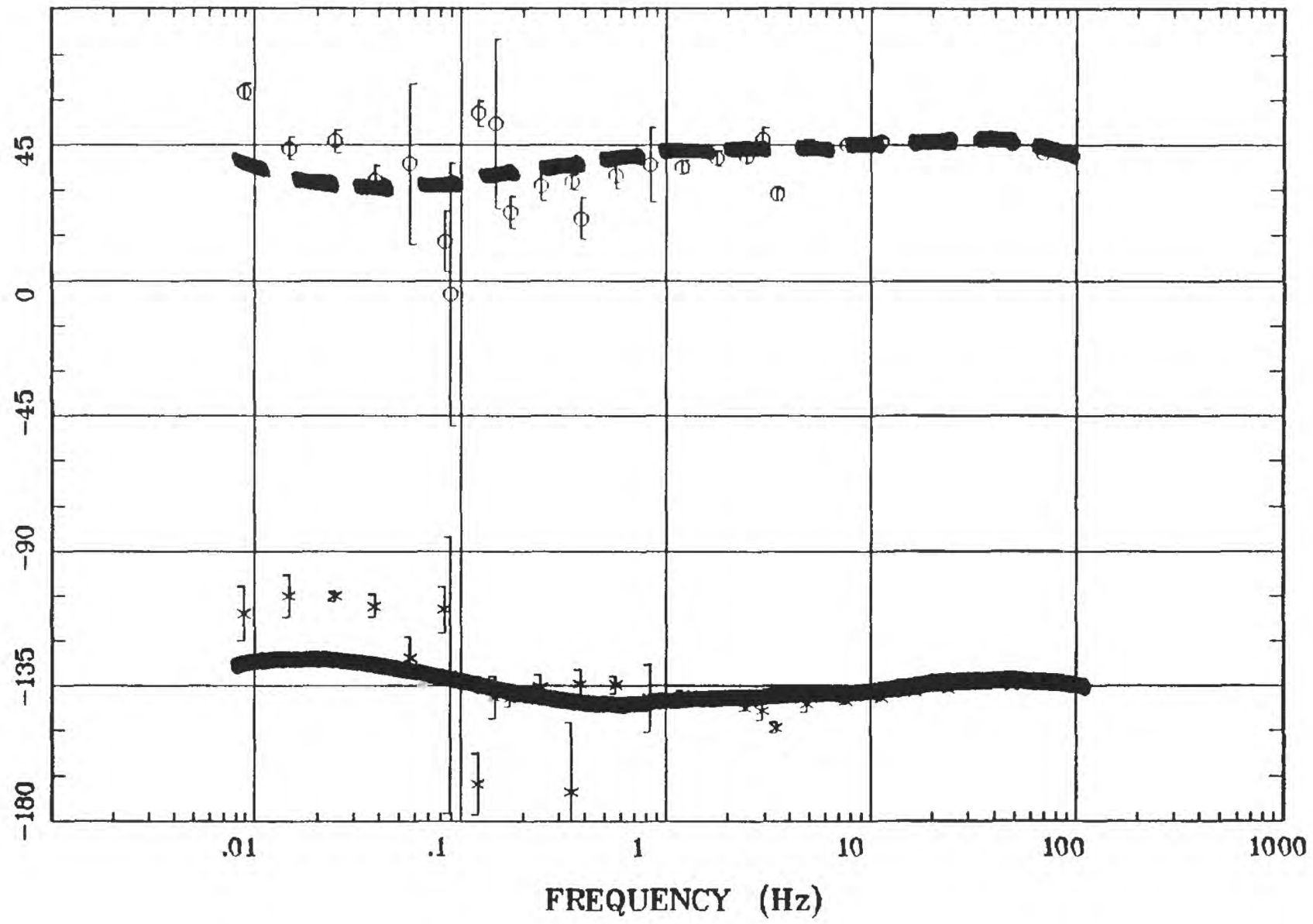

Client:
Remote: local
Acquired: 14:5 Jul 31, 1999
Survey Co:USGS

Rotation:
Filename: hr72.avg
Channels: Ch1 Ch2 Ch3 Ch4 Ch5 Ch3 Ch4
Plotted: 14:56 Feb 06, 2001
< EMI - ElectroMagnetic Instruments >

Station 67

APPARENT RESISTIVITY Boulder Valley, NV

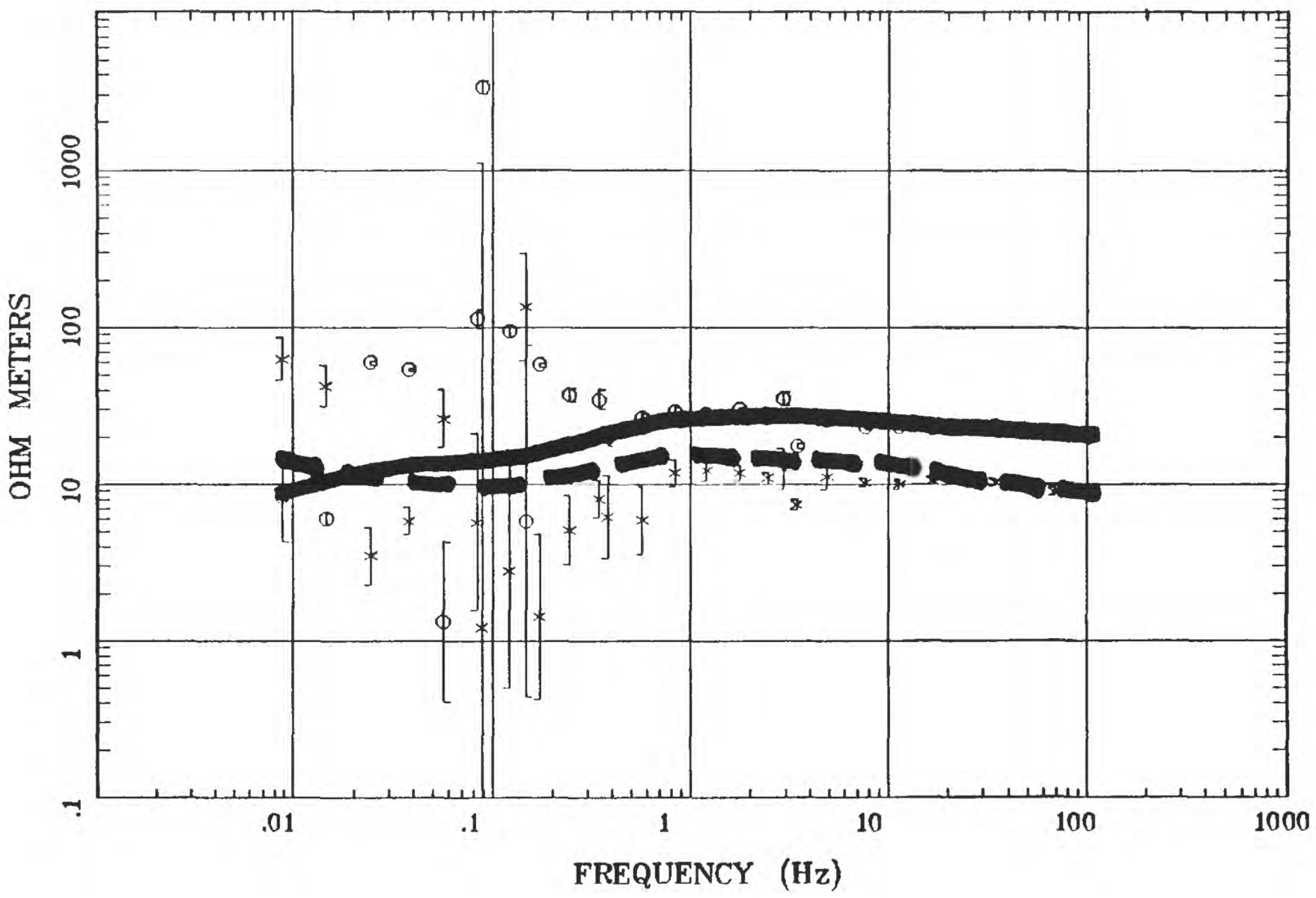

Client:
Remote: local
Acquired: 11:0 Jul 29, 1999
Survey Co:USGS

Rotation:
Filename: hr67.avg
Channels: Ch1 Ch2 Ch3 Ch4 Ch5 Ch3 Ch4
Plotted: 14:57 Feb 06, 2001
< EMI - ElectroMagnetic Instruments >

IMPEDANCE PHASE Boulder Valley, NV

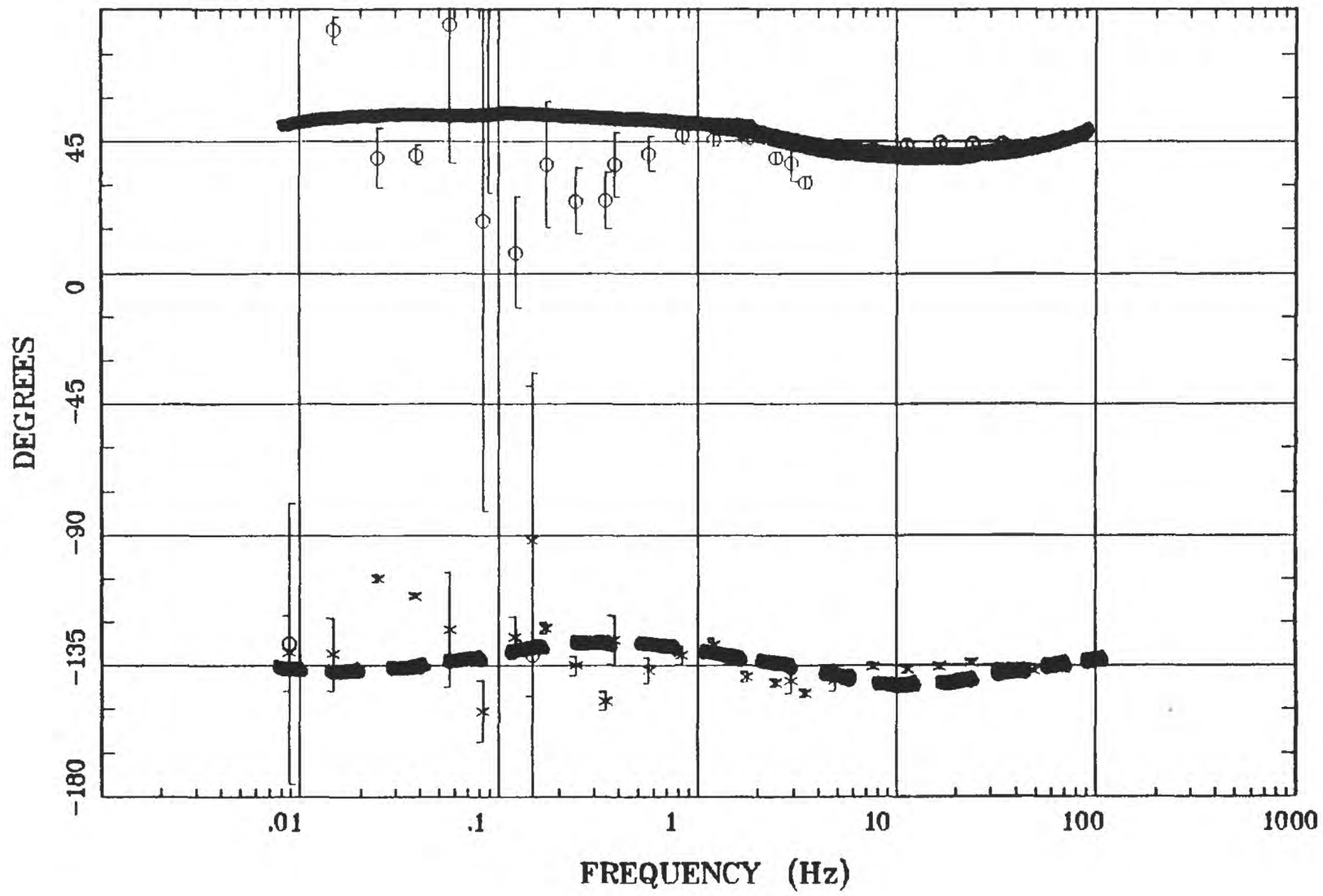

Client:
Remote: local
Acquired: 11:0 Jul 29, 1999
Survey Co:USGS

Rotation:
Filename: hr67.avg
Channels: Ch1 Ch2 Ch3 Ch4 Ch5 Ch3 Ch4
Plotted: 14:57 Feb 06, 2001
< EMI - ElectroMagnetic Instruments >

Station 65

APPARENT RESISTIVITY — Boulder Valley, NV

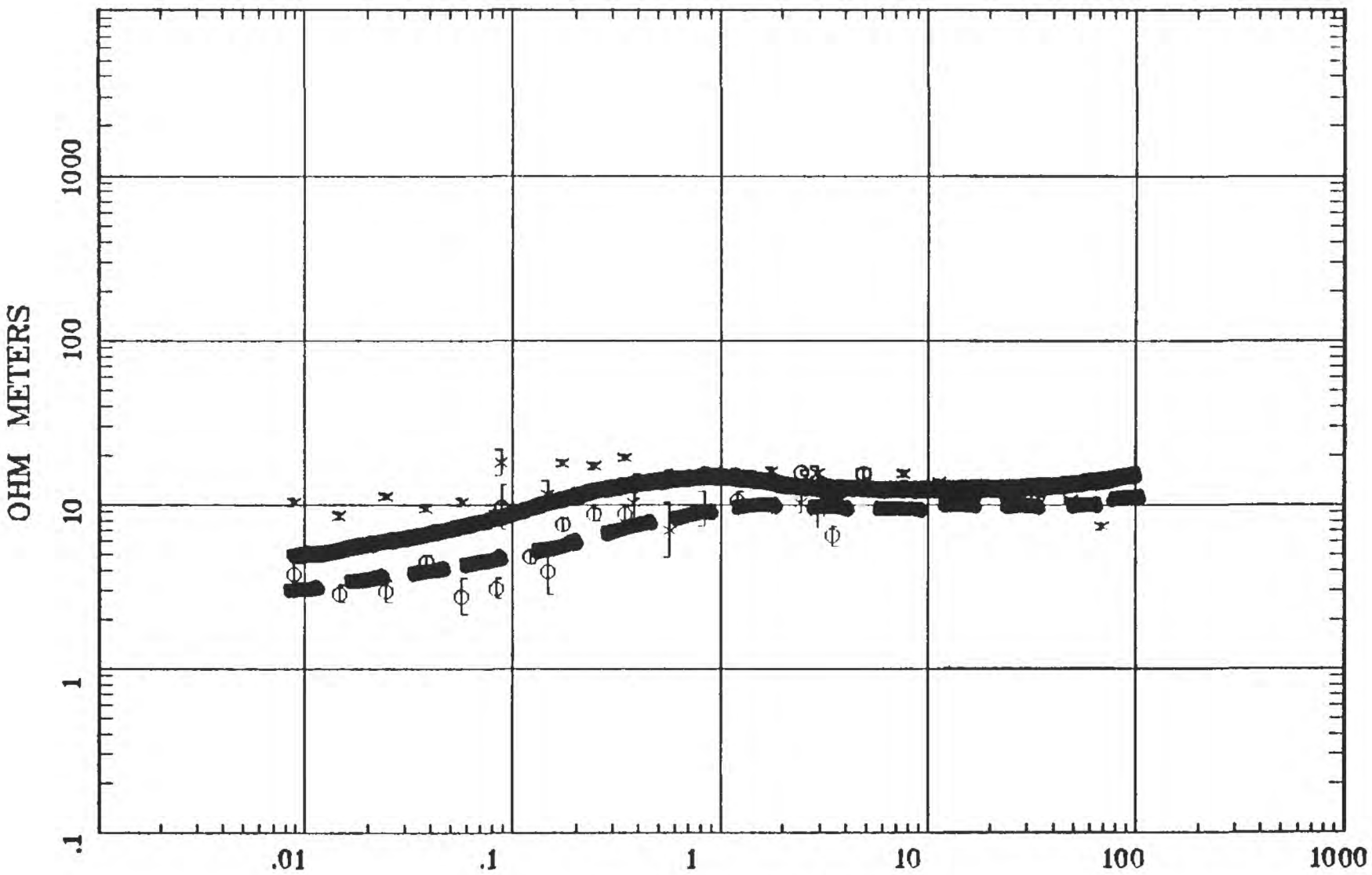

Client:
Remote: local
Acquired: 10:1 Jul 28, 1999
Survey Co:USGS

Rotation:
Filename: hr65.avg
Channels: Ch1 Ch2 Ch3 Ch4 Ch5 Ch3 Ch4
Plotted: 14:57 Feb 06, 2001
< EMI - ElectroMagnetic Instruments >

Station 65

IMPEDANCE PHASE Boulder Valley, NV

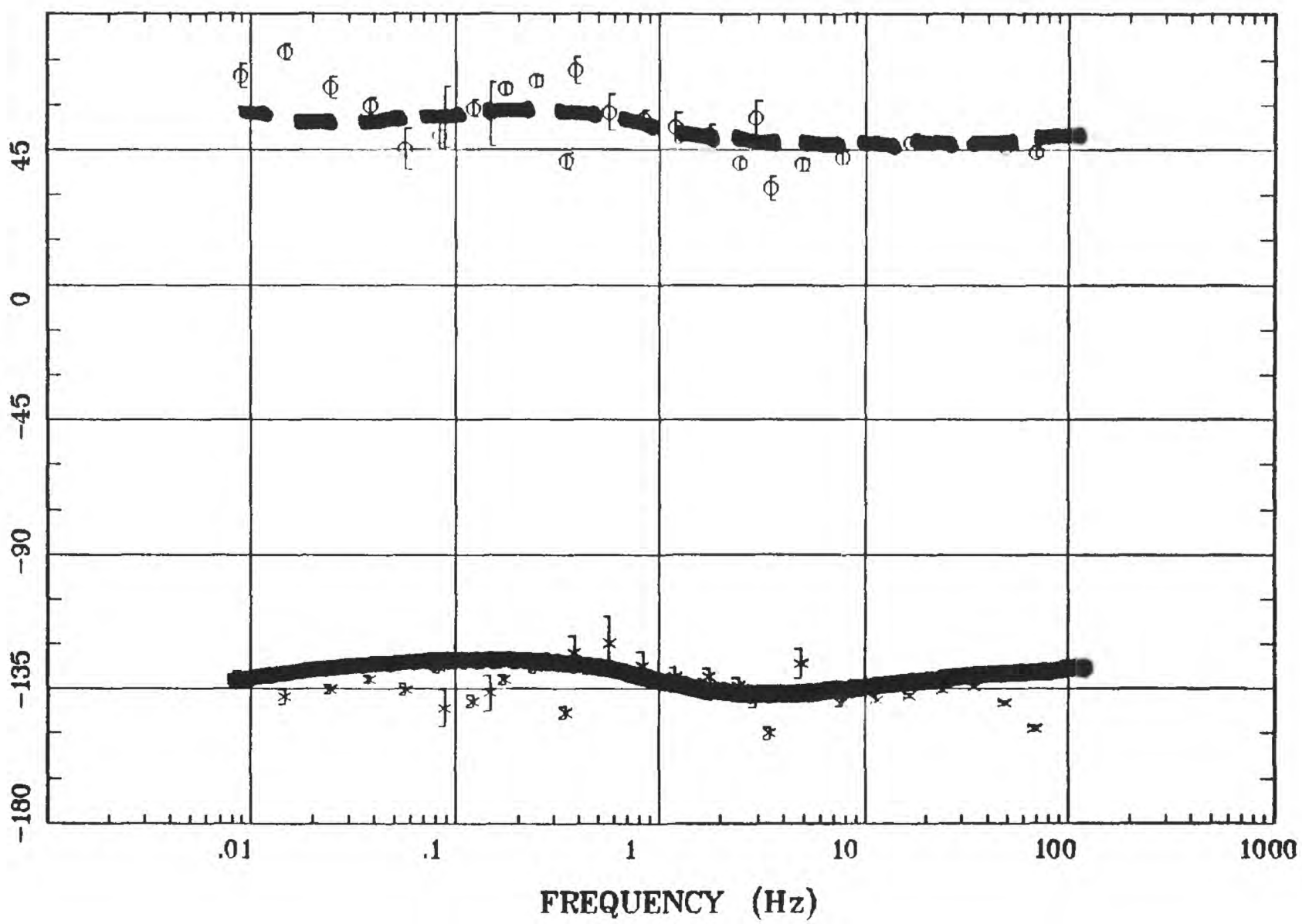

Client:
Remote: local
Acquired: 10:1 Jul 28, 1999
Survey Co:USGS

Rotation:
Filename: hr65.avg
Channels: Ch1 Ch2 Ch3 Ch4 Ch5 Ch3 Ch4
Plotted: 14:57 Feb 06, 2001
< EMI - ElectroMagnetic Instruments >

APPARENT RESISTIVITY Boulder Valley, NV

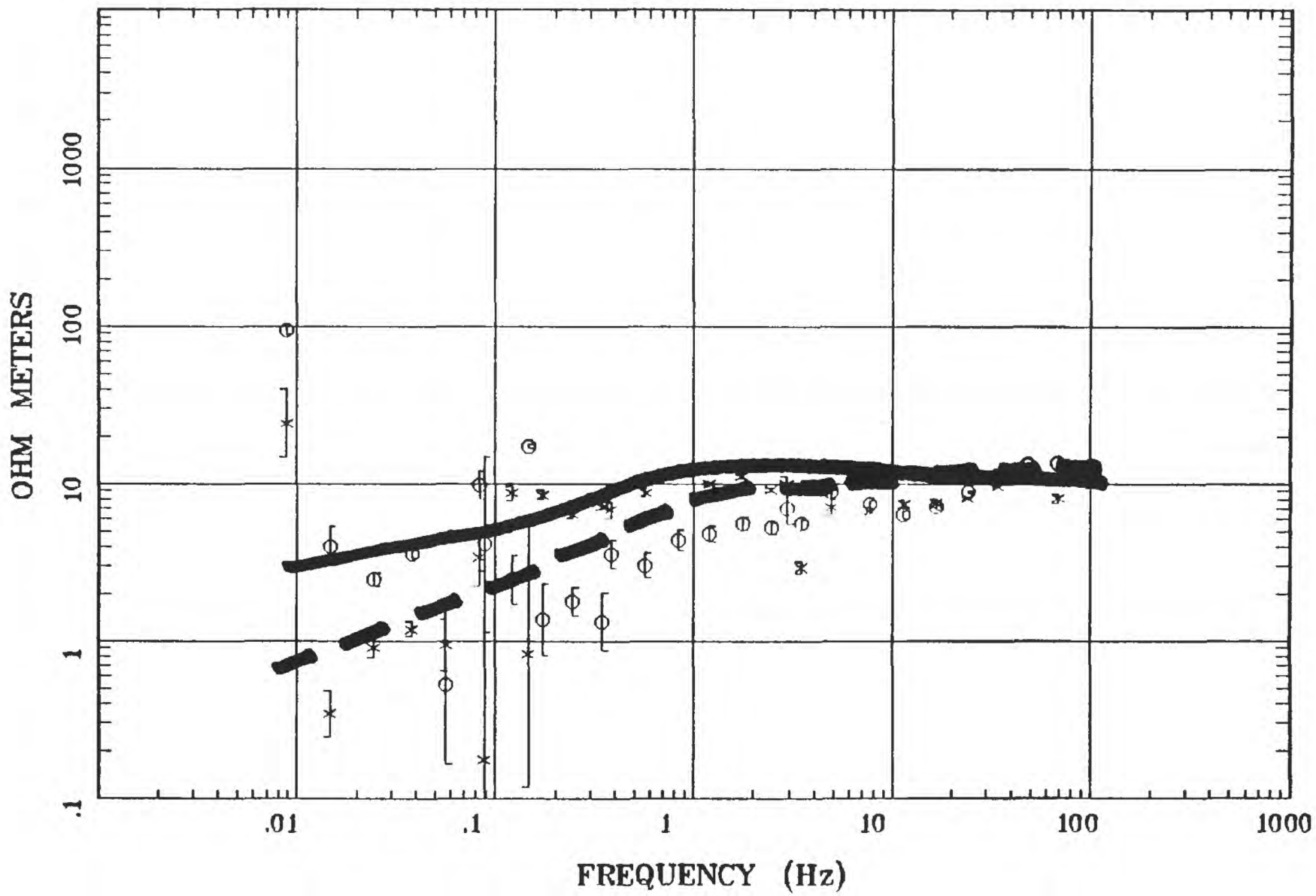

Client:
Remote: local
Acquired: 15:2 Jul 27, 1999
Survey Co:USGS

Rotation:
Filename: hr64.avg
Channels: Ch1 Ch2 Ch3 Ch4 Ch5 Ch3 Ch4
Plotted: 14:58 Feb 06, 2001
< EMI - ElectroMagnetic Instruments >

Station 64

IMPEDANCE PHASE Boulder Valley, NV

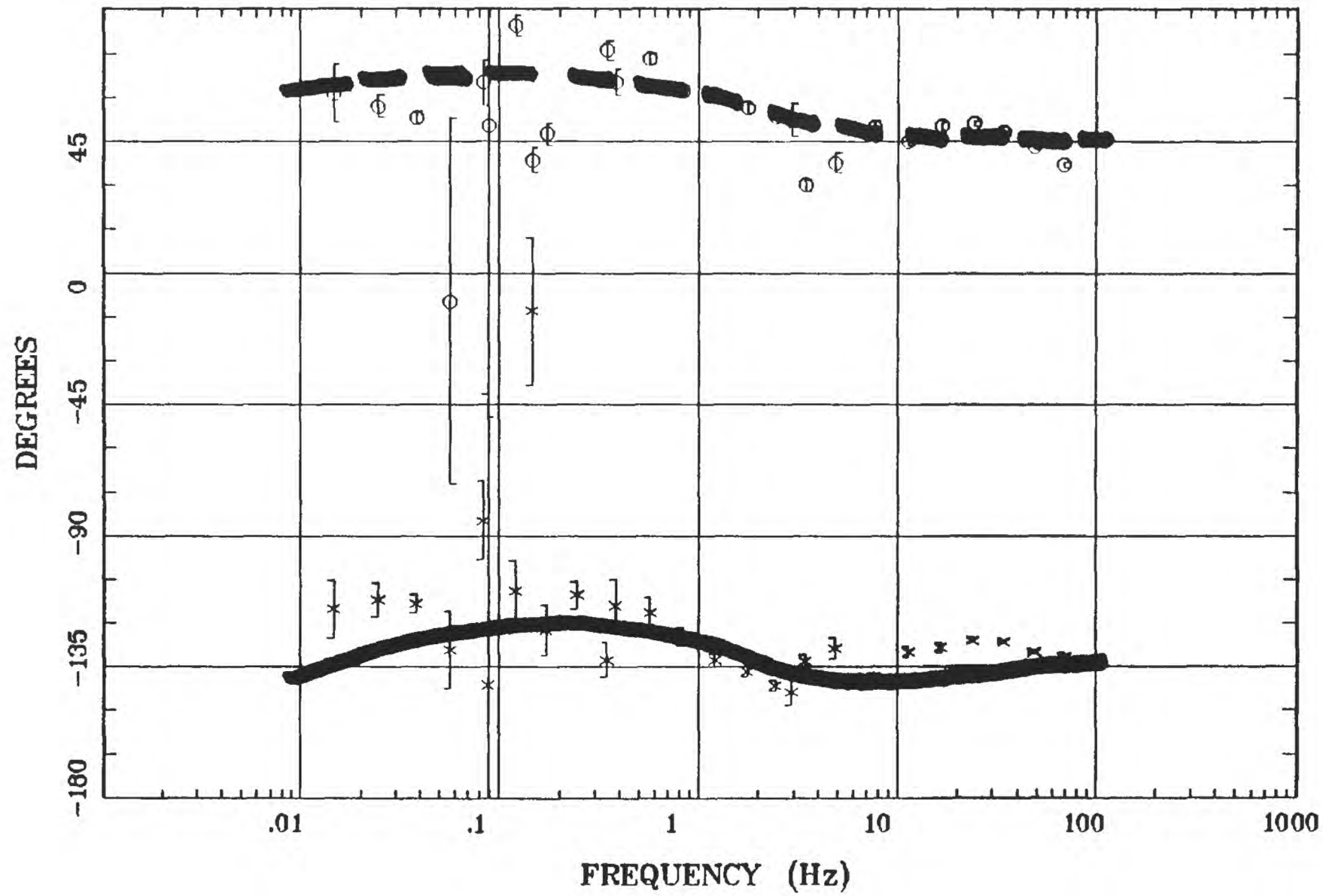

Client:
Remote: local
Acquired: 15:2 Jul 27, 1999
Survey Co:USGS

Rotation:
Filename: hr64.avg
Channels: Ch1 Ch2 Ch3 Ch4 Ch5 Ch3 Ch4
Plotted: 14:58 Feb 06, 2001
< EMI - ElectroMagnetic Instruments >

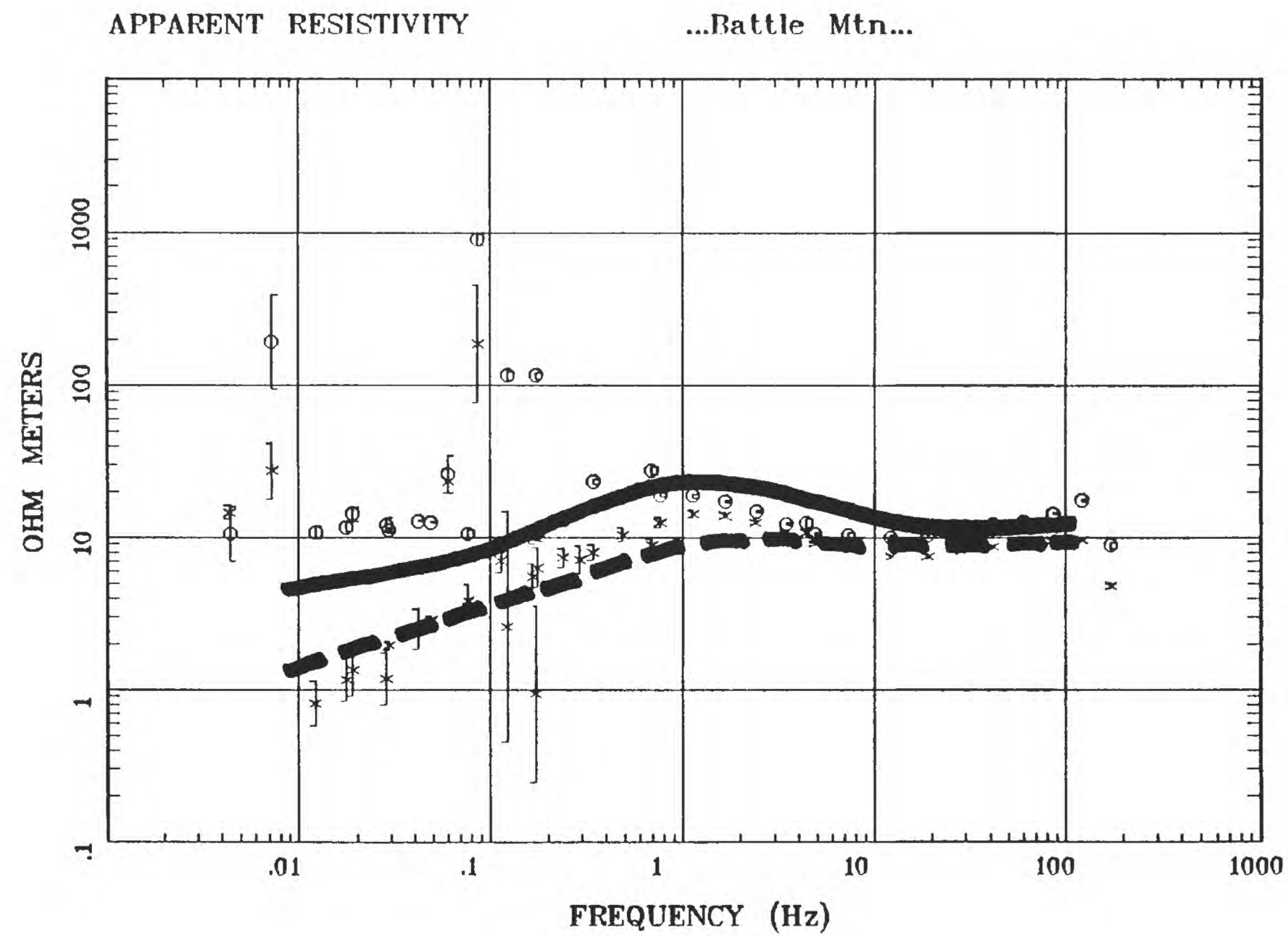

Client:
Remote: E local ref.
Acquired: 18:4 Jul 21, 1997
Survey Co:

Rotation:
Filename: nn28.all
Channels: Ch6 Ch7 Ch8 Ch9 Ch10Ch1 Ch2
Plotted: 08:44 Dec 08, 2000
< EMI - ElectroMagnetic Instruments >

Station 28A

IMPEDANCE PHASE ...Battle Mtn...

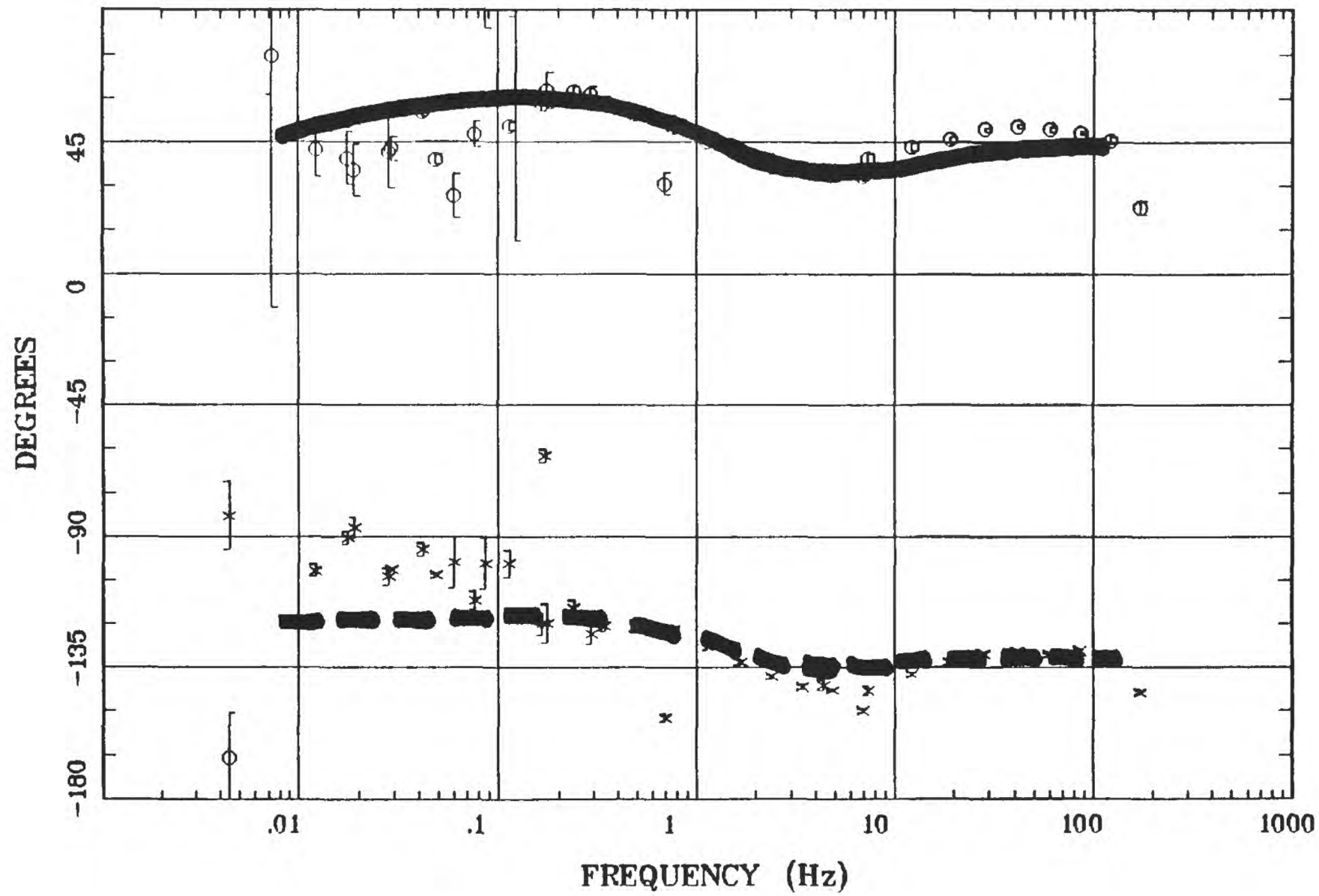

Client:
Remote: E local ref.
Acquired: 18:4 Jul 21, 1997
Survey Co:

Rotation:
Filename: nn28.all
Channels: Ch6 Ch7 Ch8 Ch9 Ch10Ch1 Ch2
Plotted: 08:44 Dec 08, 2000
< EMI - ElectroMagnetic Instruments >

APPENDIX C

OBSERVED AND CALCULATED DATA - PROFILE MT7

Magnetotelluric (MT) observed (circle and x symbols) and calculated (solid and dashed lines are TE and TM modes, respectively) resistivity and phase data for profile MT7. See the "Magnetotelluric Data" section of this report for a description of the observed data and the "Resistivity Models" section for a description of the calculated data.

Station 63

APPARENT RESISTIVITY Boulder Valley, NV

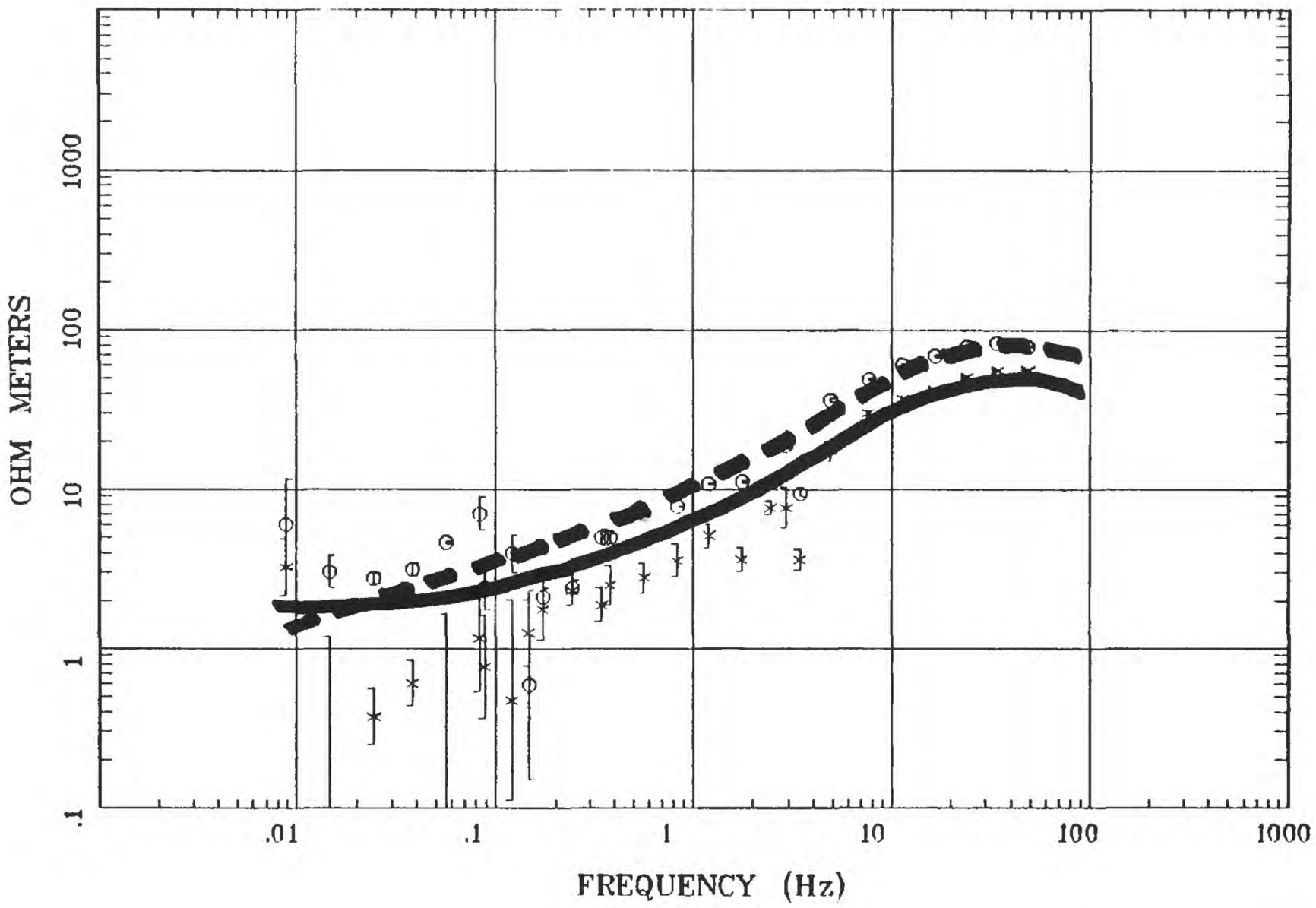

Client:
Remote: local
Acquired: 11:2 Jul 27, 1999
Survey Co:USGS

Rotation:
Filename: hr63.avg
Channels: Ch1 Ch2 Ch3 Ch4 Ch5 Ch3 Ch4
Plotted: 10:06 Mar 08, 2001
< EMI - ElectroMagnetic Instruments >

Station 63

IMPEDANCE PHASE — Boulder Valley, NV

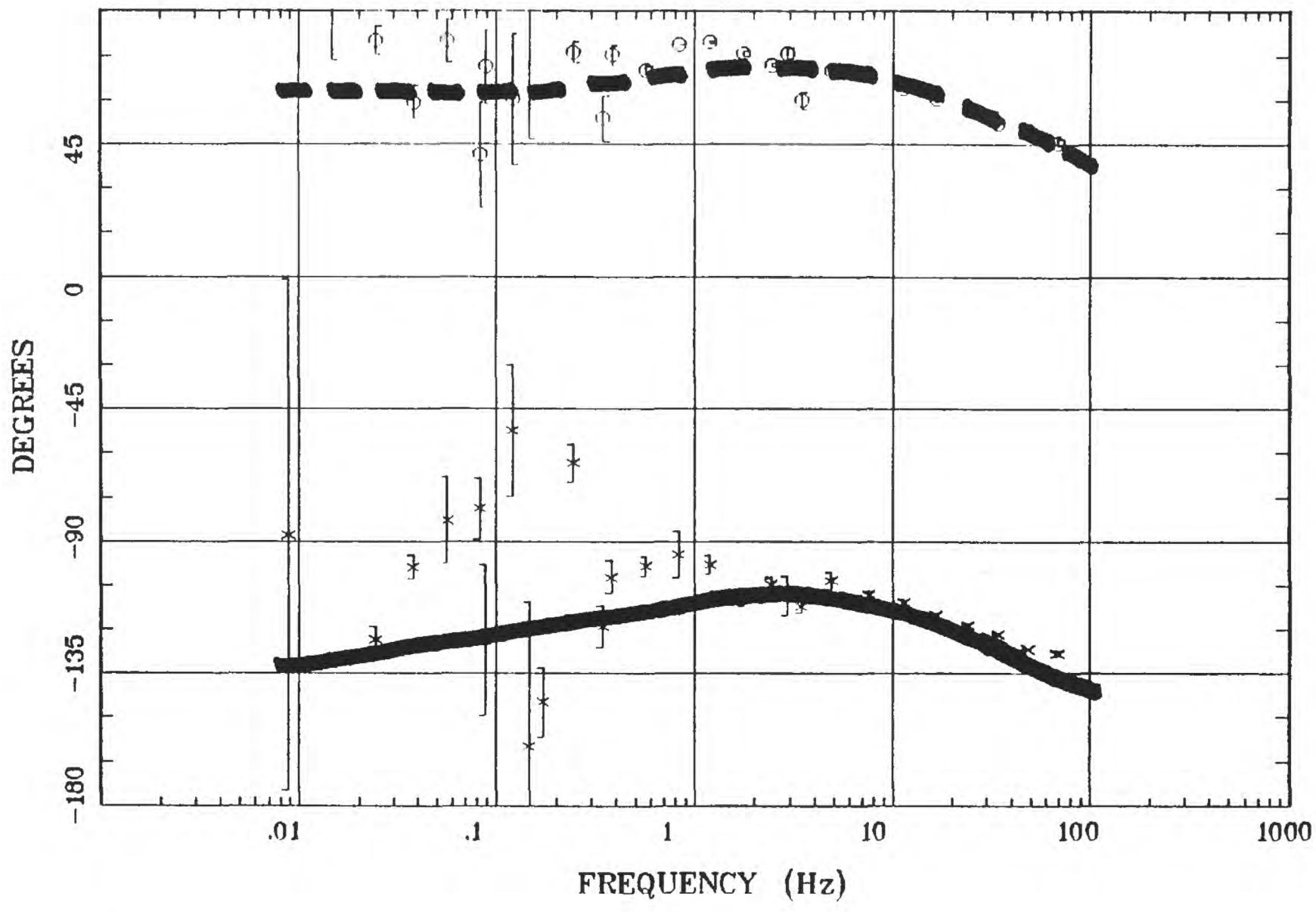

Client:
Remote: local
Acquired: 11:2 Jul 27, 1999
Survey Co:USGS

Rotation:
Filename: hr63.avg
Channels: Ch1 Ch2 Ch3 Ch4 Ch5 Ch3 Ch4
Plotted: 10:06 Mar 08, 2001
< EMI - ElectroMagnetic Instruments >

Station 64

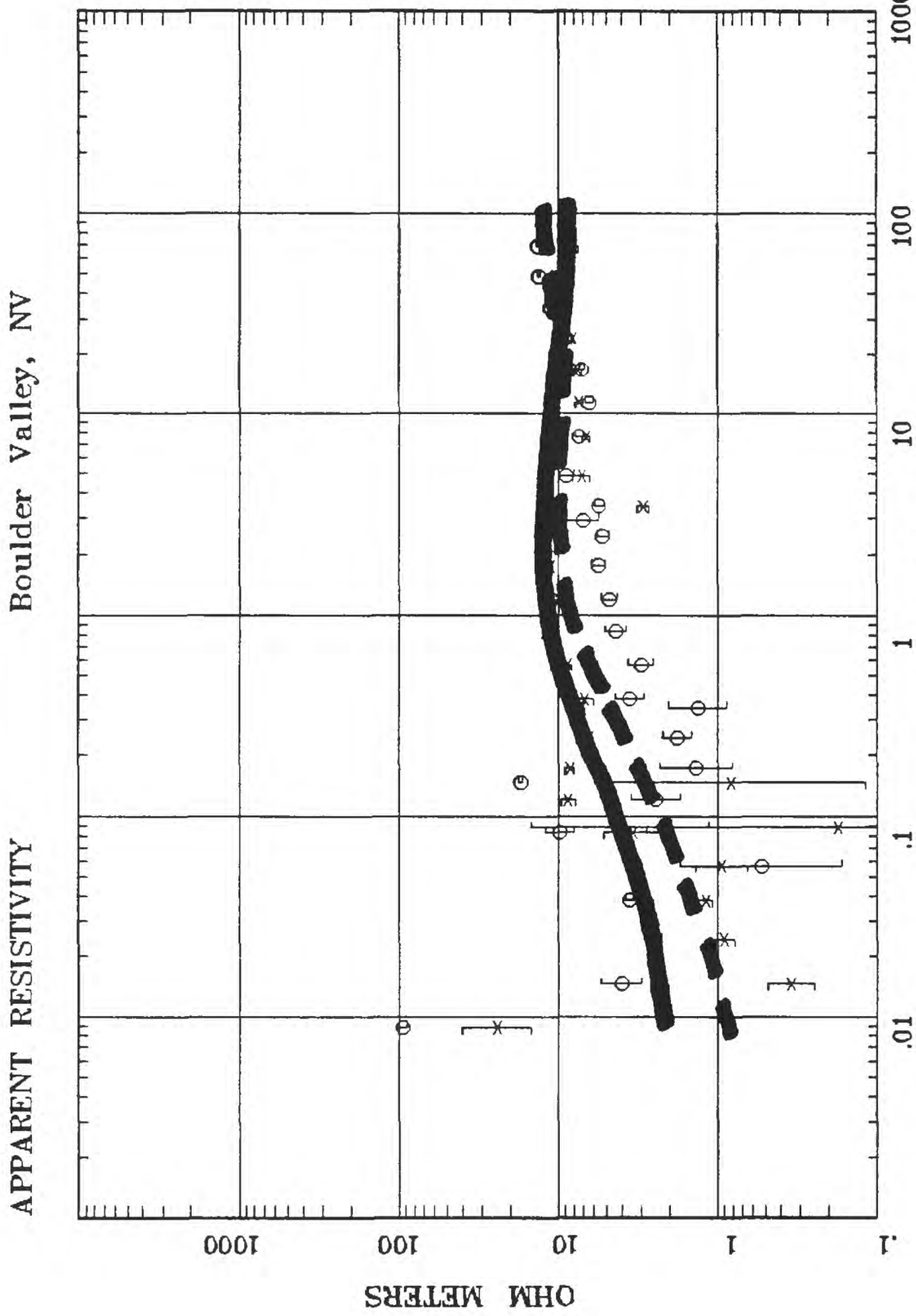

Rotation:
Filename: hr64.avg
Channels: Ch1 Ch2 Ch3 Ch4 Ch5 Ch3 Ch4
Plotted: 14:58 Feb 06, 2001
< EMI - ElectroMagnetic Instruments >

Client:
Remote: local
Acquired: 15:2 Jul 27, 1999
Survey Co:USGS

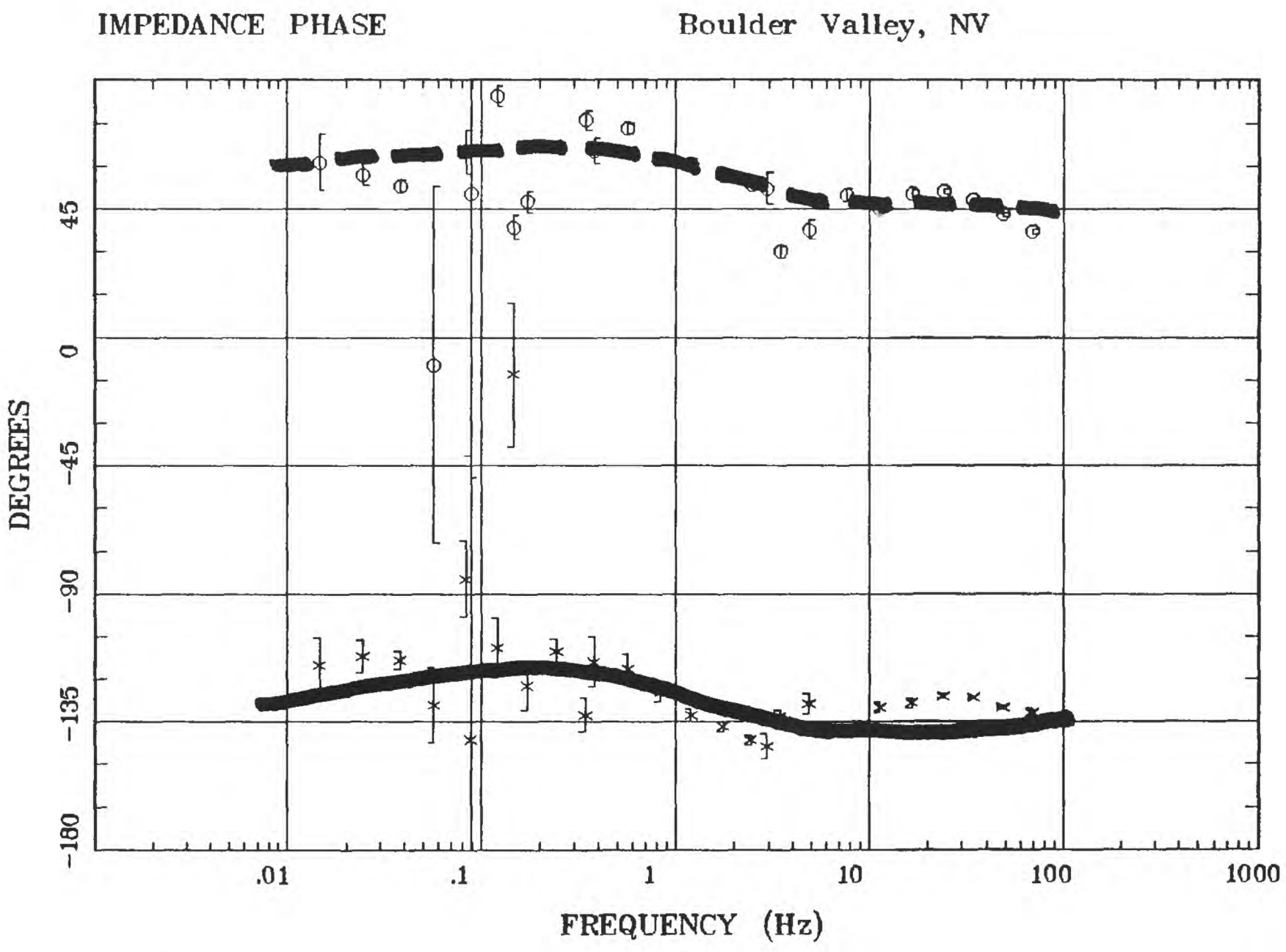

Client:
Remote: local
Acquired: 15:2 Jul 27, 1999
Survey Co:USGS

Rotation:
Filename: hr64.avg
Channels: Ch1 Ch2 Ch3 Ch4 Ch5 Ch3 Ch4
Plotted: 14:58 Feb 06, 2001
< EMI - ElectroMagnetic Instruments >

Station 28A

APPARENT RESISTIVITY ...Battle Mtn...

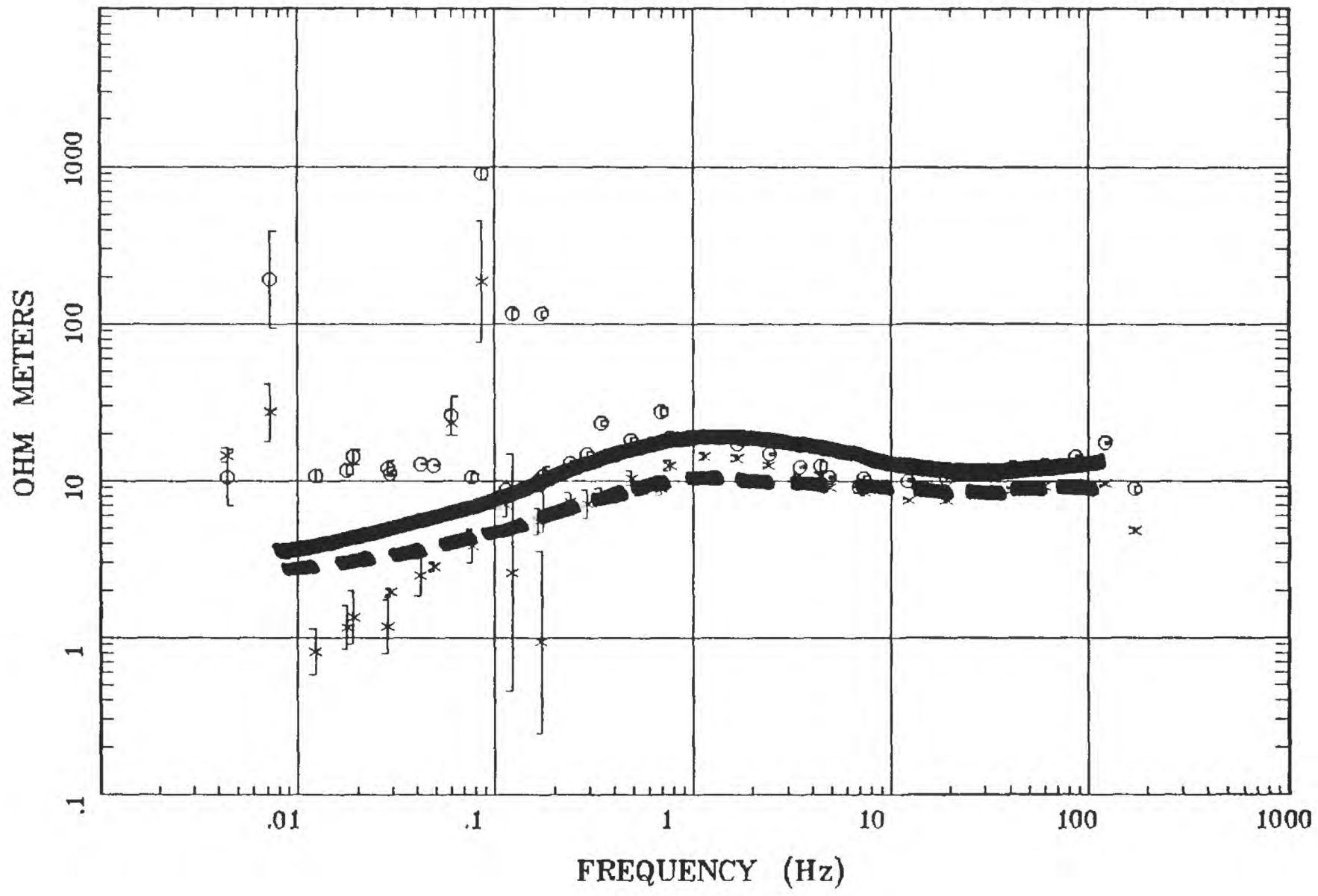

Client:
Remote: E local ref.
Acquired: 18:4 Jul 21, 1997
Survey Co:

Rotation:
Filename: nn28.all
Channels: Ch6 Ch7 Ch8 Ch9 Ch10Ch1 Ch2
Plotted: 08:44 Dec 08, 2000
< EMI - ElectroMagnetic Instruments >

Station 28A

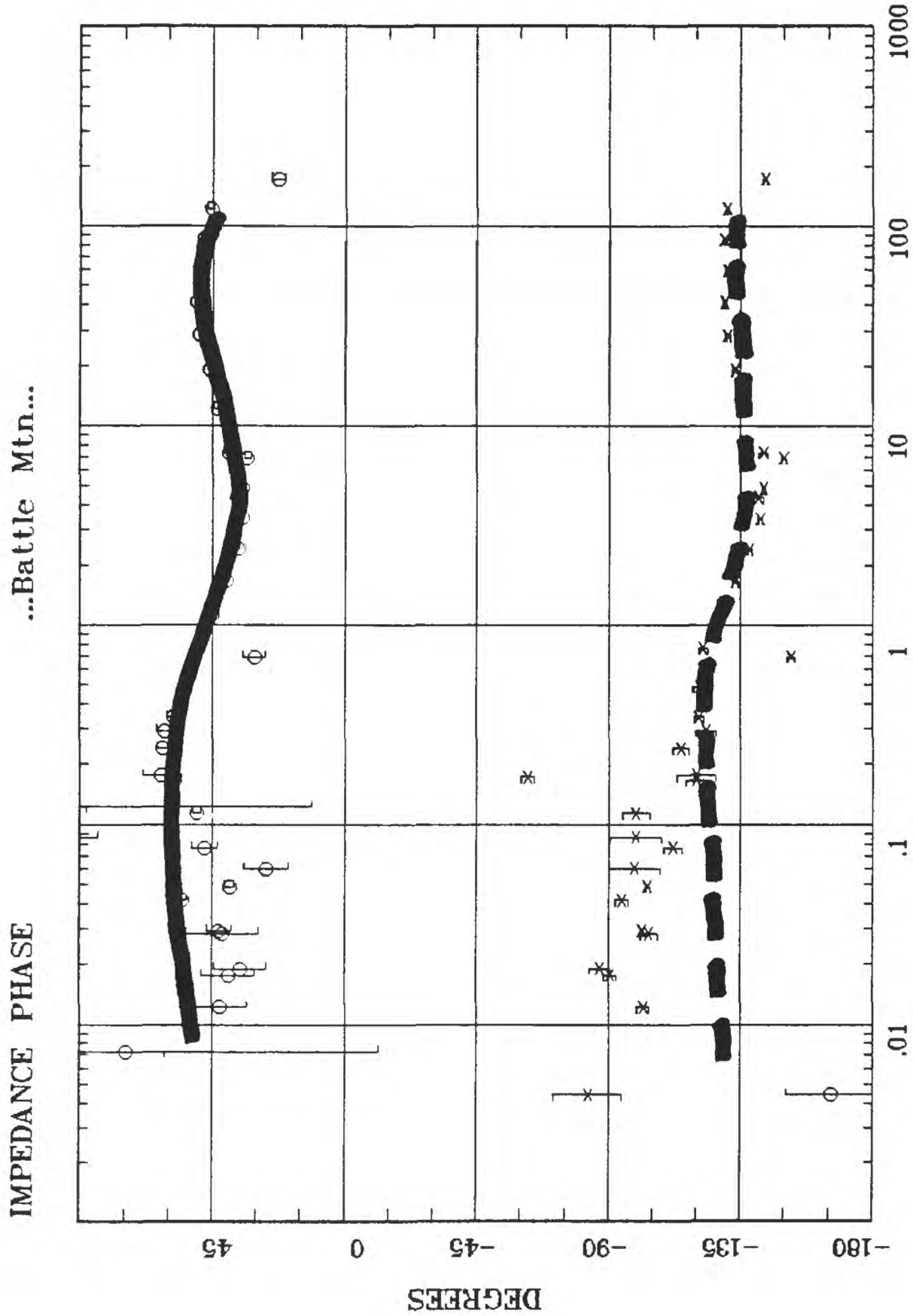
...Battle Mtn...
IMPEDANCE PHASE
DEGREES
45
0
-45
-90
-135
-180
.01
.1
1
10
100
1000
FREQUENCY (Hz)
Rotation:
Filename: nn28.all
Channels: Ch6 Ch7 Ch8 Ch9 Ch10Ch1 Ch2
Plotted: 08:44 Dec 08, 2000
< EMI - ElectroMagnetic Instruments >
Client:
Remote: E local ref.
Acquired: 18:4 Jul 2
Survey Co:

77

Station 66

APPARENT RESISTIVITY

Boulder Valley, NV

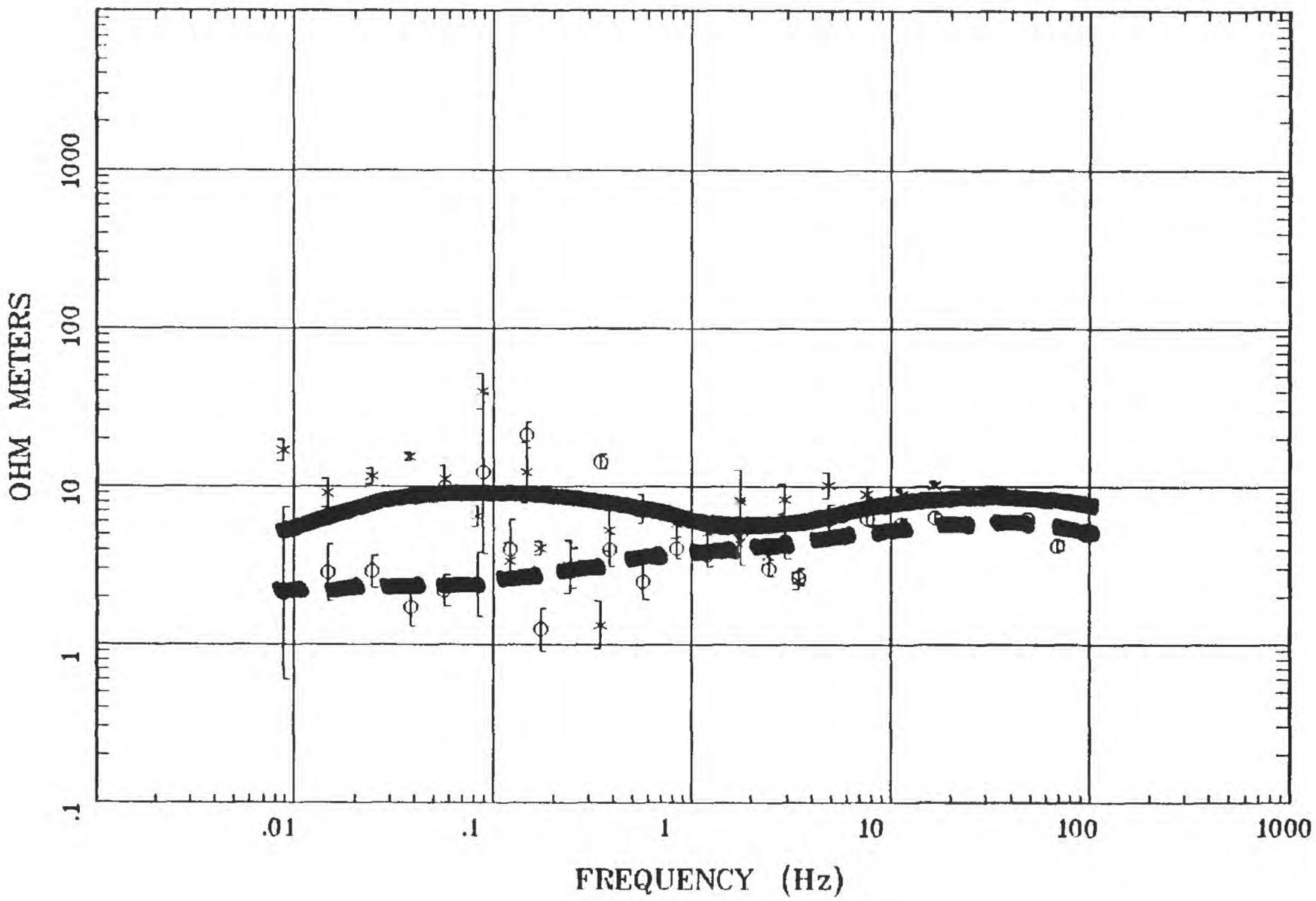

Client:
Remote: local
Acquired: 13:5 Jul 28, 1999
Survey Co:USGS

Rotation:
Filename: hr66.avg
Channels: Ch1 Ch2 Ch3 Ch4 Ch5 Ch3 Ch4
Plotted: 10:12 Mar 08, 2001
EMI - ElectroMagnetic Instruments >

IMPEDANCE PHASE Boulder Valley, NV **Station 66**

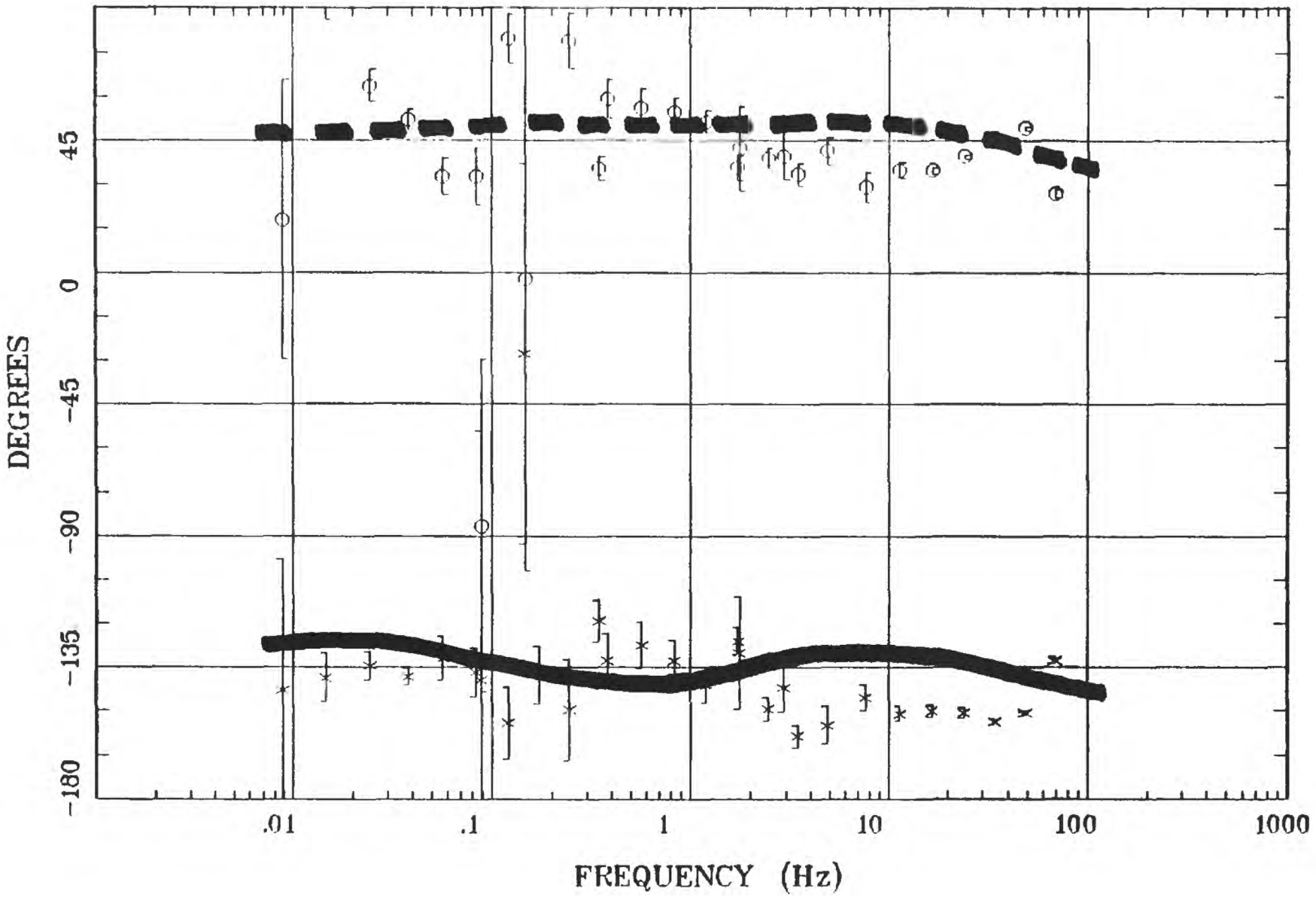

Client:
Remote: local
Acquired: 13:5 Jul 28, 1999
Survey Co:USGS

Rotation:
Filename: hr66.avg
Channels: Ch1 Ch2 Ch3 Ch4 Ch5 Ch3 Ch4
Plotted: 10:12 Mar 08, 2001
< EMI - ElectroMagnetic Instruments >

Station 68

APPARENT RESISTIVITY Boulder Valley, NV

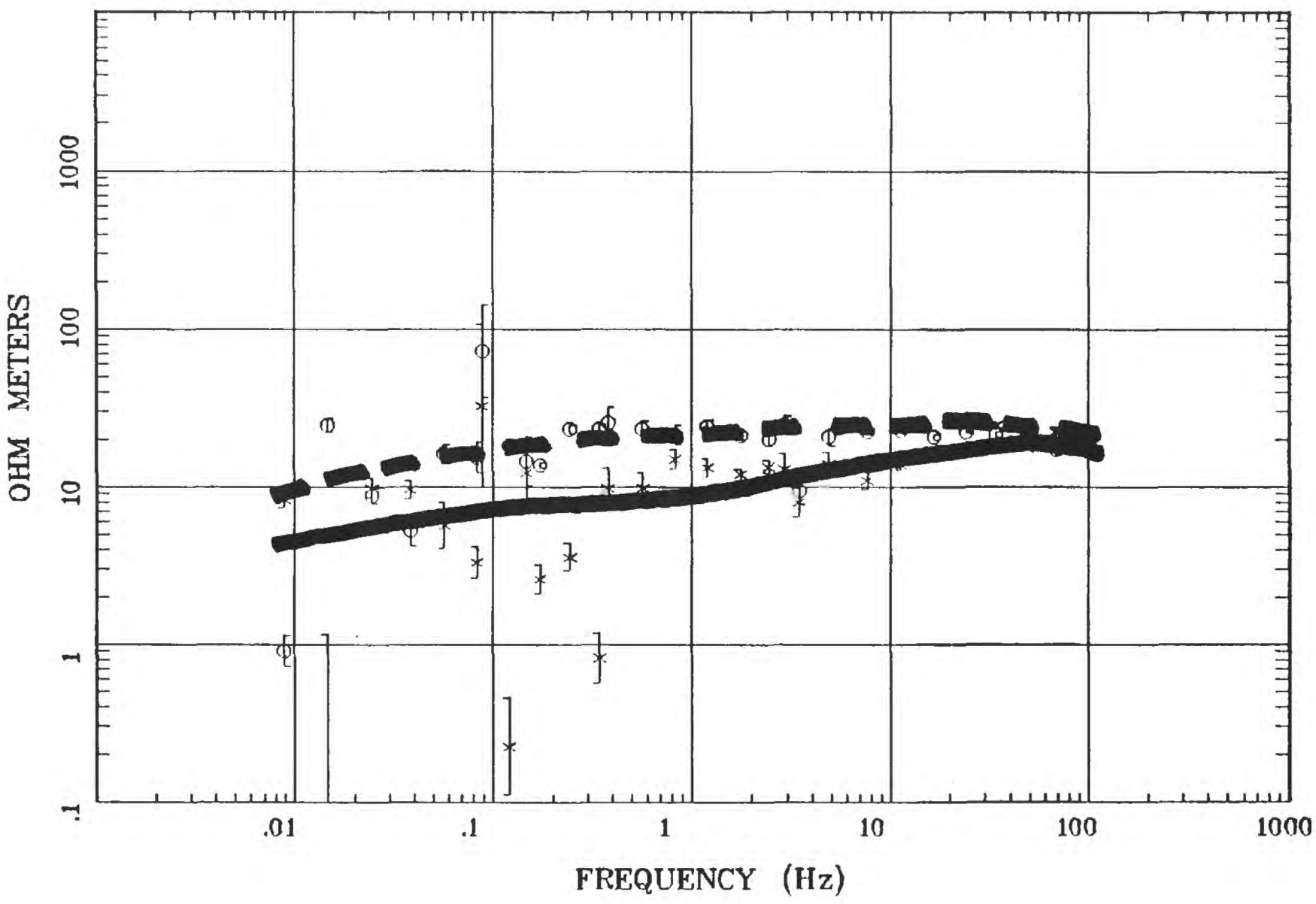

Client:
Remote: local
Acquired: 17:4 Jul 29, 1999
Survey Co:USGS

Rotation:
Filename: hr68c.avg
Channels: Ch1 Ch2 Ch3 Ch4 Ch5 Ch3 Ch4
Plotted: 10:07 Mar 08, 2001
< EMI - ElectroMagnetic Instruments >

IMPEDANCE PHASE

Boulder Valley, NV

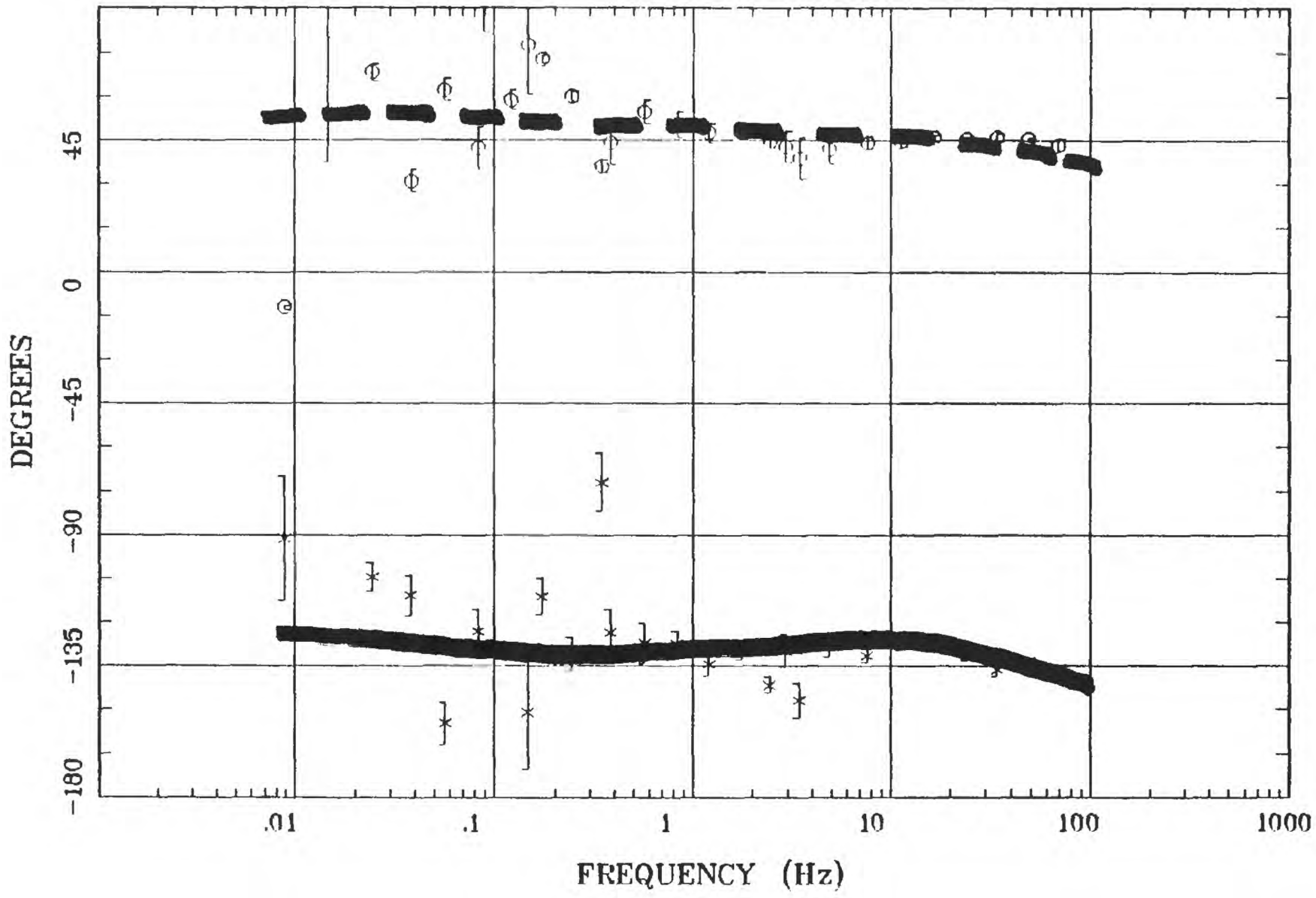

Client:
Remote: local
Acquired: 17:4 Jul 29, 1999
Survey Co:USGS

Rotation:
Filename: hr68c.avg
Channels: Ch1 Ch2 Ch3 Ch4 Ch5 Ch3 Ch4
Plotted: 10:07 Mar 08, 2001
< EMI - ElectroMagnetic Instruments >

APPARENT RESISTIVITY Boulder Valley, NV

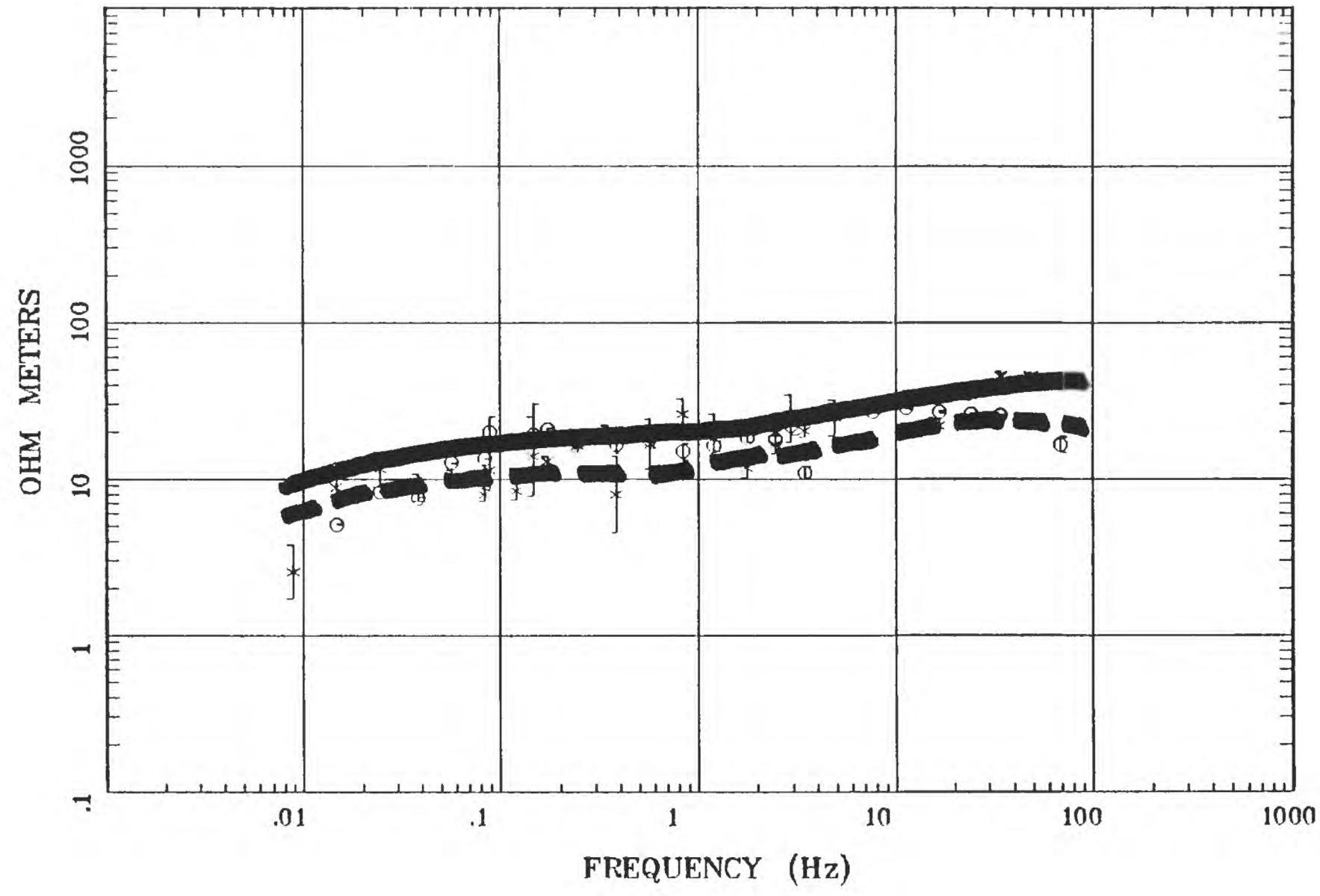

Client:
Remote: local
Acquired: 10:3 Jul 30, 1999
Survey Co:USGS

Rotation:
Filename: hr69.avg
Channels: Ch1 Ch2 Ch3 Ch4 Ch5 Ch3 Ch4
Plotted: 10:07 Mar 08, 2001
< EMI - ElectroMagnetic Instruments >

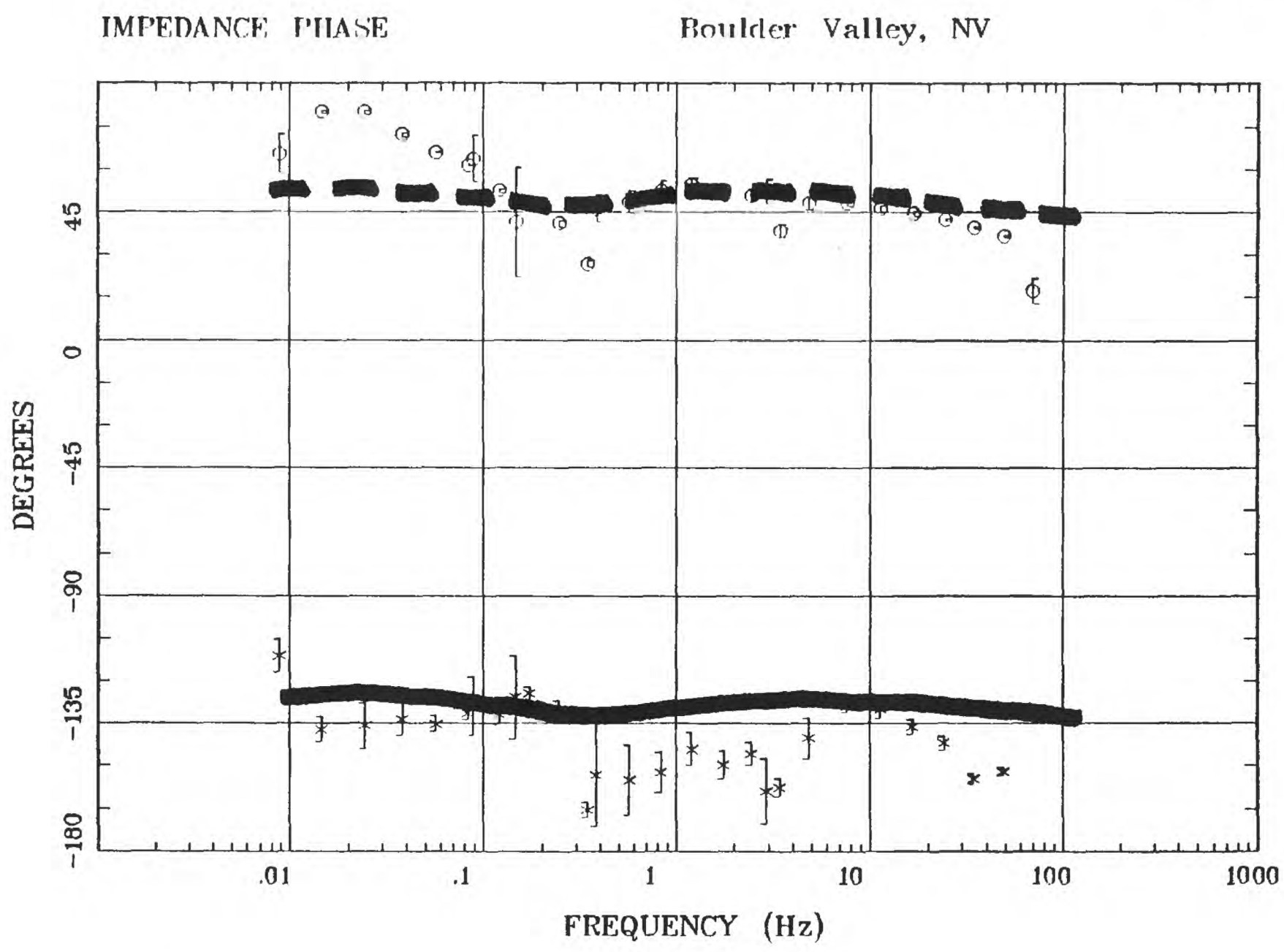

Client:
Remote: local
Acquired: 10:3 Jul 30, 1999
Survey Co:USGS

Rotation:
Filename: hr69.avg
Channels: Ch1 Ch2 Ch3 Ch4 Ch5 Ch3 Ch4
Plotted: 10:07 Mar 08, 2001
< EMI - ElectroMagnetic Instruments >

APPARENT RESISTIVITY Boulder Valley, NV

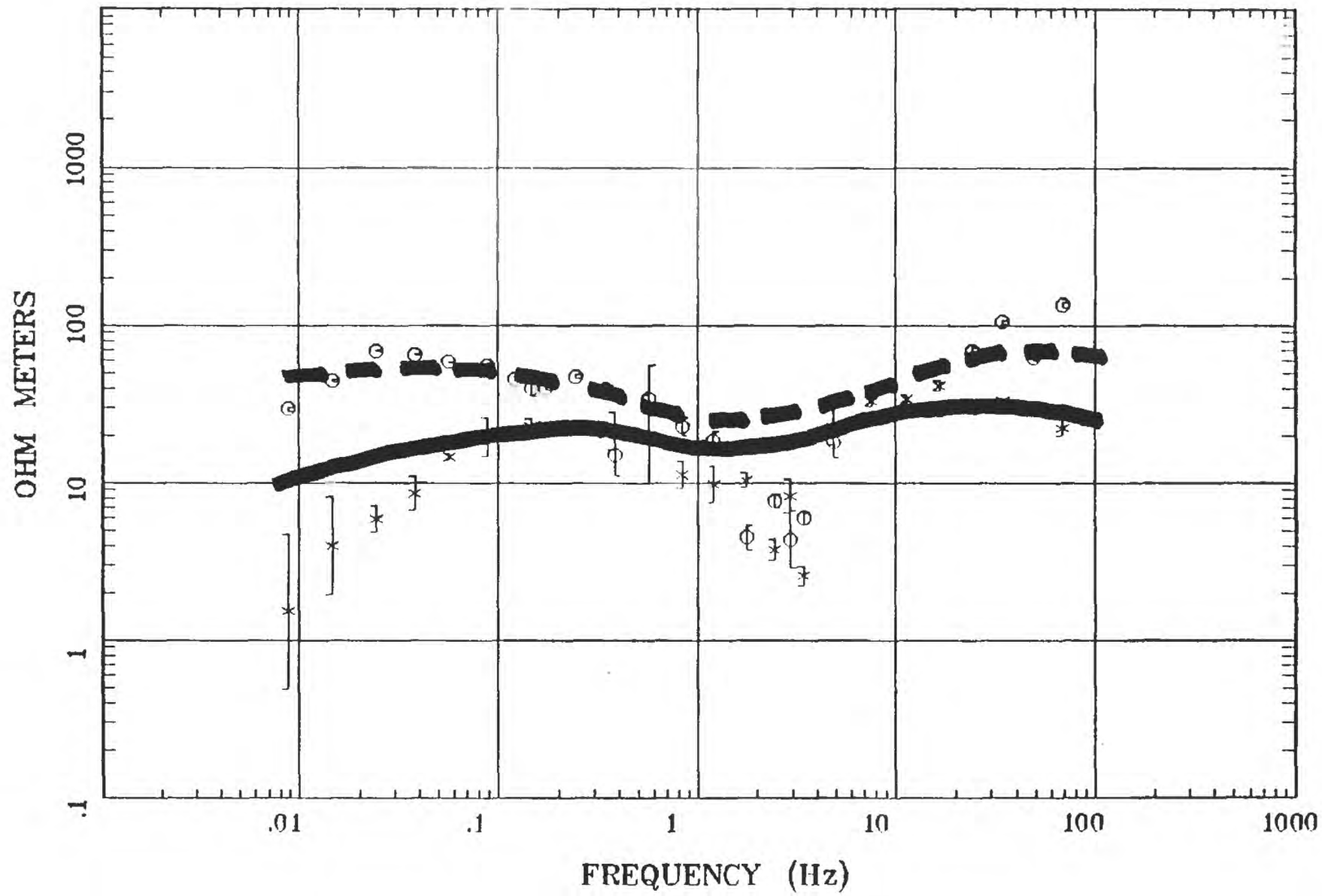

Client:
Remote: local
Acquired: 14:2 Jul 30, 1999
Survey Co:USGS

Rotation:
Filename: hr70.avg
Channels: Ch1 Ch2 Ch3 Ch4 Ch5 Ch3 Ch4
Plotted: 10:08 Mar 08, 2001
< EMI - ElectroMagnetic Instruments >

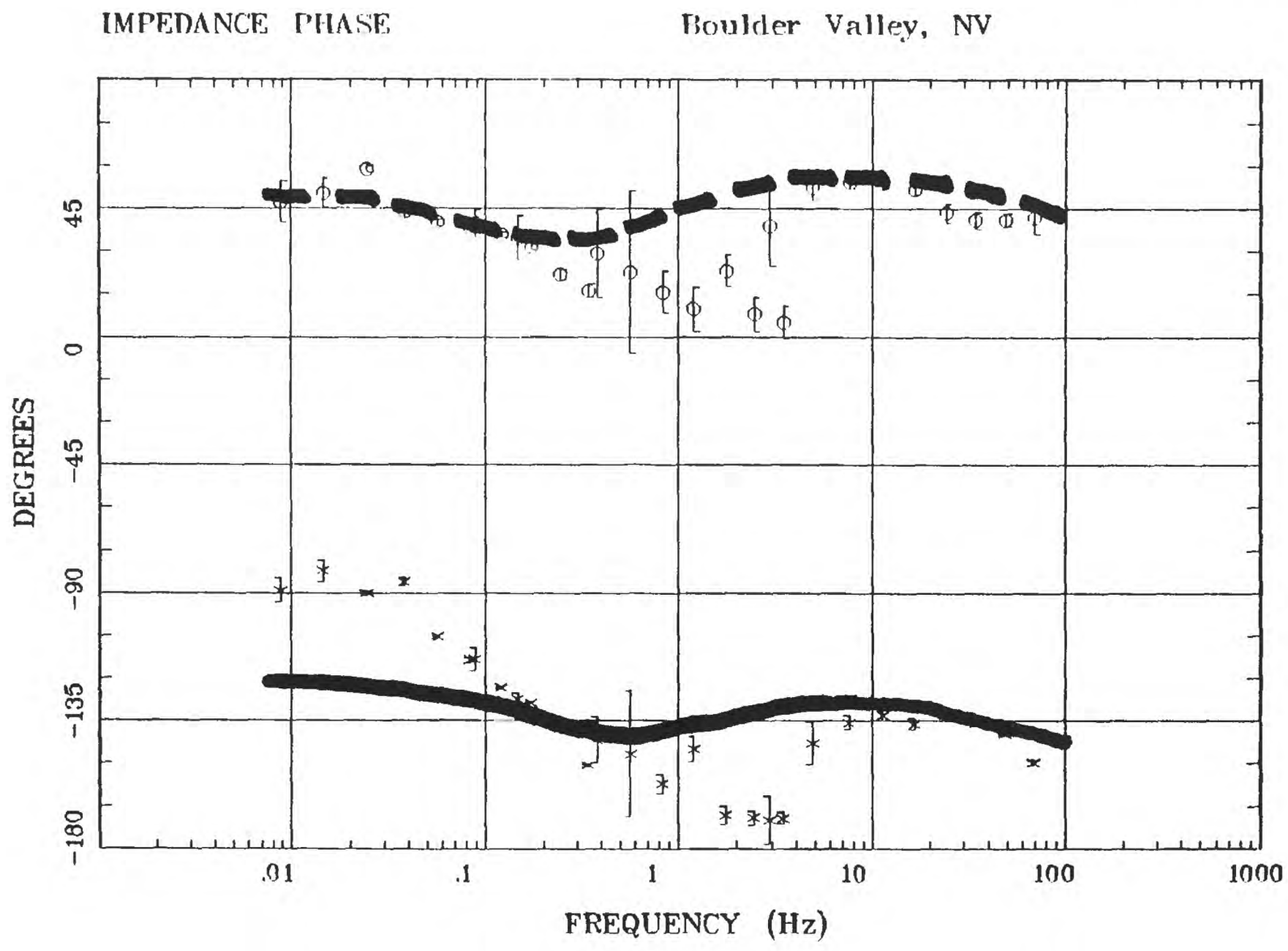

Client:
Remote: local
Acquired: 14:2 Jul 30, 1999
Survey Co:USGS

Rotation:
Filename: hr70.avg
Channels: Ch1 Ch2 Ch3 Ch4 Ch5 Ch3 Ch4
Plotted: 10:08 Mar 08, 2001
< EMI - ElectroMagnetic Instruments >

APPENDIX D

OBSERVED AND CALCULATED DATA - PROFILE MT8

Magnetotelluric (MT) observed (circle and x symbols) and calculated (solid and dashed lines are TE and TM modes, respectively) resistivity and phase data for profile MT8. See the "Magnetotelluric Data" section of this report for a description of the observed data and the "Resistivity Models" section for a description of the calculated data.

APPARENT RESISTIVITY Boulder Valley, NV **Station 76**

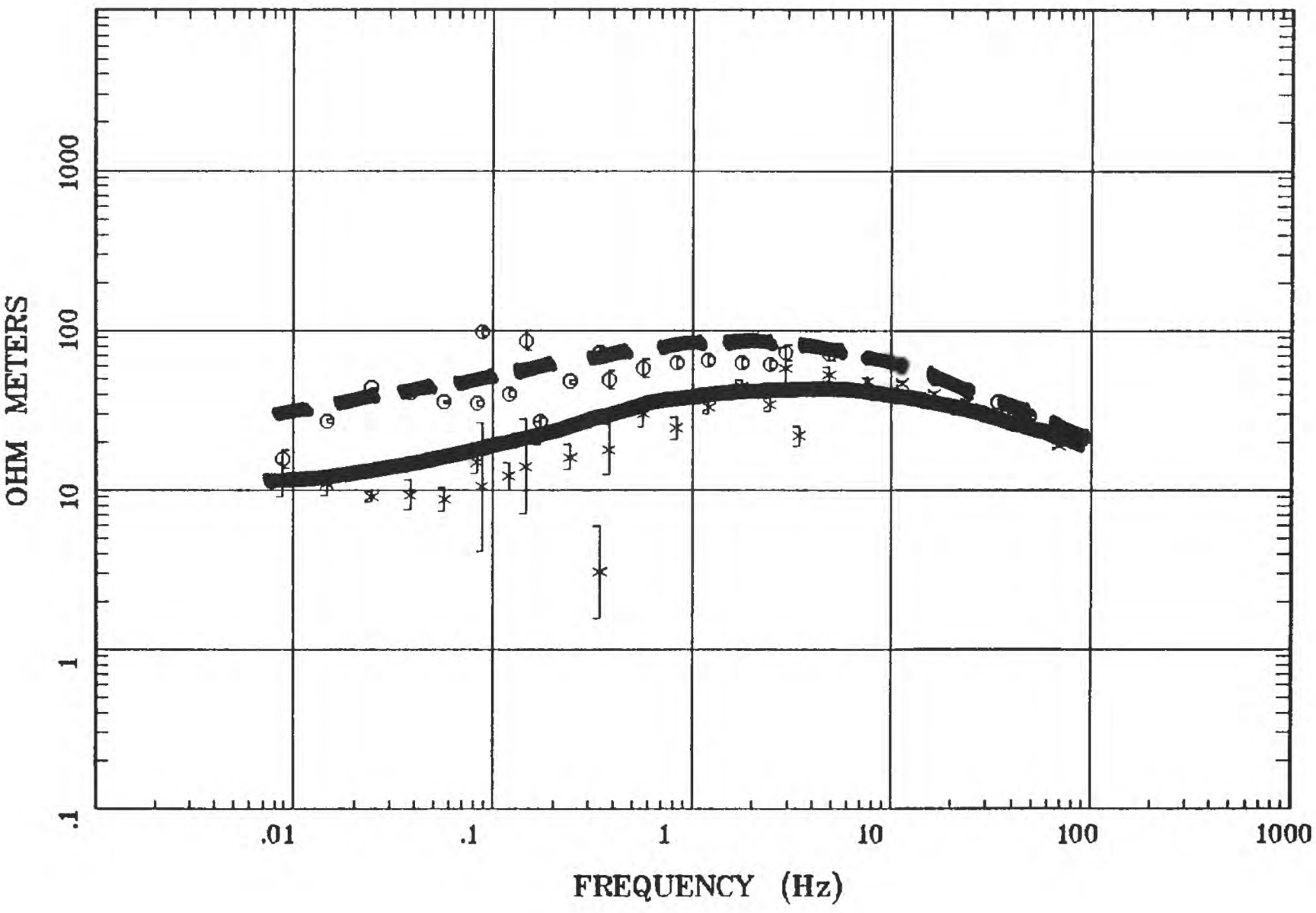

Client:
Remote: none
Acquired: 12:0 Aug 02, 1999
Survey Co:USGS

Rotation:
Filename: hr76.avg
Channels: Ch1 Ch2 Ch3 Ch4 Ch5 Ch3 Ch4
Plotted: 12:25 Jan 25, 2001
< EMI - ElectroMagnetic Instruments >

IMPEDANCE PHASE Boulder Valley, NV **Station 76**

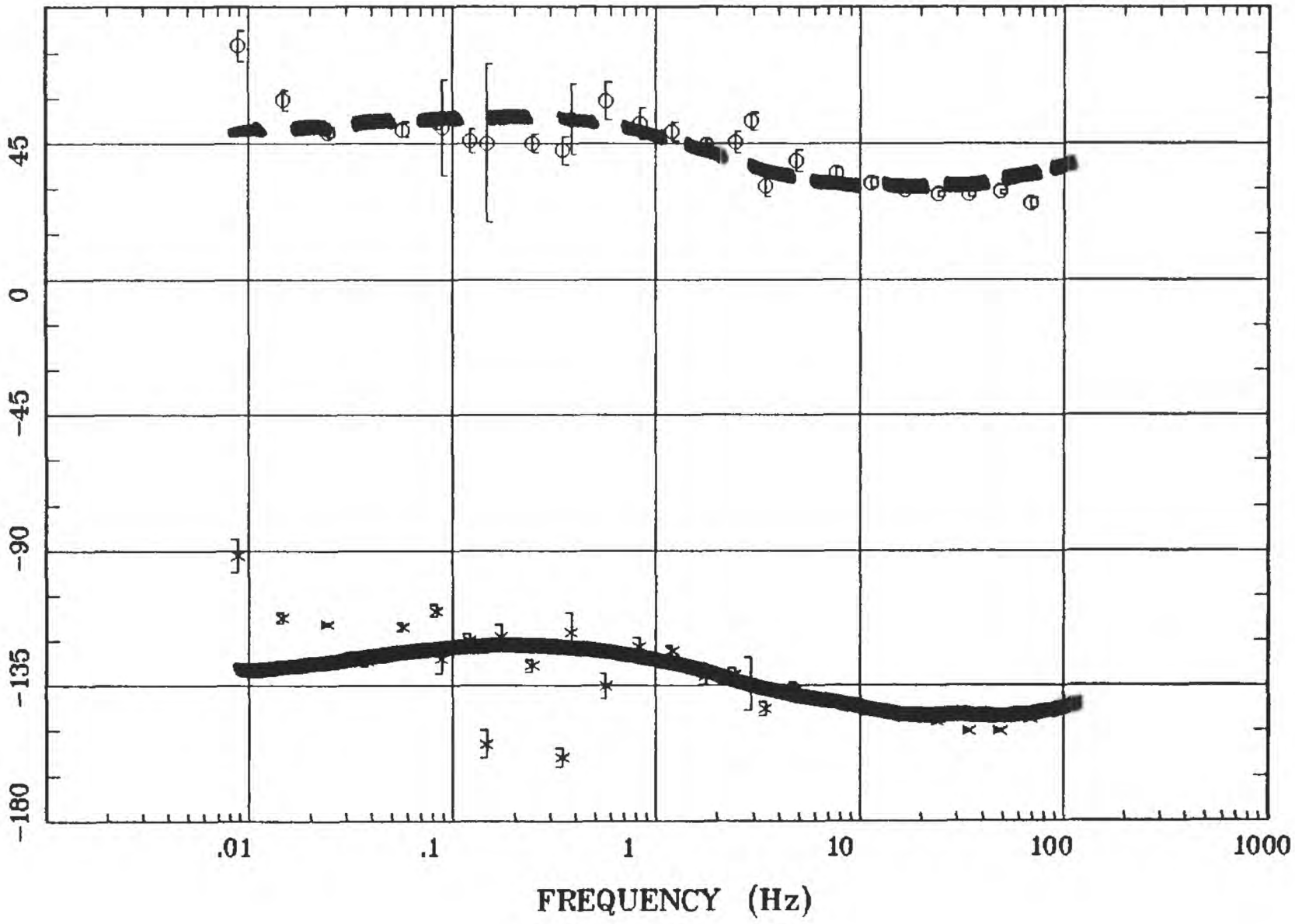

Client:
Remote: none
Acquired: 12:0 Aug 02, 1999
Survey Co:USGS

Rotation:
Filename: hr76.avg
Channels: Ch1 Ch2 Ch3 Ch4 Ch5 Ch3 Ch4
Plotted: 12:25 Jan 25, 2001
< EMI - ElectroMagnetic Instruments >

Station 75

APPARENT RESISTIVITY Boulder Valley, NV

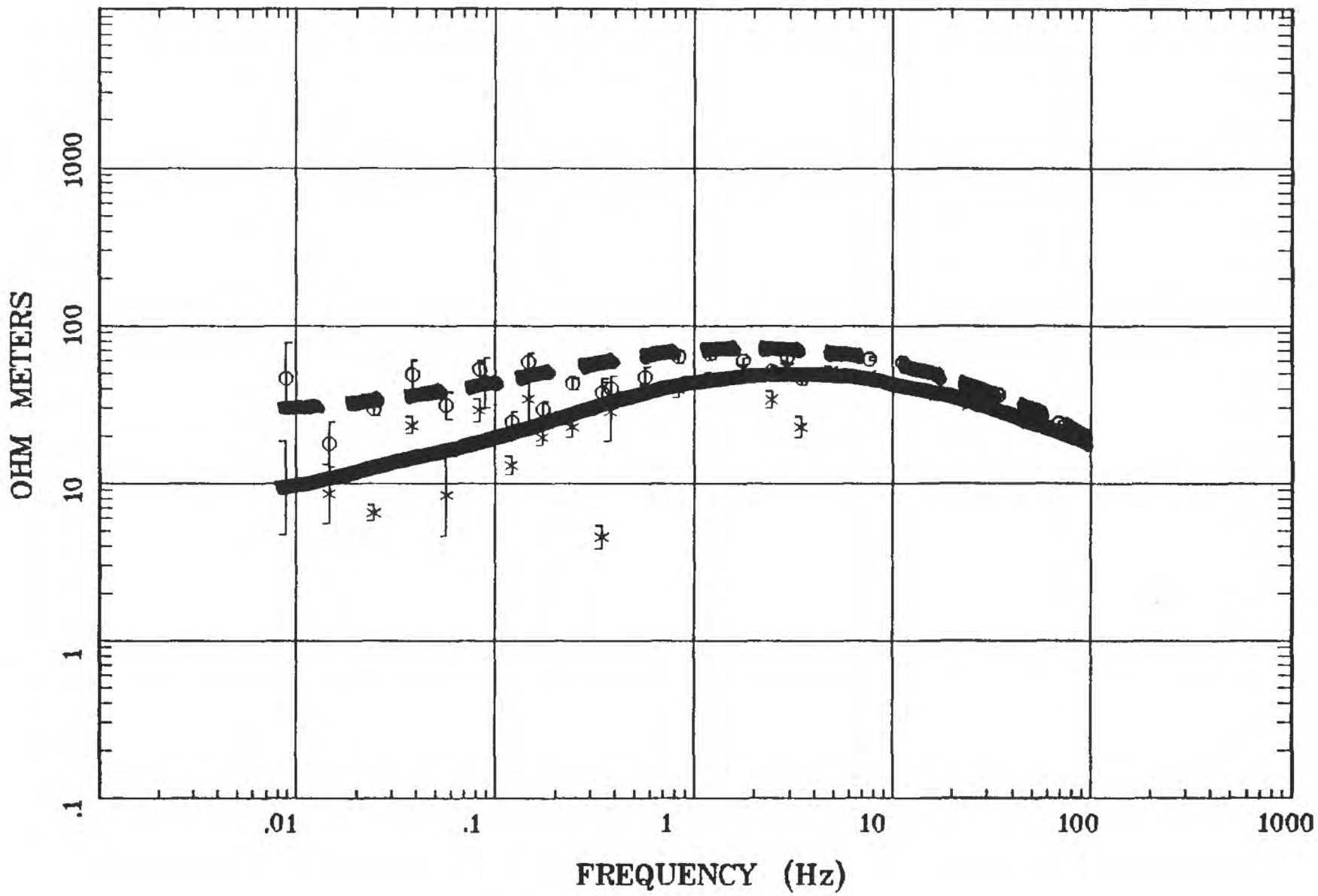

Client:
Remote: none
Acquired: 08:4 Aug 02, 1999
Survey Co:USGS

Rotation:
Filename: hr75b.avg
Channels: Ch1 Ch2 Ch3 Ch4 Ch5 Ch3 Ch4
Plotted: 12:31 Jan 25, 2001
< EMI - ElectroMagnetic Instruments >

Station 75

IMPEDANCE PHASE Boulder Valley, NV

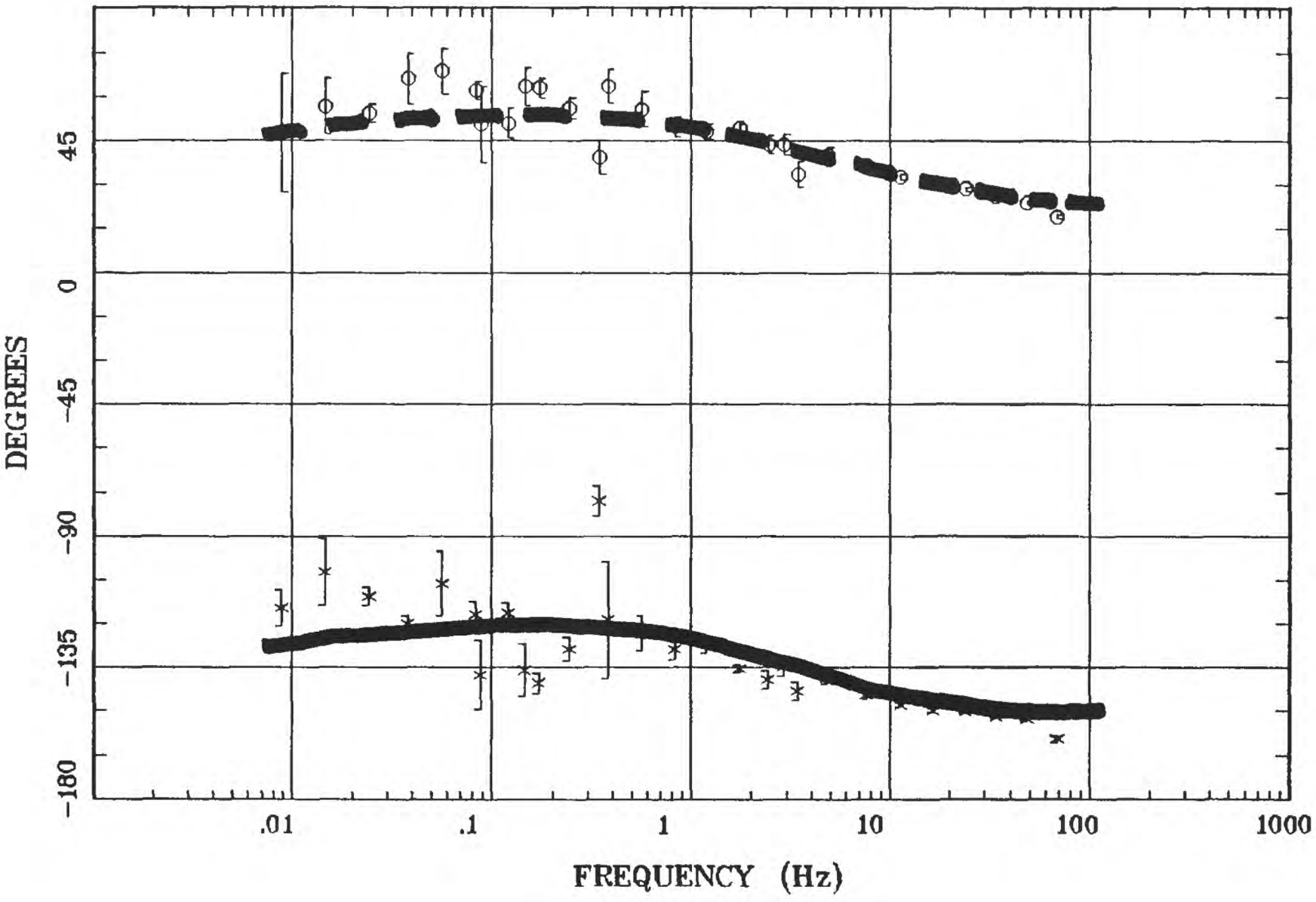

Client:
Remote: none
Acquired: 08:4 Aug 02, 1999
Survey Co:USGS

Rotation:
Filename: hr75b.avg
Channels: Ch1 Ch2 Ch3 Ch4 Ch5 Ch3 Ch4
Plotted: 12:31 Jan 25, 2001
< EMI - ElectroMagnetic Instruments >

Station 74

APPARENT RESISTIVITY Boulder Valley, NV

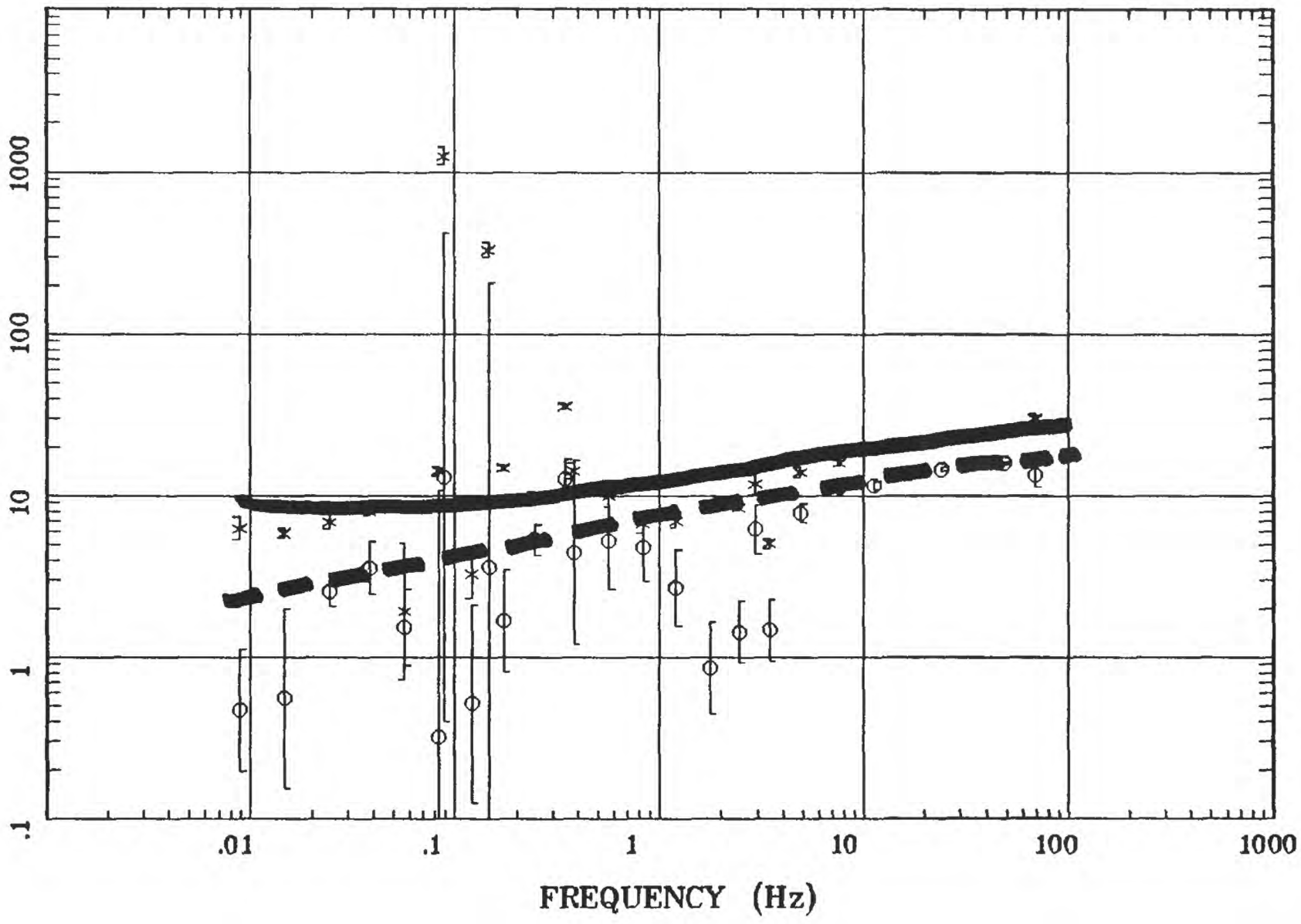

Client:
Remote: none
Acquired: 14:0 Aug 01, 1999
Survey Co:USGS

Rotation:
Filename: hr74b.avg
Channels: Ch1 Ch2 Ch3 Ch4 Ch5 Ch3 Ch4
Plotted: 12:36 Jan 25, 2001
< EMI - ElectroMagnetic Instruments >

IMPEDANCE PHASE

Boulder Valley, NV

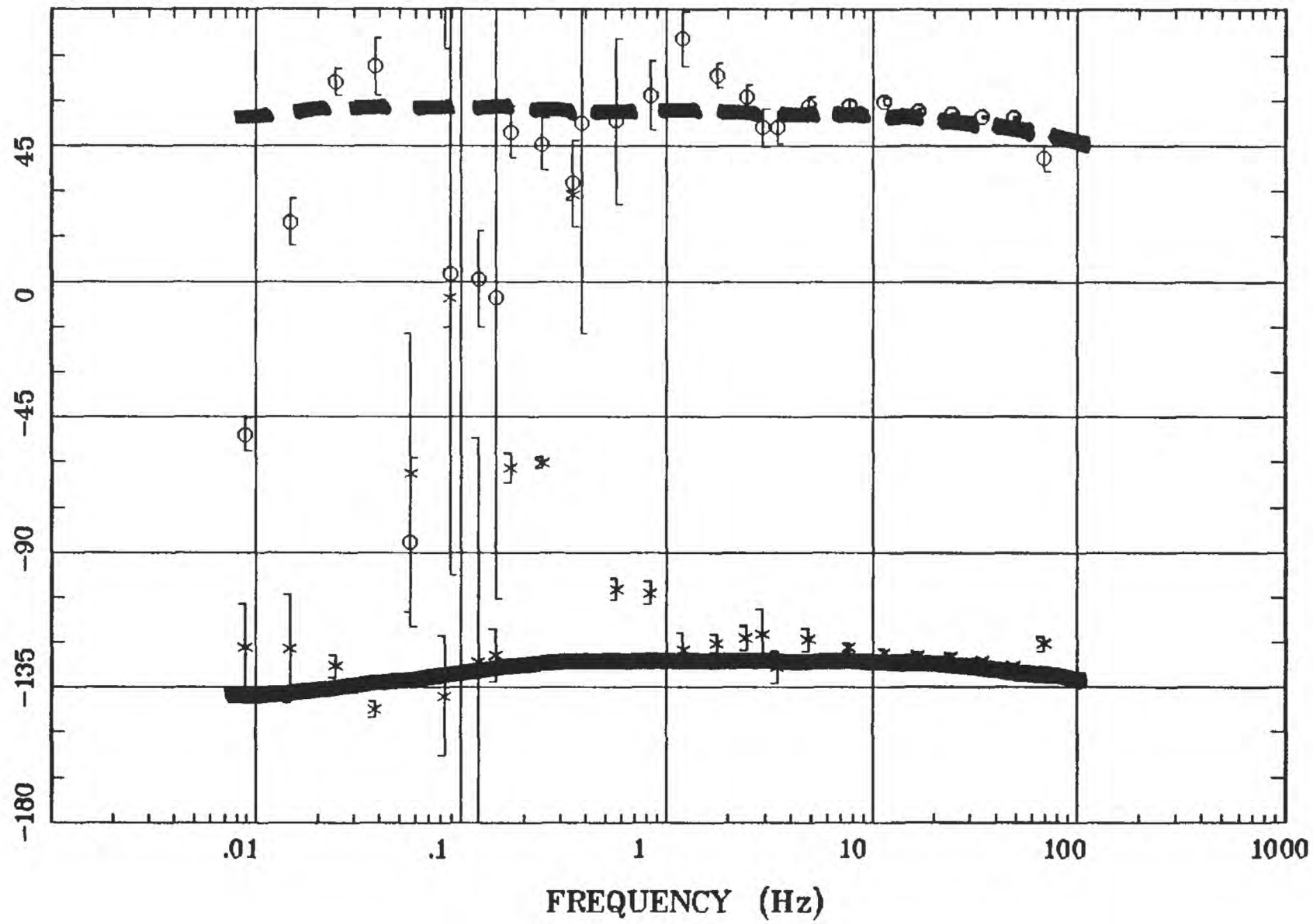

Client:
Remote: none
Acquired: 14:0 Aug 01, 1999
Survey Co:USGS

Rotation:
Filename: hr74b.avg
Channels: Ch1 Ch2 Ch3 Ch4 Ch5 Ch3 Ch4
Plotted: 12:36 Jan 25, 2001
< EMI - ElectroMagnetic Instruments >

Station 73

APPARENT RESISTIVITY

Boulder Valley, NV

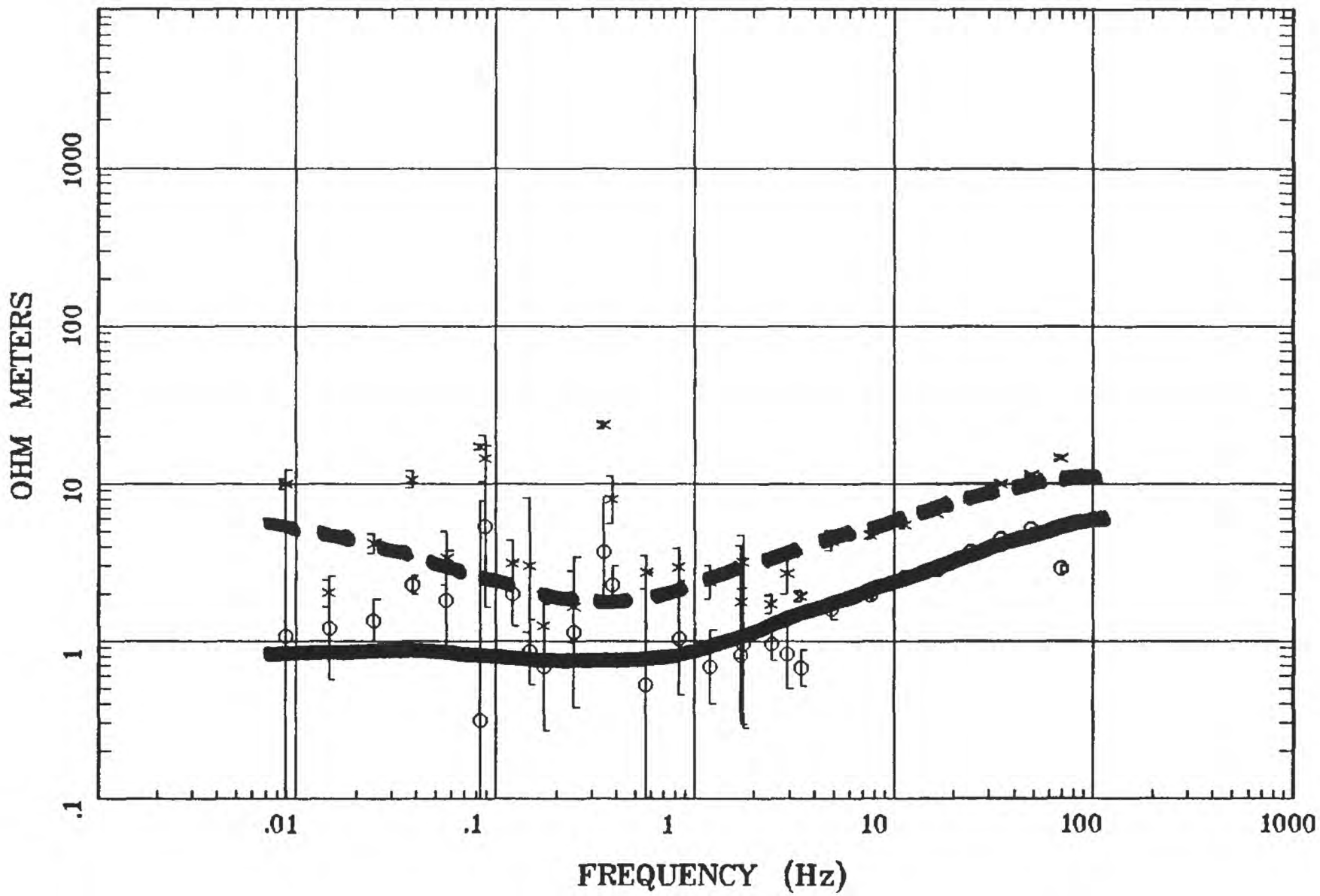

Client:
Remote: local
Acquired: 09:3 Aug 01, 1999
Survey Co:USGS

Rotation:
Filename: hr73all.avg
Channels: Ch1 Ch2 Ch3 Ch4 Ch5 Ch3 Ch4
Plotted: 12:40 Jan 25, 2001
< EMI - ElectroMagnetic Instruments >

Station 73

IMPEDANCE PHASE

Boulder Valley, NV

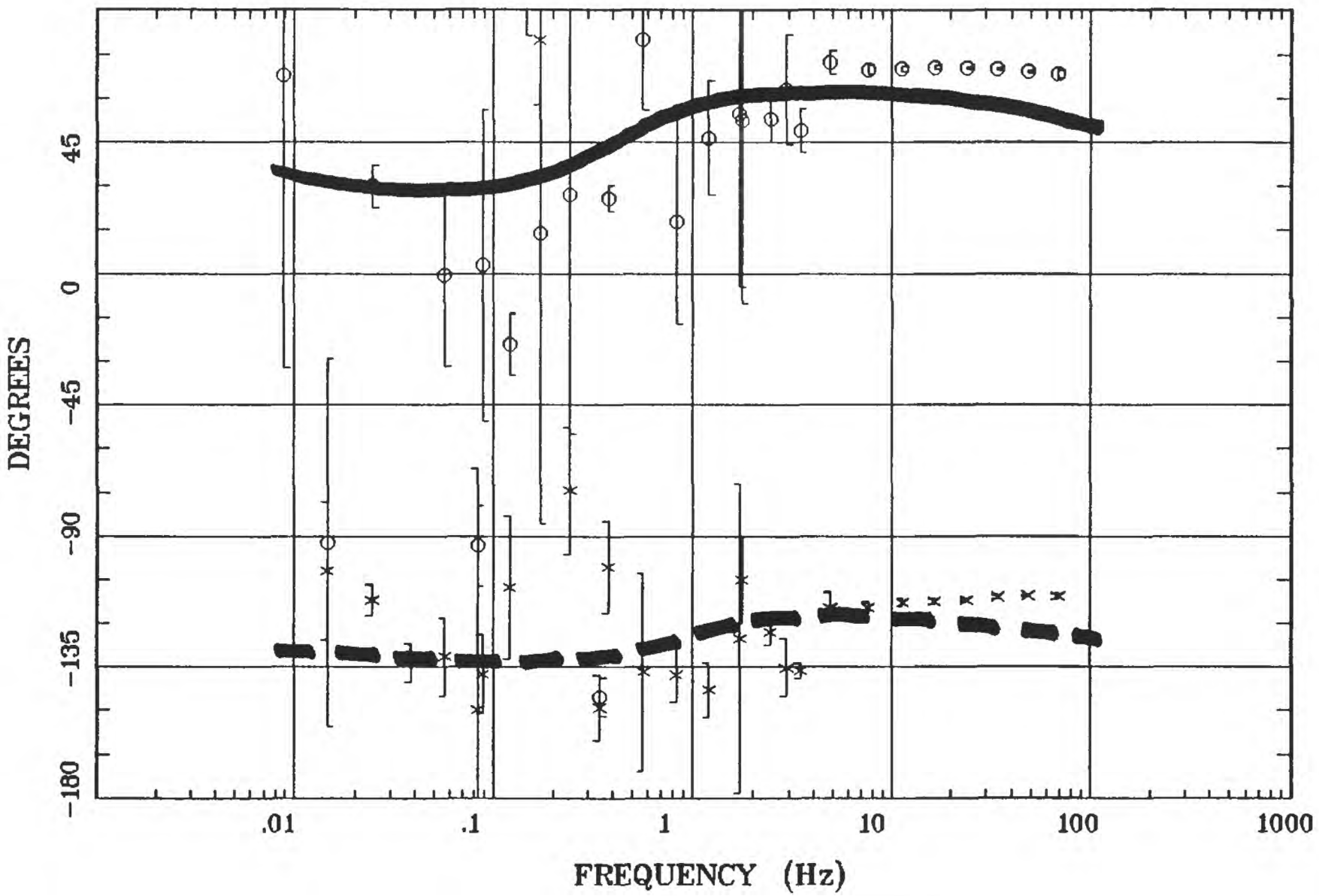

Client:
Remote: local
Acquired: 09:3 Aug 01, 1999
Survey Co:USGS

Rotation:
Filename: hr73all.avg
Channels: Ch1 Ch2 Ch3 Ch4 Ch5 Ch3 Ch4
Plotted: 12:40 Jan 25, 2001
< EMI - ElectroMagnetic Instruments >

APPENDIX E

OBSERVED AND CALCULATED DATA - PROFILE MT9

Magnetotelluric (MT) observed (circle and x symbols) and calculated (solid and dashed lines are TE and TM modes, respectively) resistivity and phase data for profile MT9. See the "Magnetotelluric Data" section of this report for a description of the observed data and the "Resistivity Models" section for a description of the calculated data.

APPARENT RESISTIVITY Winnemucca, NV 100K

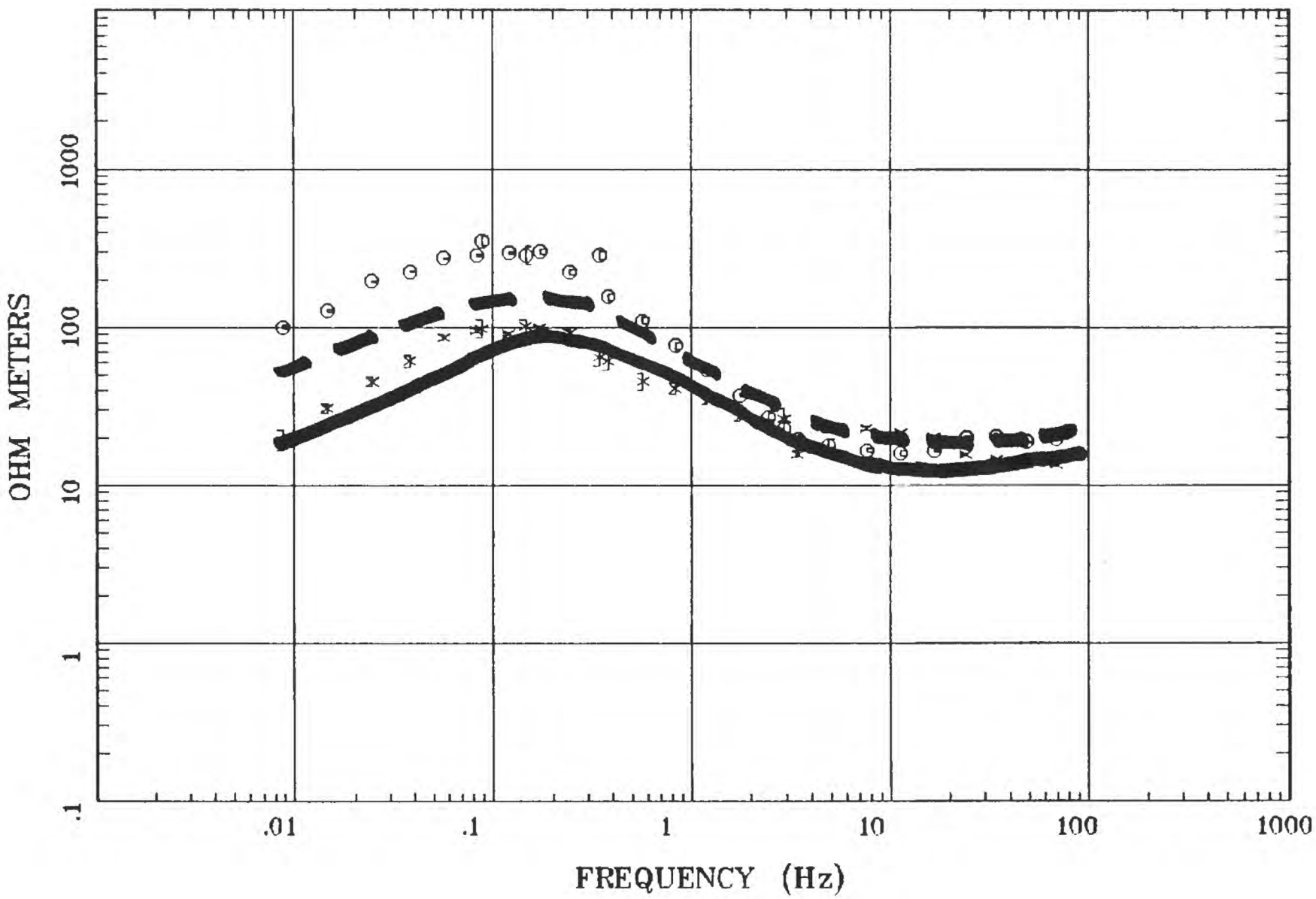

Client:
Remote: none
Acquired: 09:4 Jul 23, 2000
Survey Co:USGS

Rotation:
Filename: hr90b.avg
Channels: Ch1 Ch2 Ch3 Ch4 Ch5 Ch3 Ch4
Plotted: 11:06 Feb 06, 2001
< EMI - ElectroMagnetic Instruments >

Station 90

IMPEDANCE PHASE

Winnemucca, NV 100K

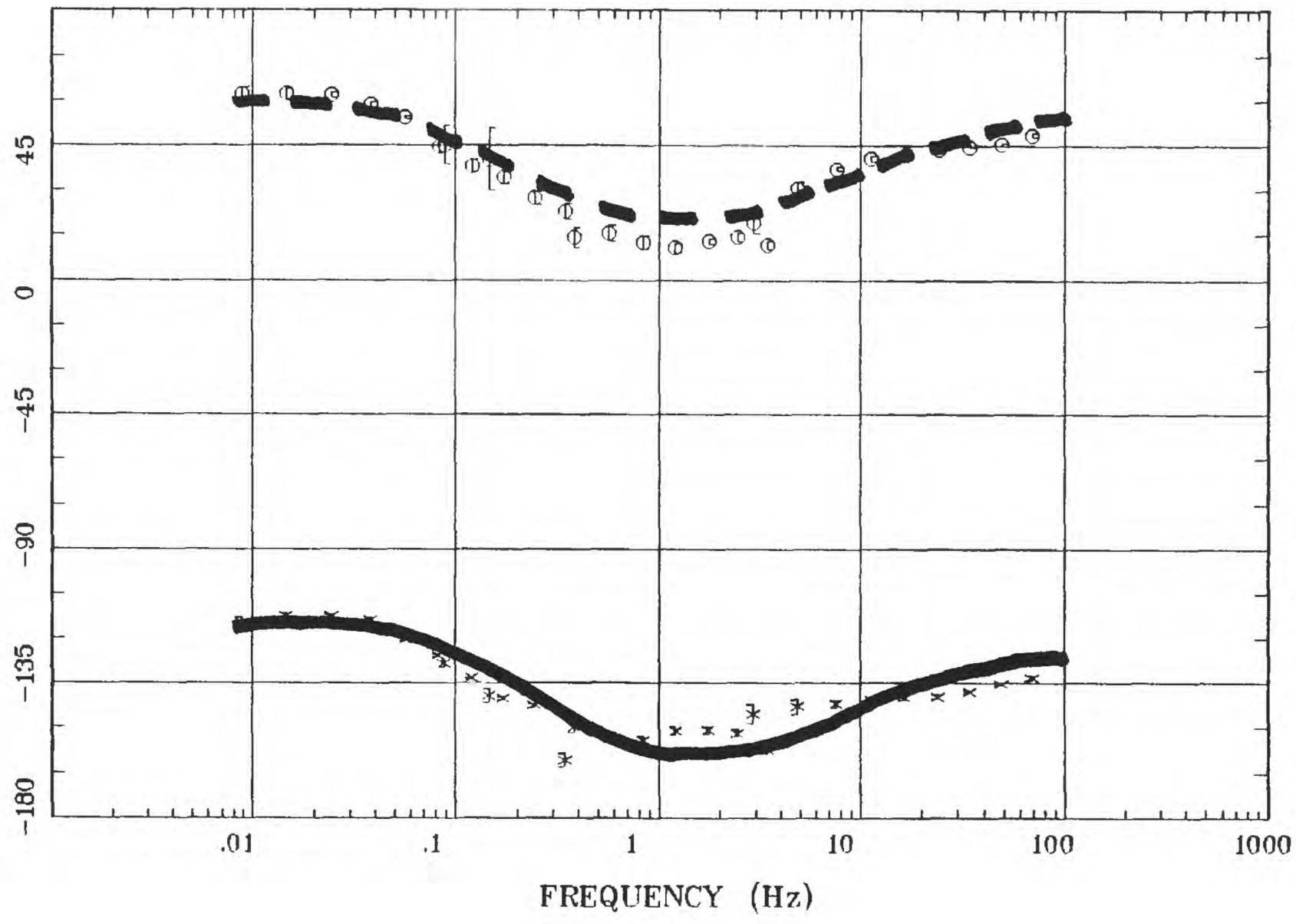

Client:
Remote: none
Acquired: 09:4 Jul 23, 2000
Survey Co:USGS

Rotation:
Filename: hr90b.avg
Channels: Ch1 Ch2 Ch3 Ch4 Ch5 Ch3 Ch4
Plotted: 11:06 Feb 06, 2001
< EMI - ElectroMagnetic Instruments >

Station 91

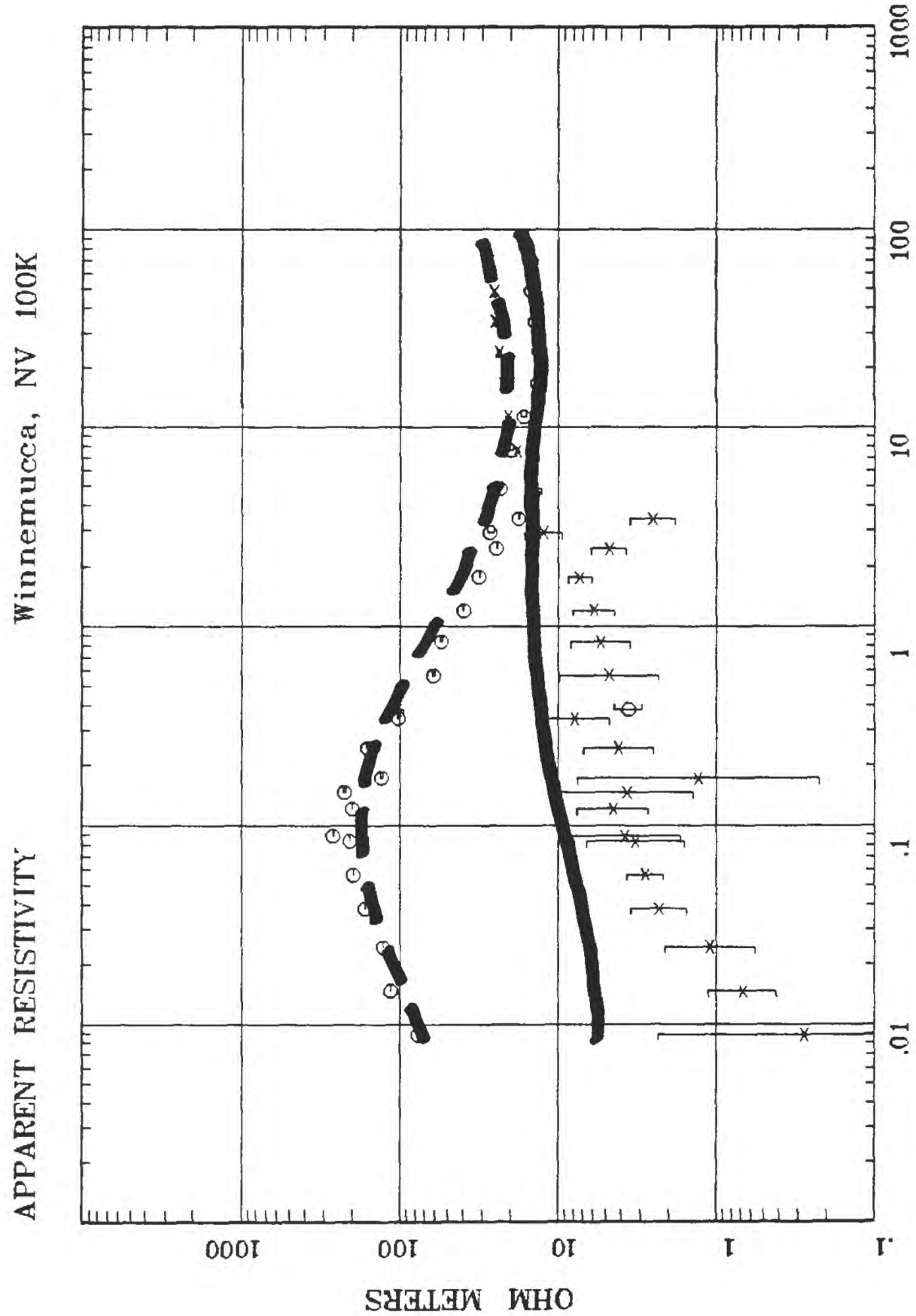

Rotation:
Filename: hr91b.avg
Channels: Ch1 Ch2 Ch3 Ch4 Ch5 Ch3 Ch4
Plotted: 11:07 Feb 08, 2001
< EMI - ElectroMagnetic Instruments >

Client:
Remote: none
Acquired: 13:0 Jul 23, 2000
Survey Co:USGS

Station 91

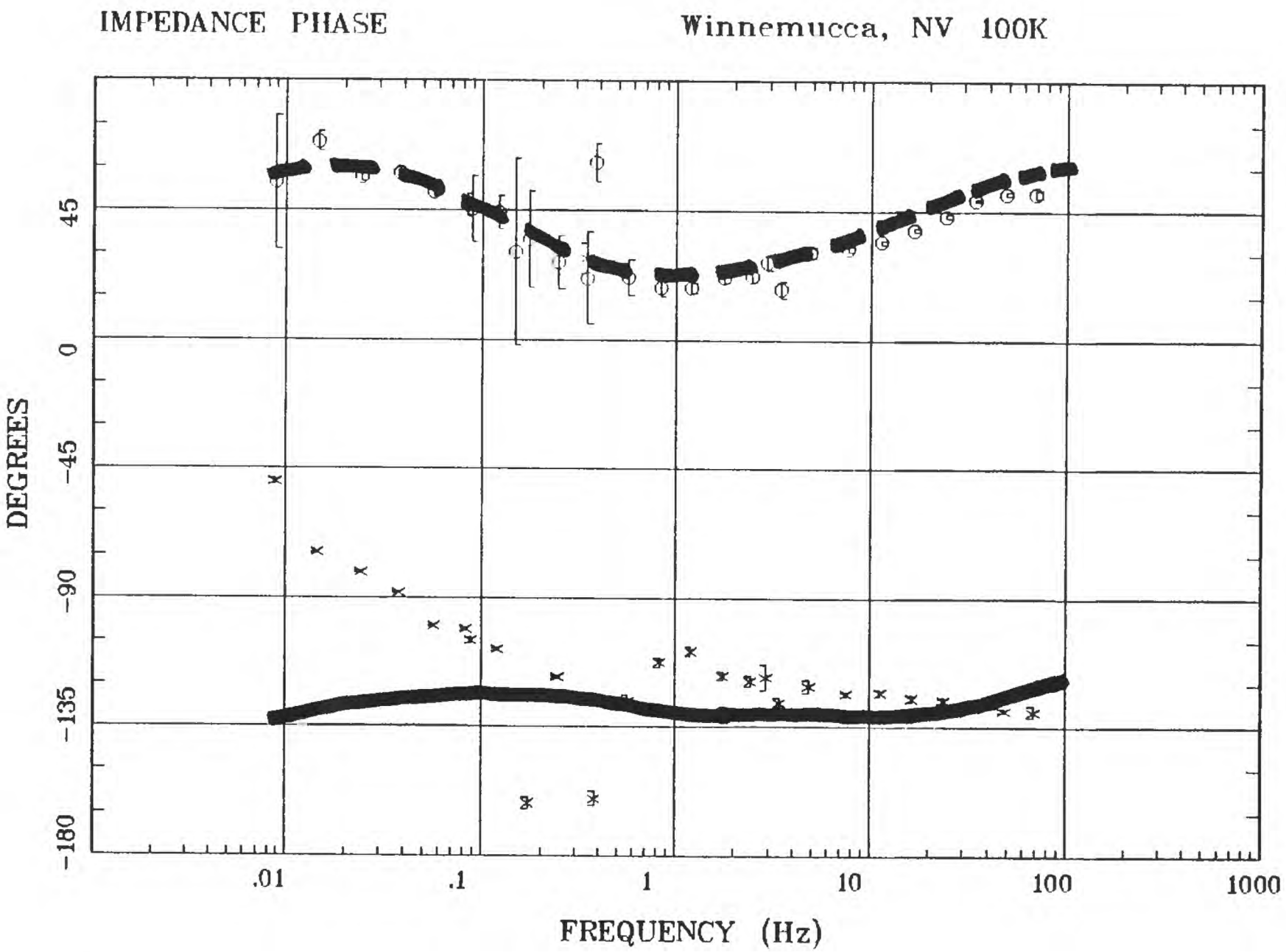

Client:
Remote: none
Acquired: 13:0 Jul 23, 2000
Survey Co:USGS

Rotation:
Filename: hr91b.avg
Channels: Ch1 Ch2 Ch3 Ch4 Ch5 Ch3 Ch4
Plotted: 11:07 Feb 06, 2001
< EMI - ElectroMagnetic Instruments >

66

Station 92

APPARENT RESISTIVITY

Winnemucca, NV 100K

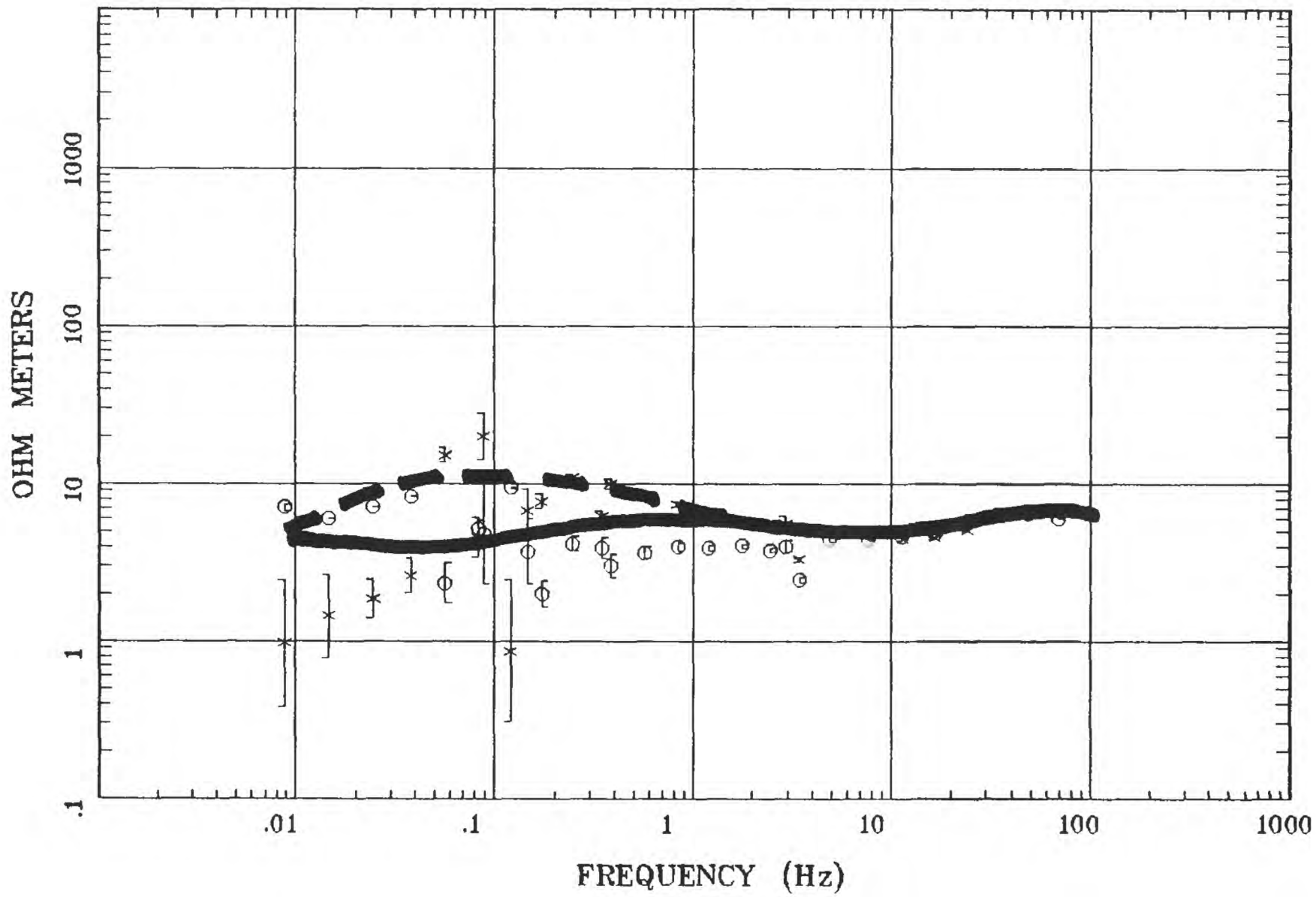

Client:
Remote: none
Acquired: 13:4 Jul 27, 2000
Survey Co:USGS

Rotation:
Filename: hr92all.avg
Channels: Ch1 Ch2 Ch3 Ch4 Ch5 Ch3 Ch4
Plotted: 11:07 Feb 06, 2001
< EMI - ElectroMagnetic Instruments >

IMPEDANCE PHASE

Winnemucca, NV 100K

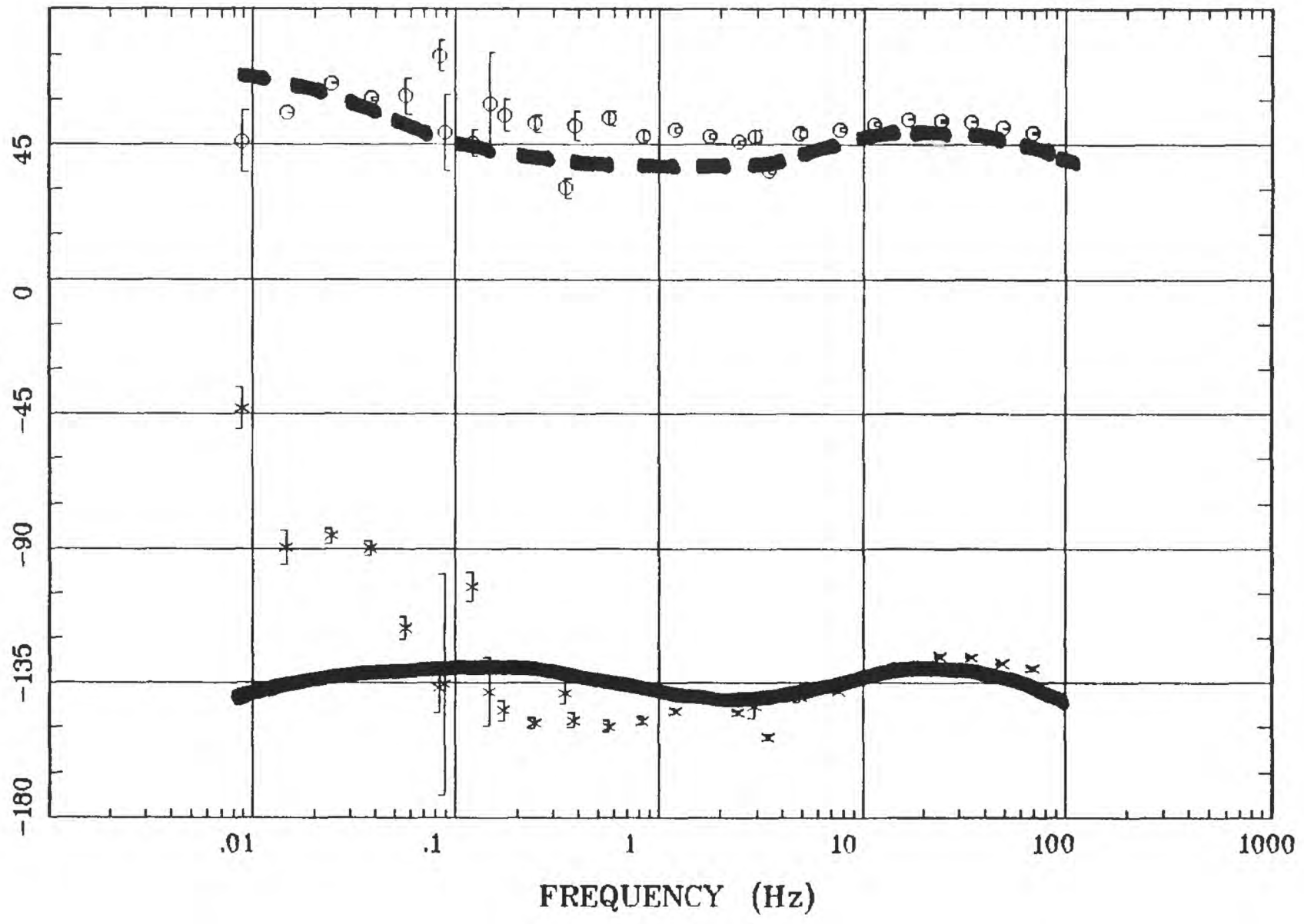

Client:
Remote: none
Acquired: 13:4 Jul 27, 2000
Survey Co:USGS

Rotation:
Filename: hr92all.avg
Channels: Ch1 Ch2 Ch3 Ch4 Ch5 Ch3 Ch4
Plotted: 11:07 Feb 06, 2001
< EMI - ElectroMagnetic Instruments >

100

APPARENT RESISTIVITY Winnemucca, NV 100K **Station 93**

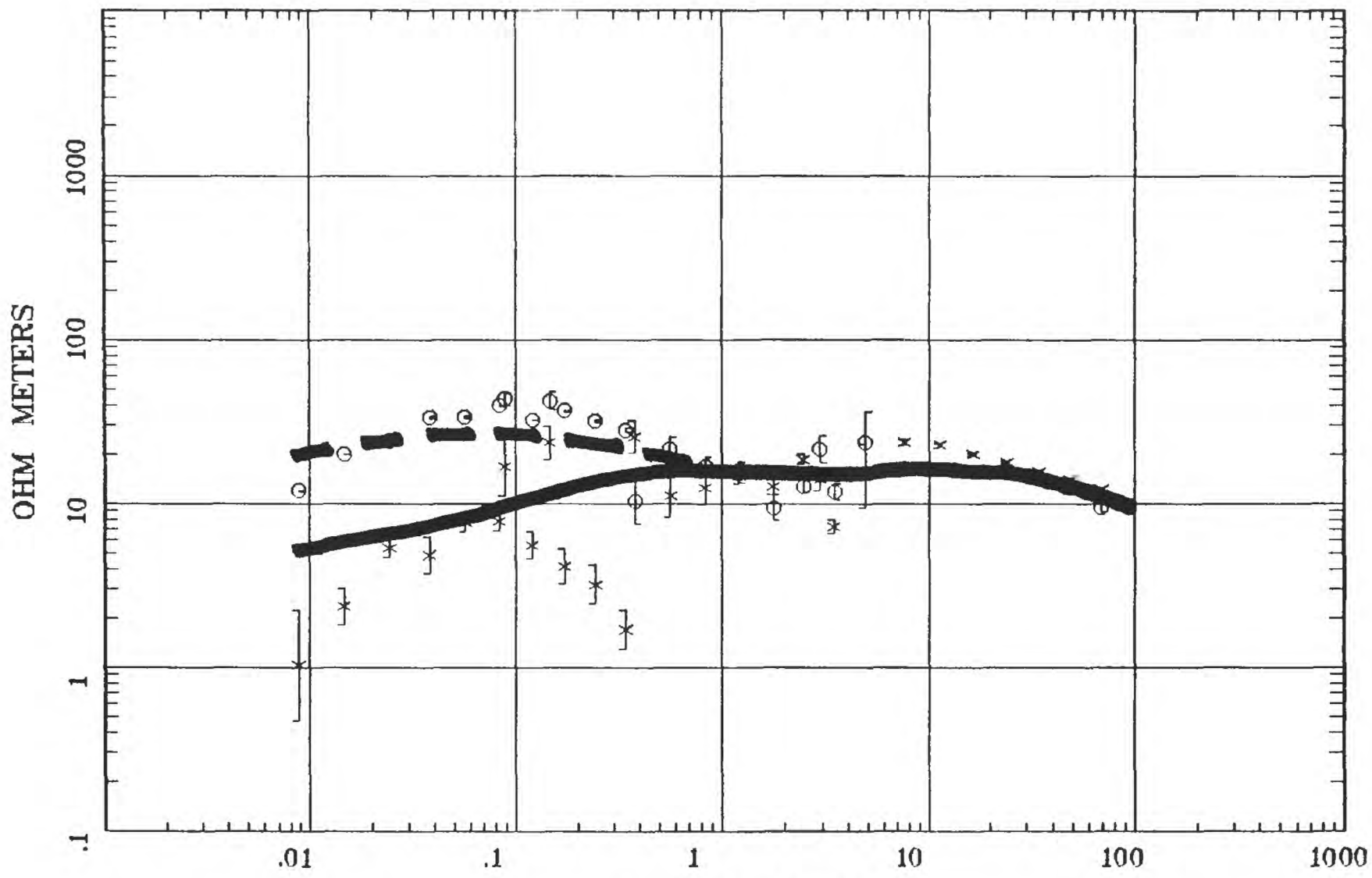

Client:
Remote: none
Acquired: 09:2 Jul 28, 2000
Survey Co:USGS

Rotation:
Filename: hr93b.avg
Channels: Ch1 Ch2 Ch3 Ch4 Ch5 Ch3 Ch4
Plotted: 11:08 Feb 06, 2001
< EMI - ElectroMagnetic Instruments >

Station 93

IMPEDANCE PHASE Winnemucca, NV 100K

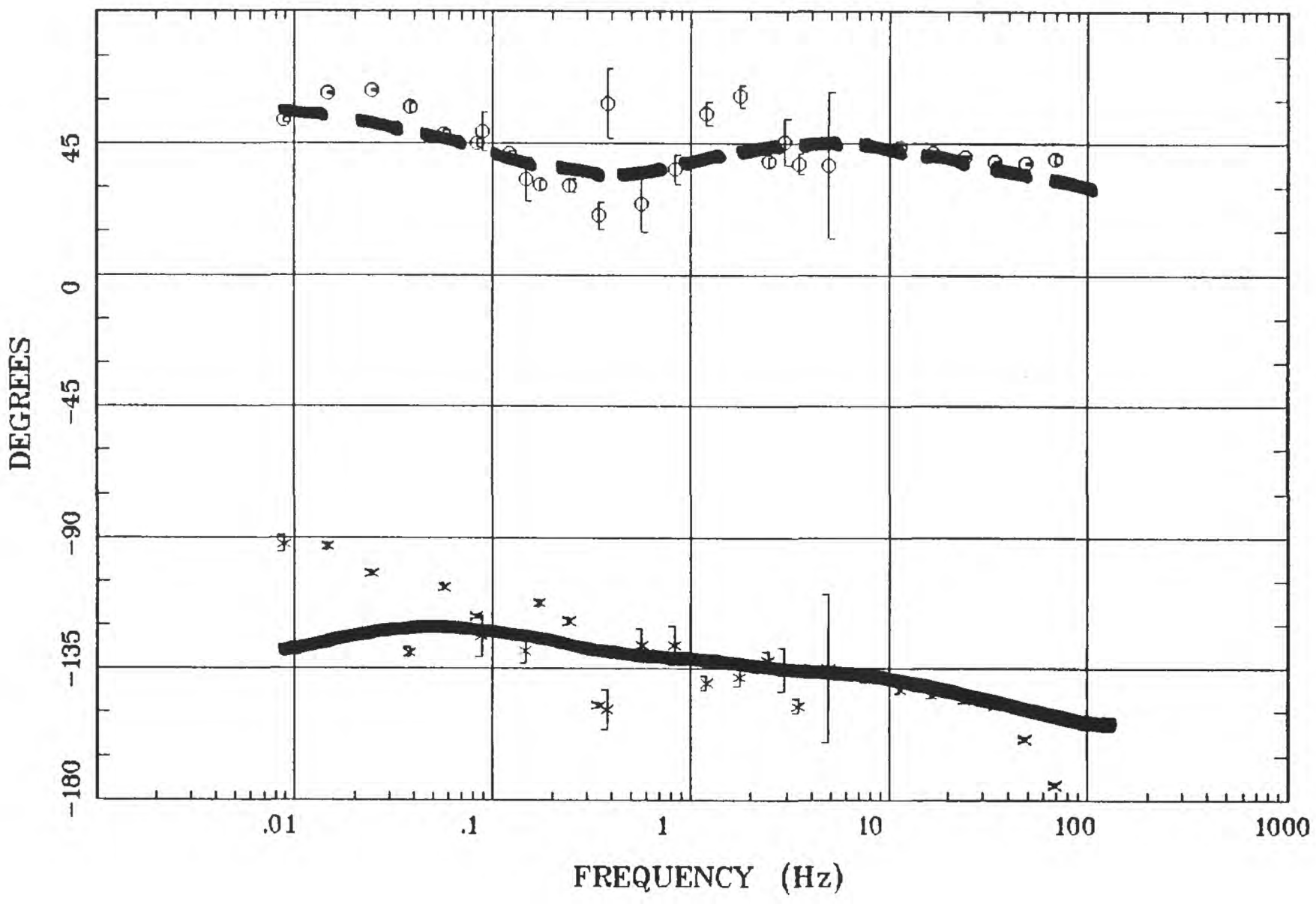

Client:
Remote: none
Acquired: 09:2 Jul 28, 2000
Survey Co:USGS

Rotation:
Filename: hr93b.avg
Channels: Ch1 Ch2 Ch3 Ch4 Ch5 Ch3 Ch4
Plotted: 11:08 Feb 06, 2001
< EMI - ElectroMagnetic Instruments >

APPARENT RESISTIVITY Winnemucca, NV 100K

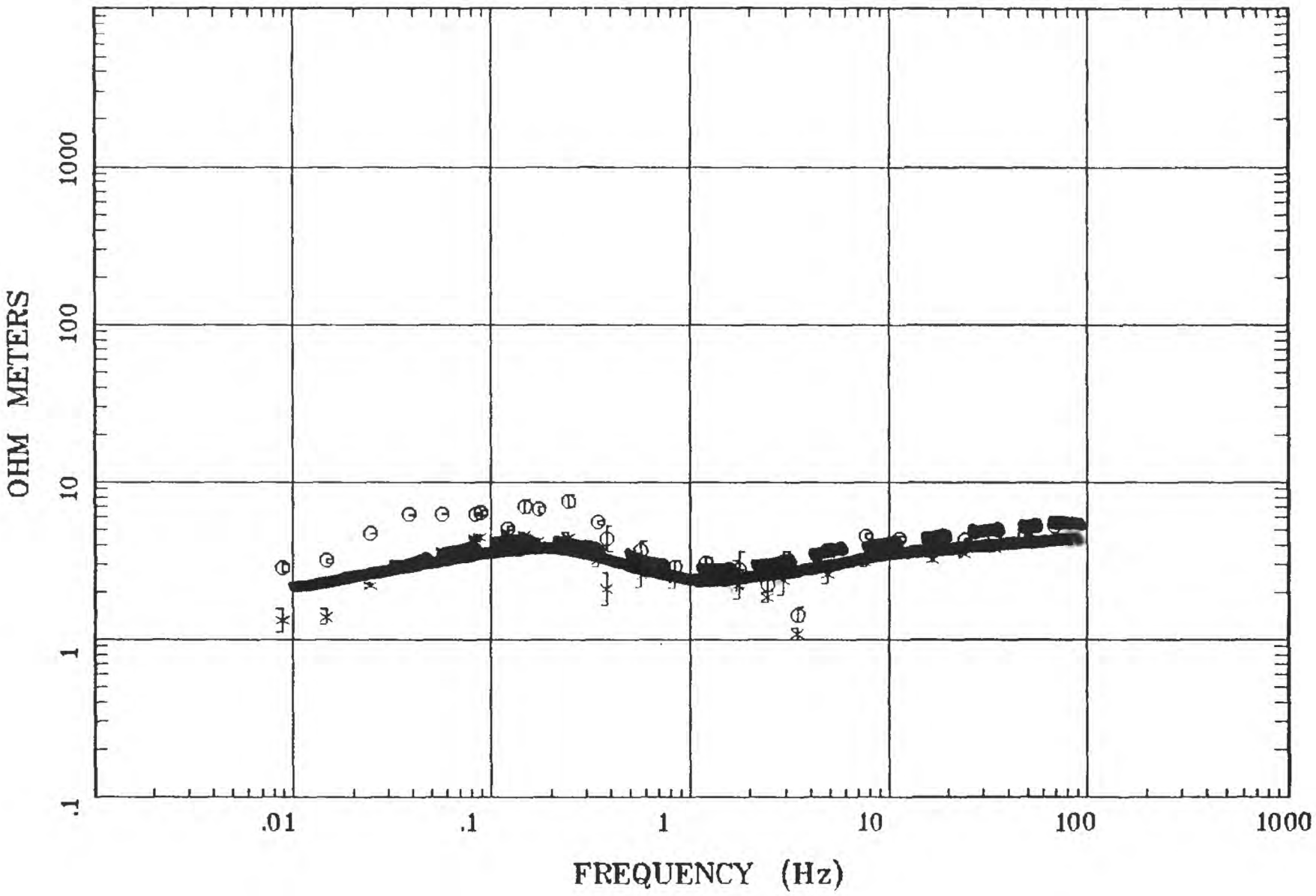

Client:
Remote: none
Acquired: 12:2 Jul 28, 2000
Survey Co:USGS

Rotation:
Filename: hr94all.avg
Channels: Ch1 Ch2 Ch3 Ch4 Ch5 Ch3 Ch4
Plotted: 11:08 Feb 06, 2001
< EMI - ElectroMagnetic Instruments >

Station 94

IMPEDANCE PHASE Winnemucca, NV 100K

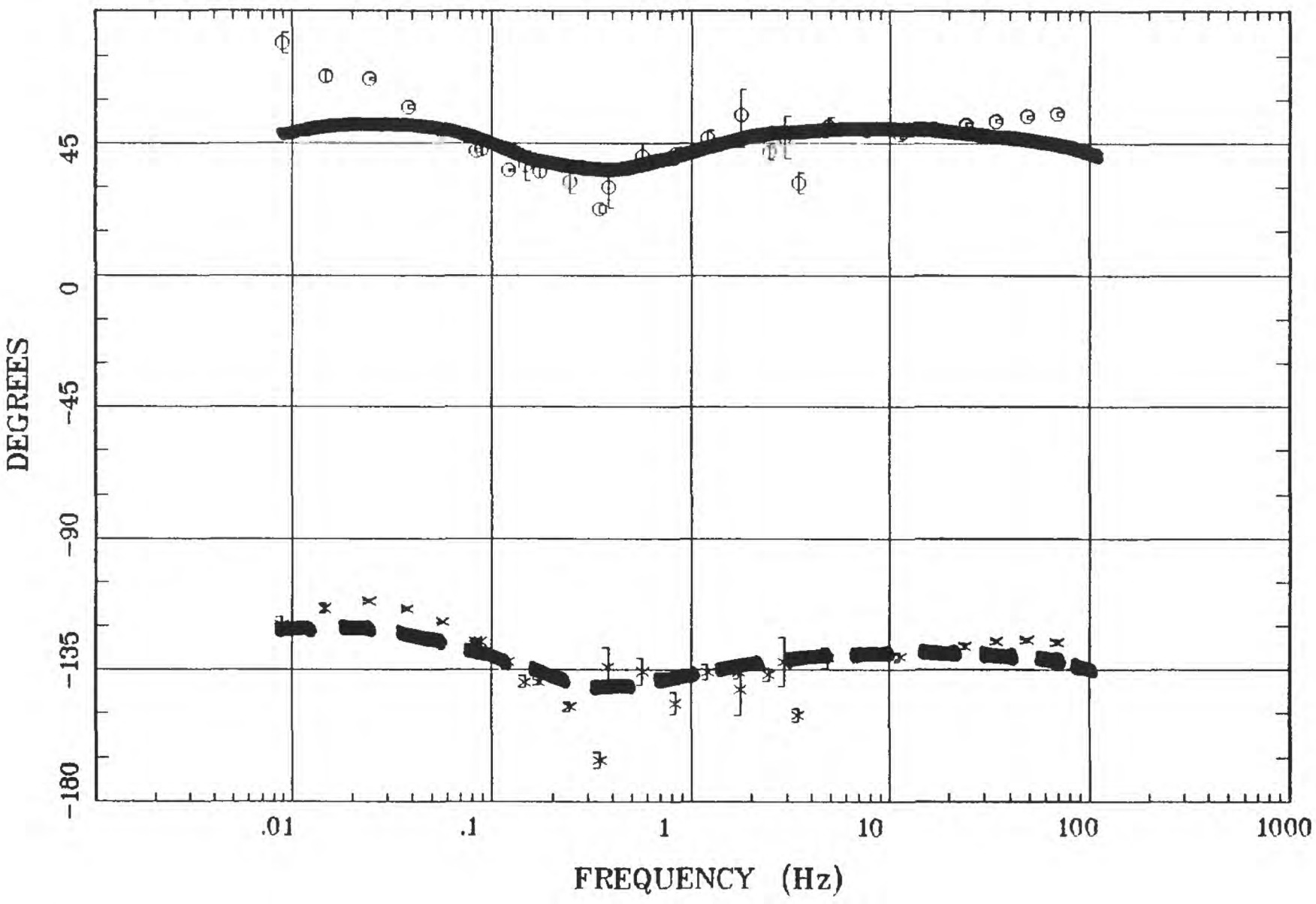

Client:
Remote: none
Acquired: 12:2 Jul 28, 2000
Survey Co:USGS

Rotation:
Filename: hr94all.avg
Channels: Ch1 Ch2 Ch3 Ch4 Ch5 Ch3 Ch4
Plotted: 11:08 Feb 06, 2001
< EMI - ElectroMagnetic Instruments >

Station 48

APPARENT RESISTIVITY Osgood Mtns, NV 100K

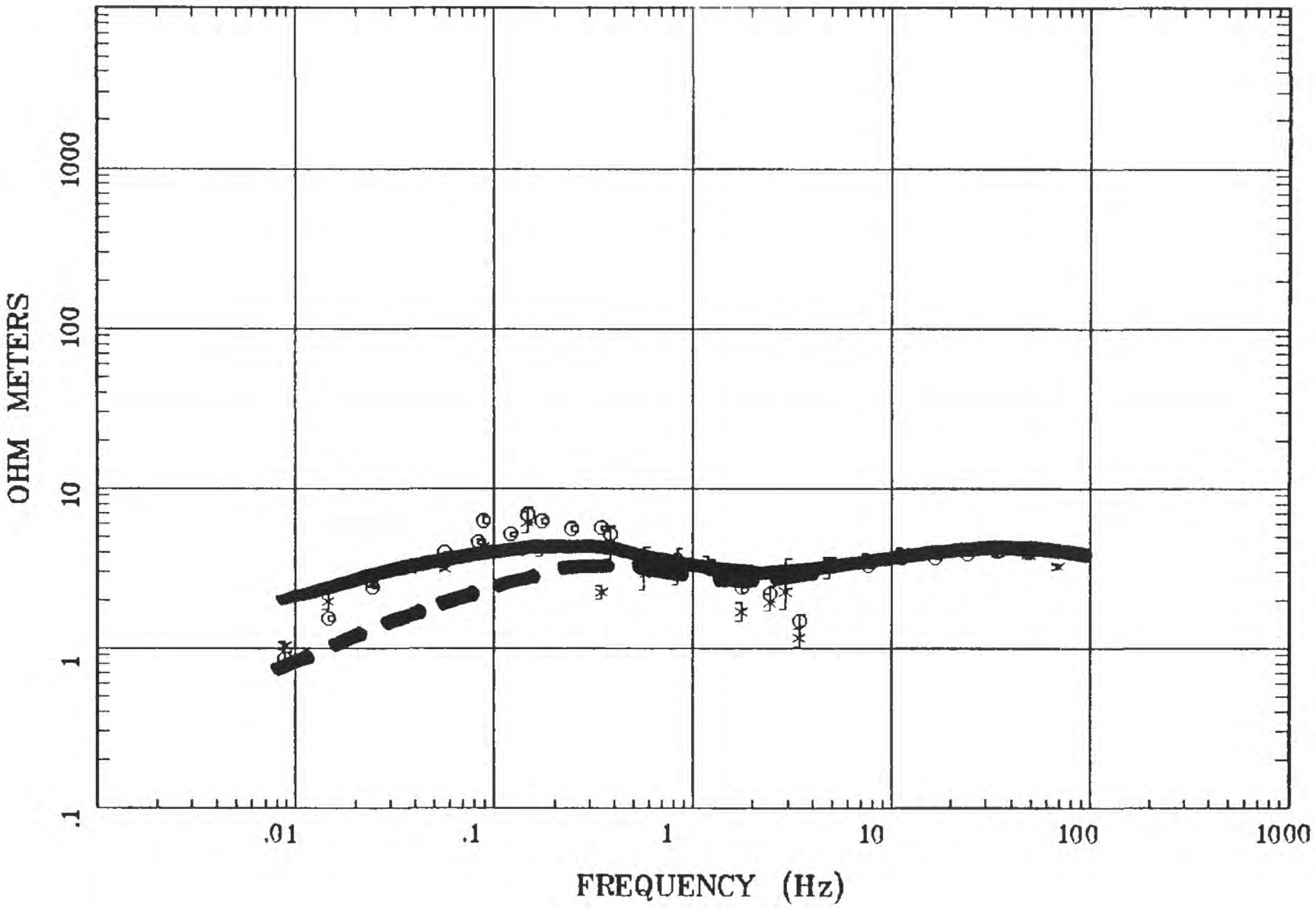

Client:
Remote: none
Acquired: 10:4 Jul 22, 2000
Survey Co:USGS

Rotation:
Filename: hr48c.avg
Channels: Ch1 Ch2 Ch3 Ch4 Ch5 Ch3 Ch4
Plotted: 11:05 Feb 06, 2001
< EMI - ElectroMagnetic Instruments >

Station 48

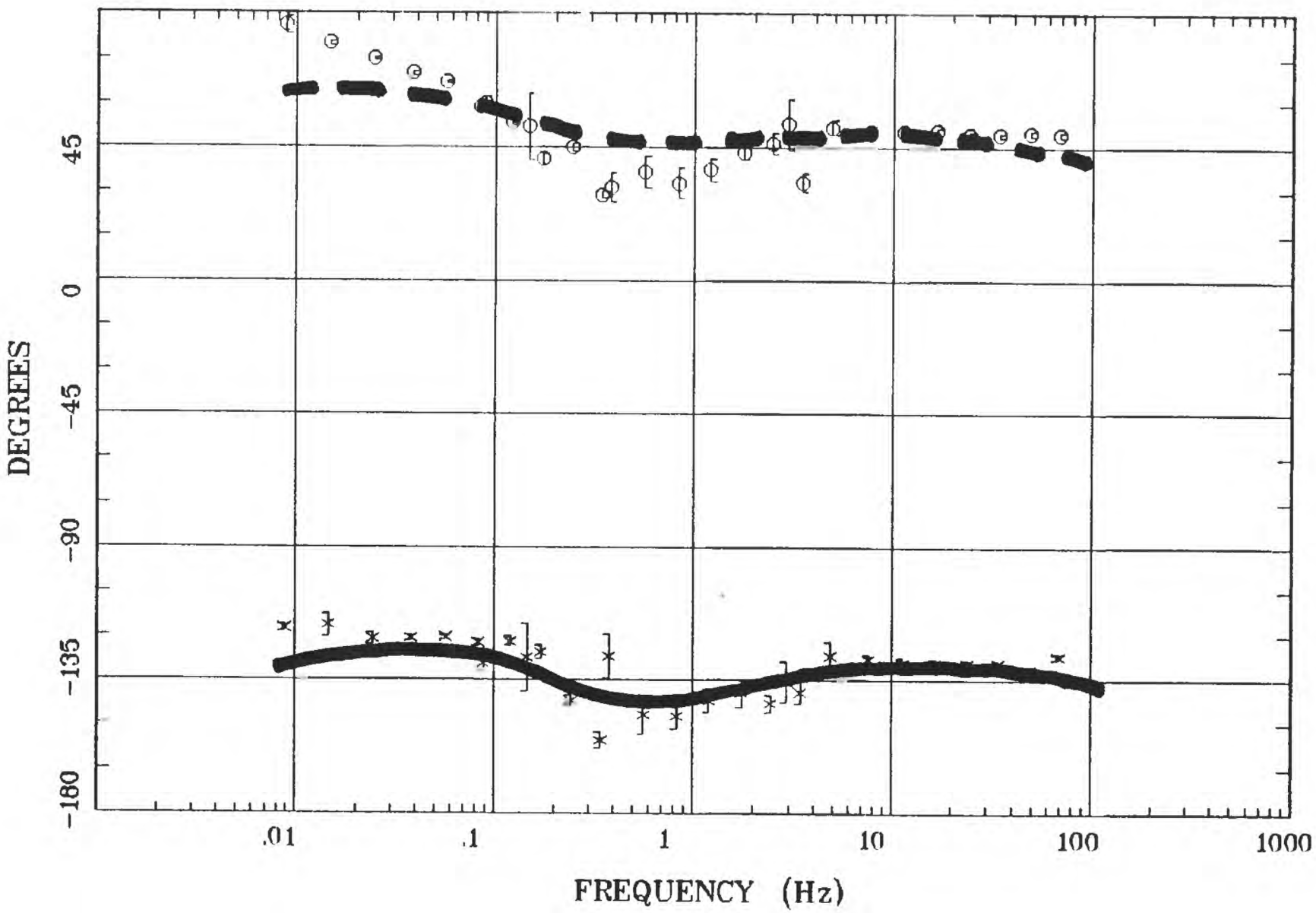

Client:
Remote: none
Acquired: 10:4 Jul 22, 2000
Survey Co:USGS

Rotation:
Filename: hr48c.avg
Channels: Ch1 Ch2 Ch3 Ch4 Ch5 Ch3 Ch4
Plotted: 11:05 Feb 06, 2001
< EMI - ElectroMagnetic Instruments >

Station 49

APPARENT RESISTIVITY Osgood Mtns, NV 100K

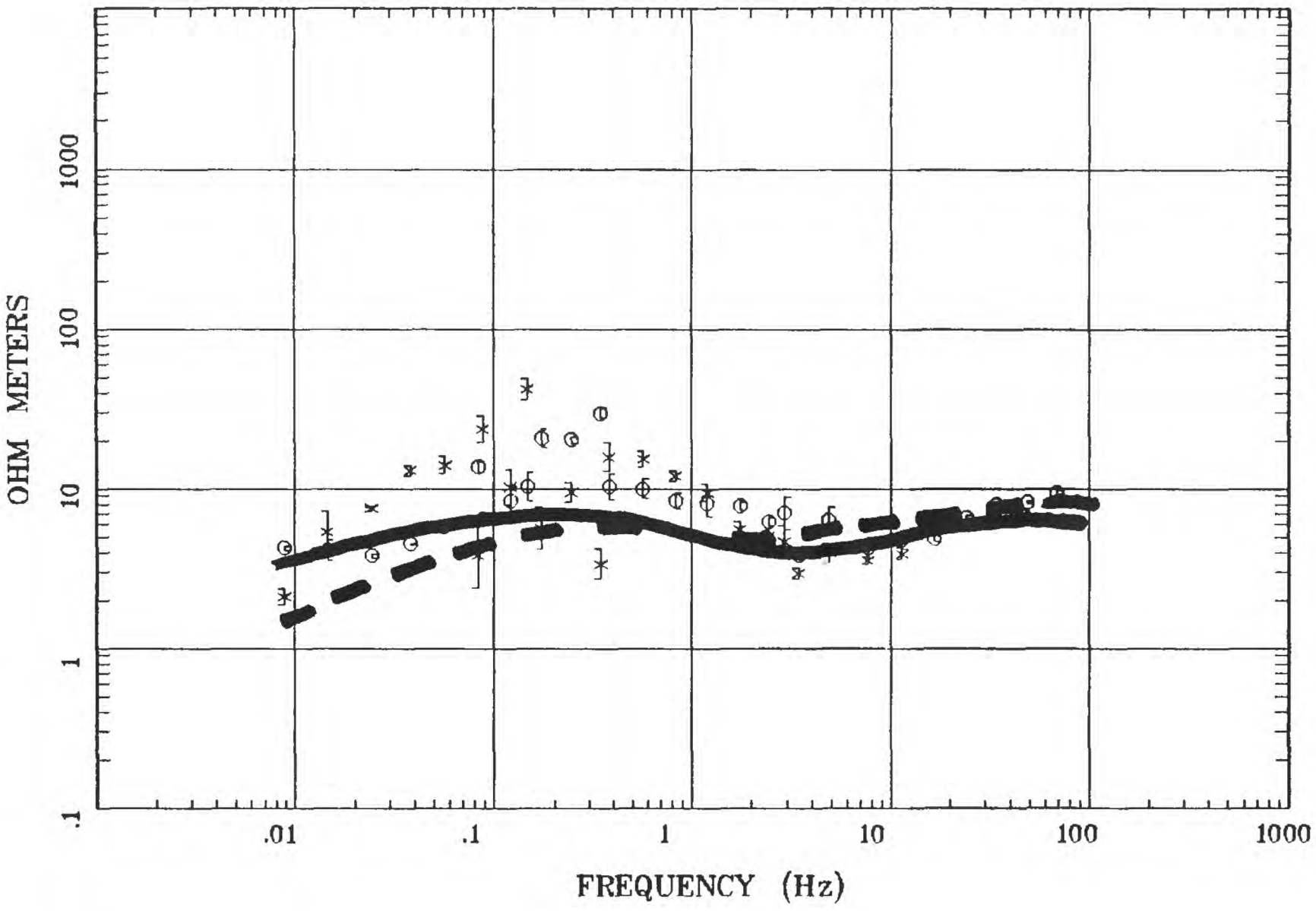

Client:
Remote: none
Acquired: 14:4 Jul 22, 2000
Survey Co:USGS

Rotation:
Filename: hr49a.avg
Channels: Ch1 Ch2 Ch3 Ch4 Ch5 Ch3 Ch4
Plotted: 11:06 Feb 06, 2001
< EMI - ElectroMagnetic Instruments >

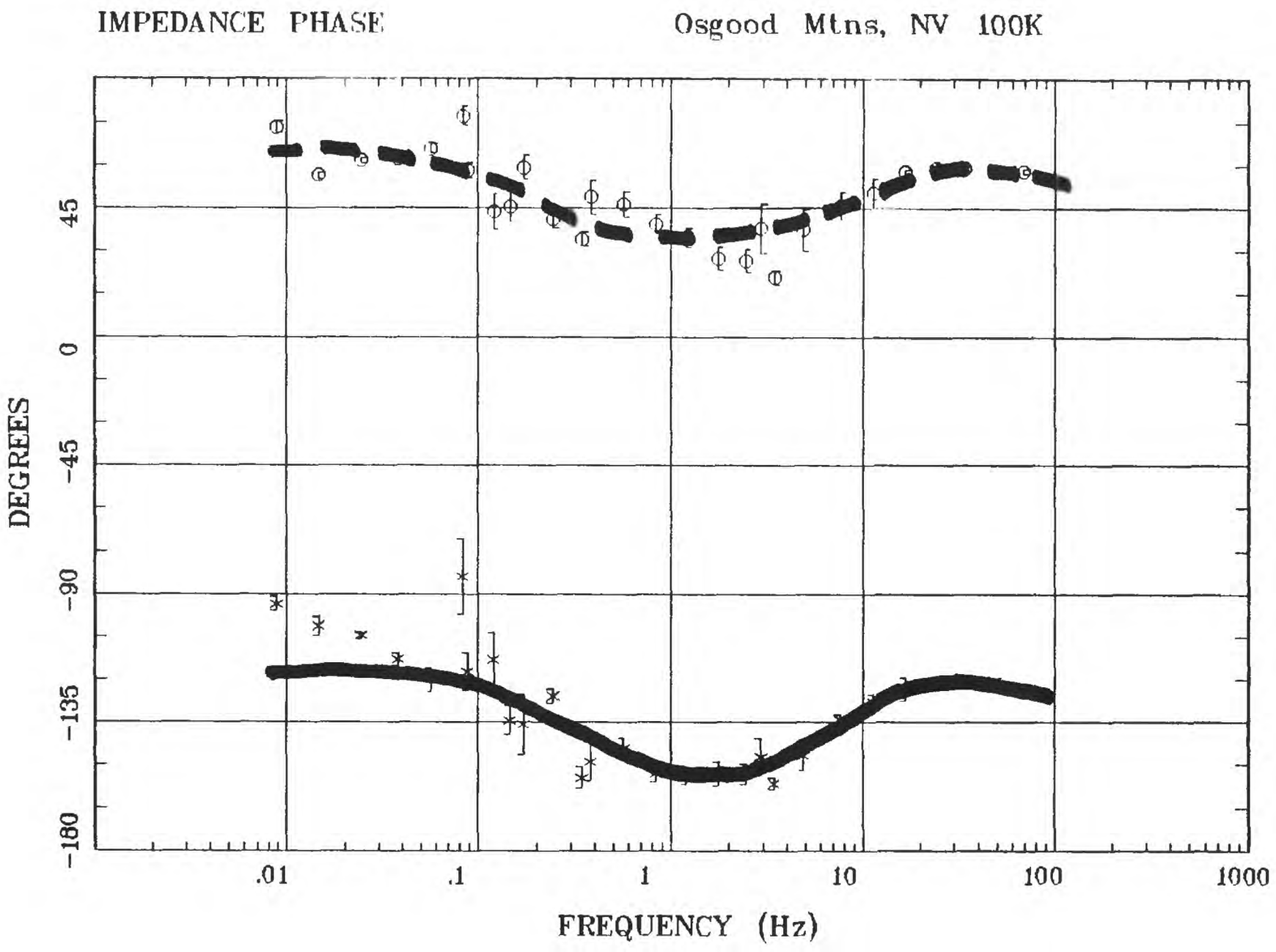

Client:
Remote: none
Acquired: 14:4 Jul 22, 2000
Survey Co:USGS

Rotation:
Filename: hr49a.avg
Channels: Ch1 Ch2 Ch3 Ch4 Ch5 Ch3 Ch4
Plotted: 11:06 Feb 06, 2001
< EMI - ElectroMagnetic Instruments >

APPARENT RESISTIVITY Osgood Mtns, NV 100K

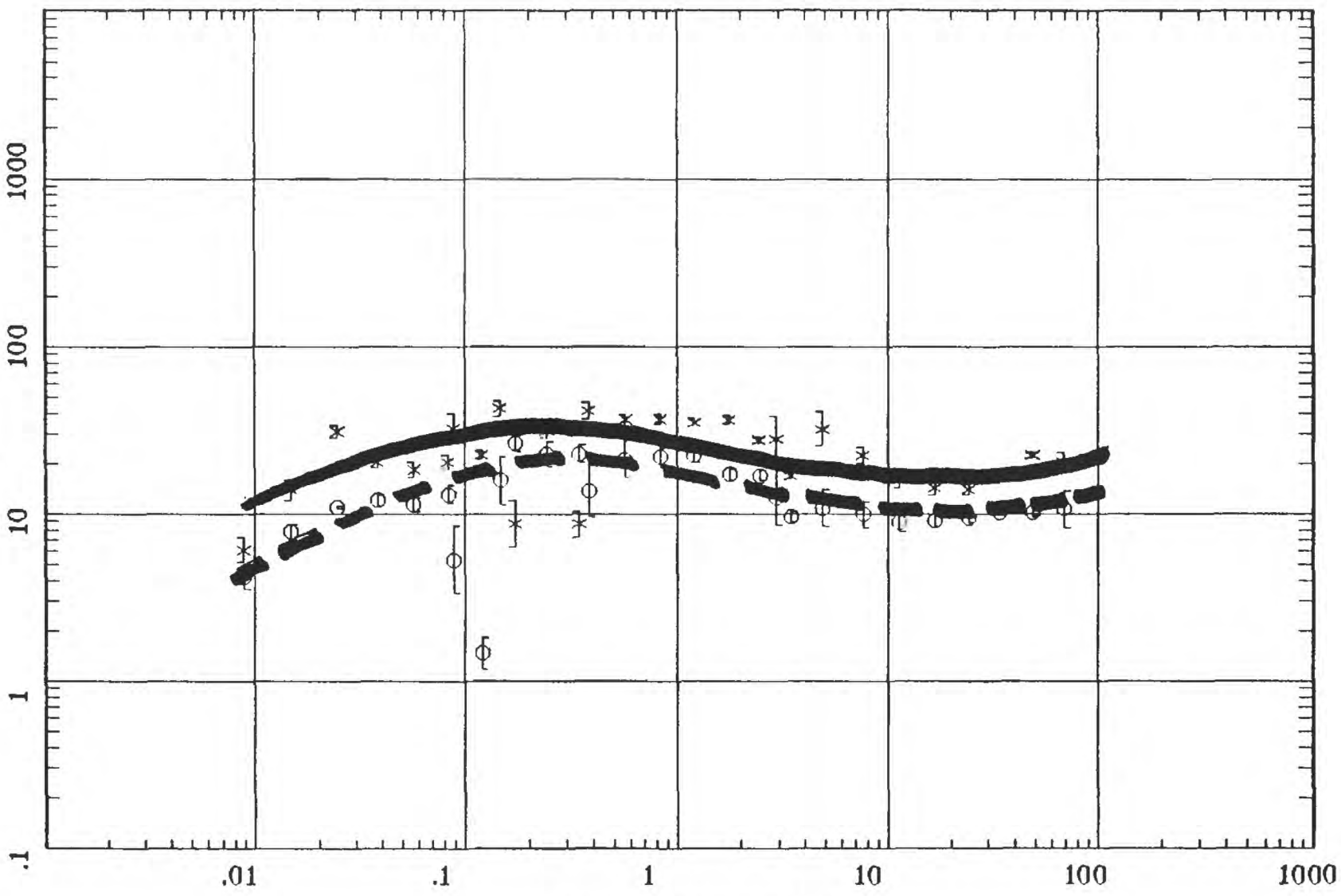

Client:
Remote: none
Acquired: 10:1 Jul 29, 2000
Survey Co:USGS

Rotation:
Filename: hr95b.avg
Channels: Ch1 Ch2 Ch3 Ch4 Ch5 Ch3 Ch4
Plotted: 11:09 Feb 06, 2001
< EMI - ElectroMagnetic Instruments >

Station 95

IMPEDANCE PHASE

Osgood Mtns, NV 100K

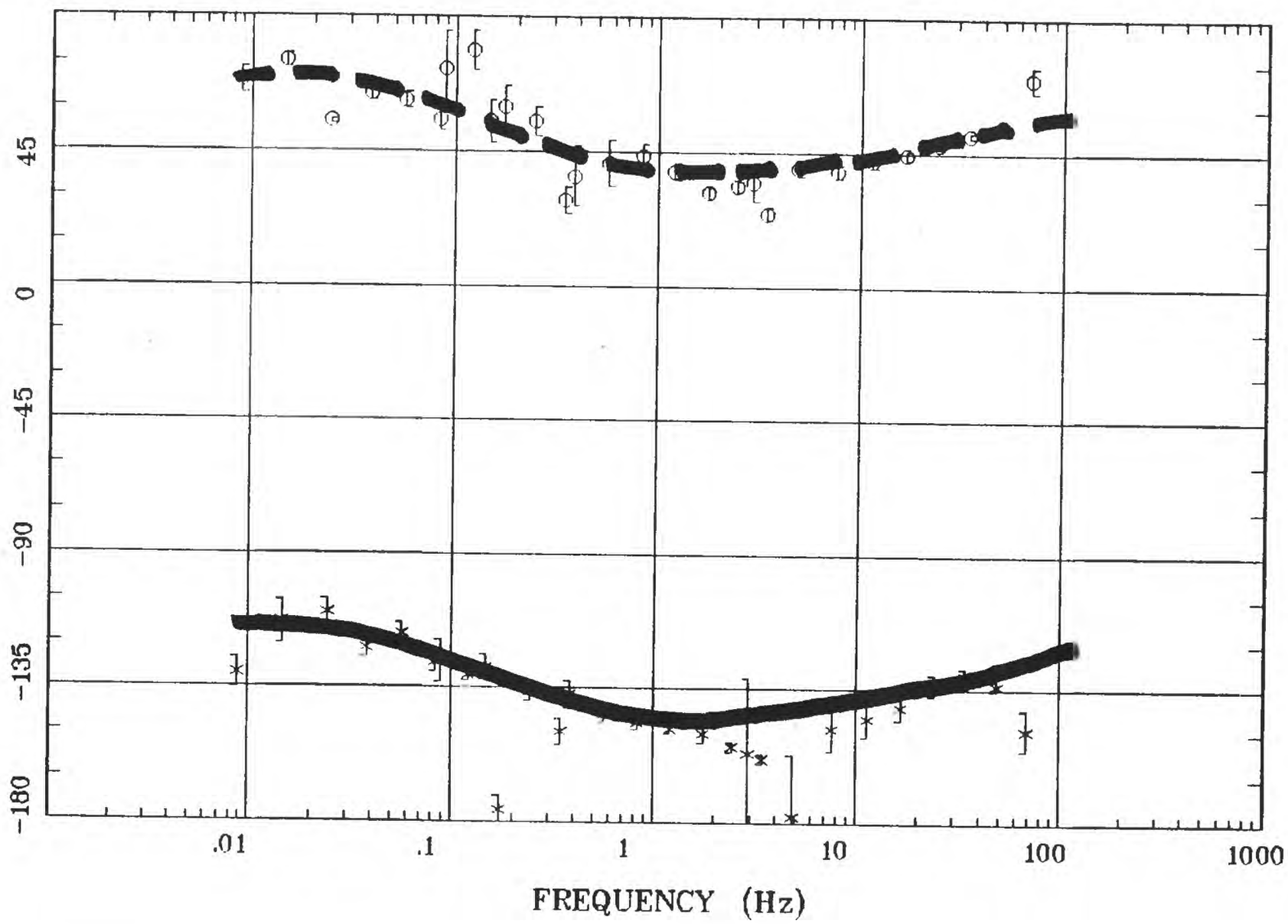

Client:
Remote: none
Acquired: 10:1 Jul 29, 2000
Survey Co:USGS

Rotation:
Filename: hr95b.avg
Channels: Ch1 Ch2 Ch3 Ch4 Ch5 Ch3 Ch4
Plotted: 11:09 Feb 06, 2001
< EMI - ElectroMagnetic Instruments >

Station 96

APPARENT RESISTIVITY Tuscarora, NV 100K

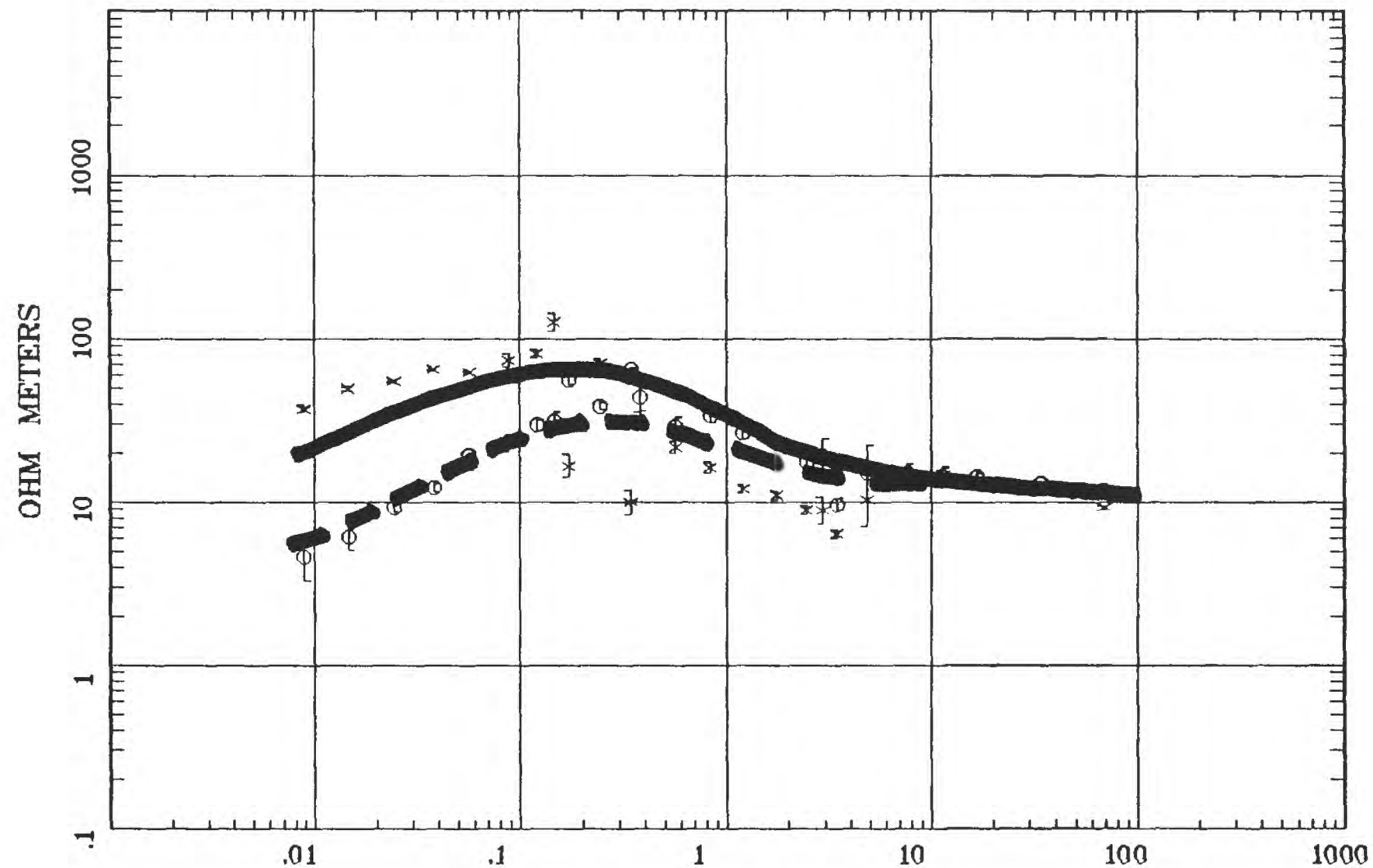

Client:
Remote: none
Acquired: 13:2 Jul 29, 2000
Survey Co:USGS

Rotation:
Filename: hr96a.avg
Channels: Ch1 Ch2 Ch3 Ch4 Ch5 Ch3 Ch4
Plotted: 11:09 Feb 06, 2001
< EMI - ElectroMagnetic Instruments >

Station 96

IMPEDANCE PHASE Tuscarora, NV 100K

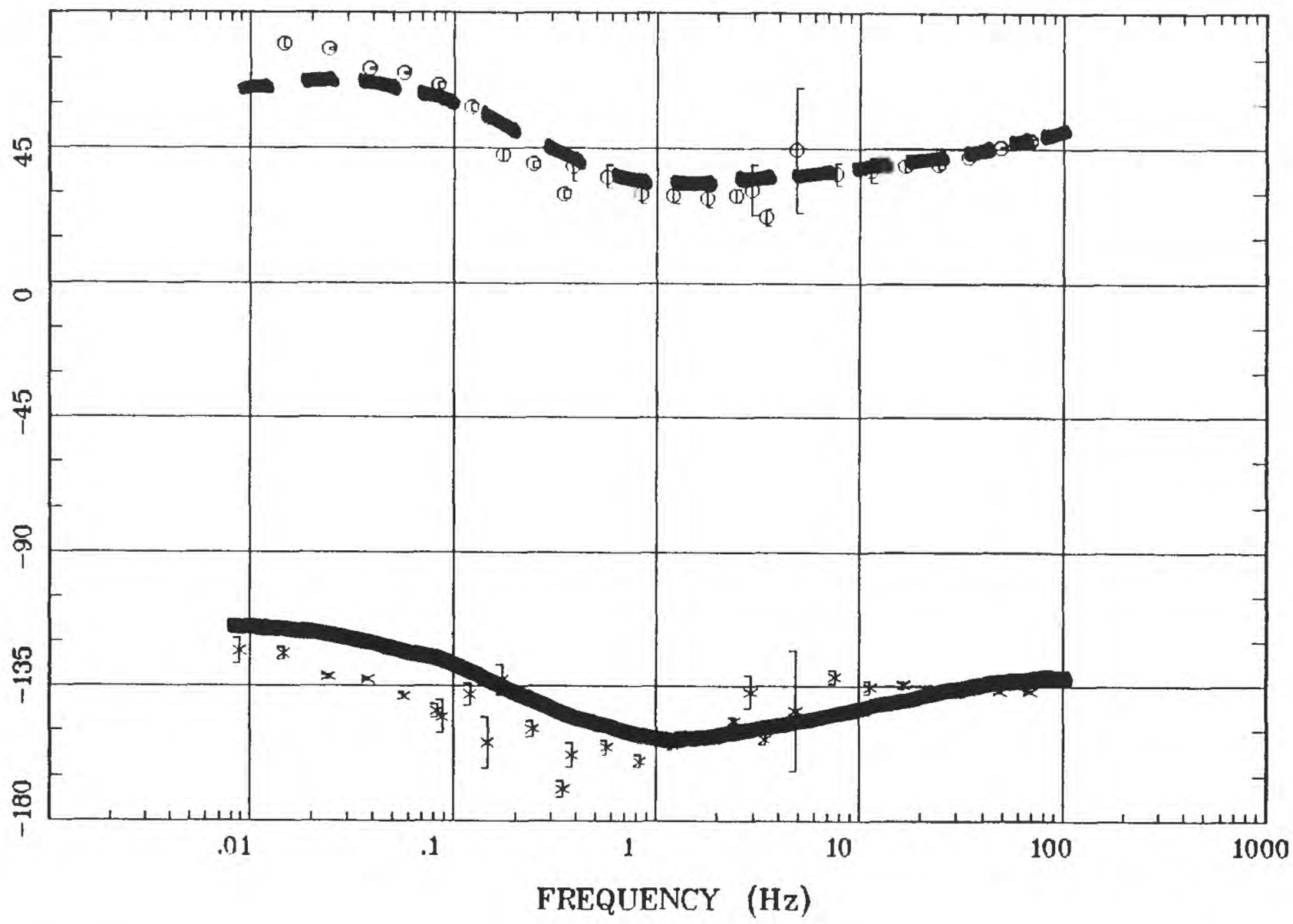

Client:
Remote: none
Acquired: 13:2 Jul 29, 2000
Survey Co:USGS

Rotation:
Filename: hr96a.avg
Channels: Ch1 Ch2 Ch3 Ch4 Ch5 Ch3 Ch4
Plotted: 11:09 Feb 06, 2001
< EMI - ElectroMagnetic Instruments >

APPARENT RESISTIVITY Winnemucca, NV 100K

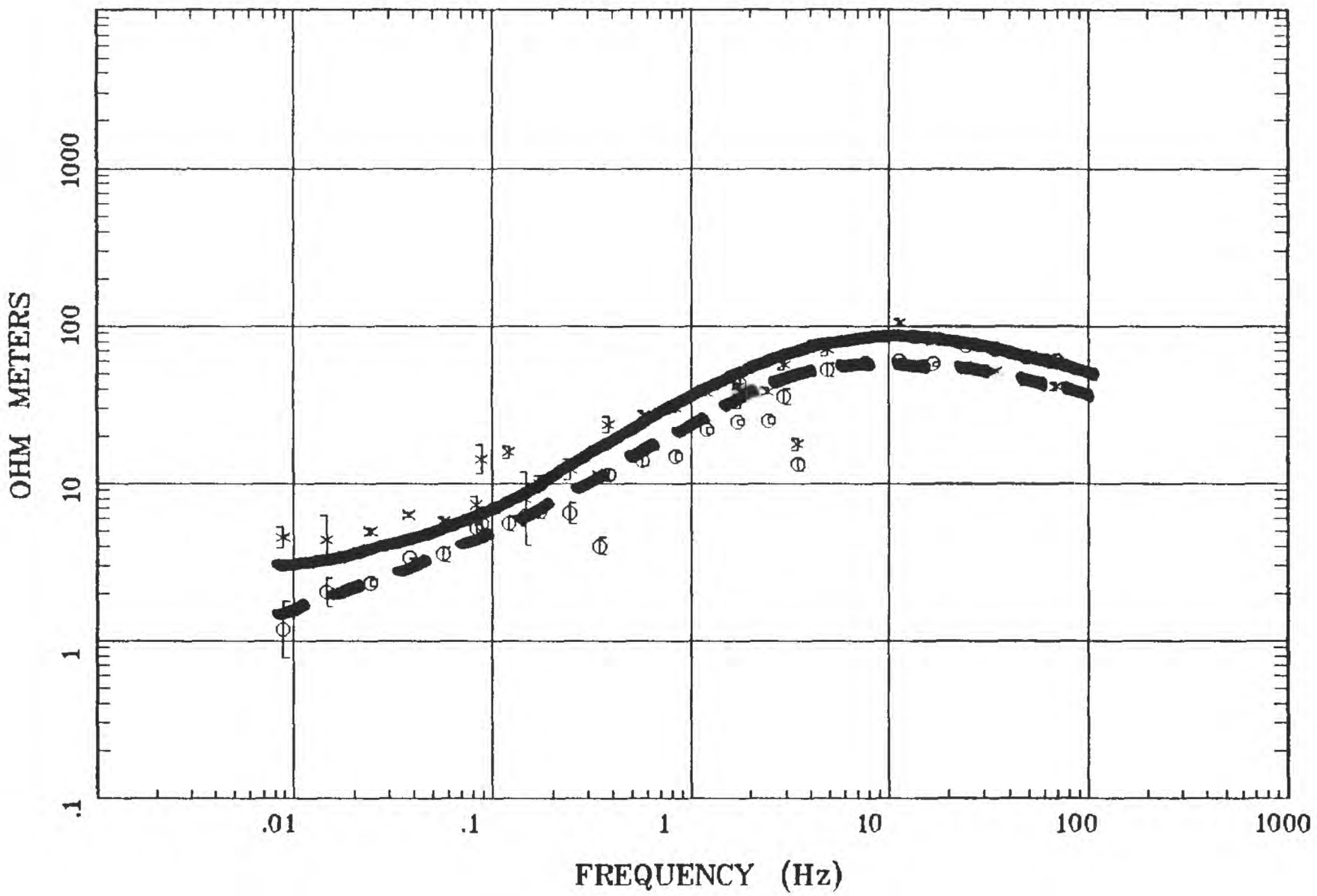

Client:
Remote: none
Acquired: 09:2 Jul 30, 2000
Survey Co:USGS

Rotation:
Filename: hr97all.avg
Channels: Ch1 Ch2 Ch3 Ch4 Ch5 Ch3 Ch4
Plotted: 11:10 Feb 06, 2001
< EMI - ElectroMagnetic Instruments >

Station 97

IMPEDANCE PHASE Winnemucca, NV 100K

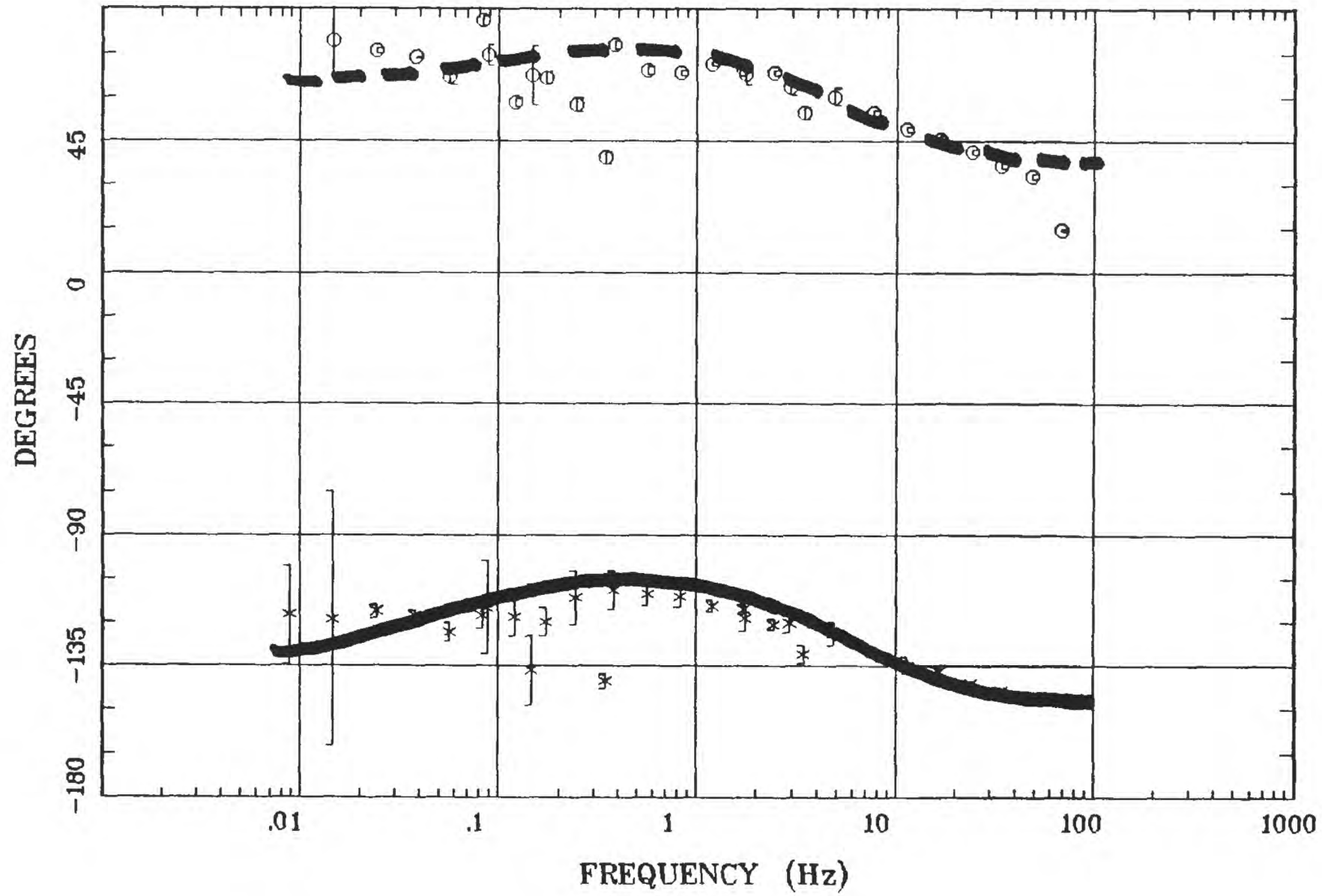

Client:
Remote: none
Acquired: 09:2 Jul 30, 2000
Survey Co:USGS

Rotation:
Filename: hr97all.avg
Channels: Ch1 Ch2 Ch3 Ch4 Ch5 Ch3 Ch4
Plotted: 11:10 Feb 06, 2001
< EMI - ElectroMagnetic Instruments >